The Impact of Tooth Brushing on Teeth Affected by Molar Incisor Hypomineralisation (MIH)

Eastman Dental Institute University College London

2017-2021

Submitted by:

Sarah Alfahad

Word count: 38841

Project supervisors:

Dr. Laurent Bozec (Faculty of Dentistry, University of Toronto)

Dr. Susan Parekh (Department of Paediatric Dentistry, Eastman Dental Institute-University College London)

Contents

List of Tables

List of Figures

List of Abbreviations

AI:	Amelogenesis imperfecta
AmF:	Amine fluoride
BEWE:	Basic erosive wear examination
CNN:	Conventional neural network
CPP-ACP:	Casein phosphopeptide-amorphous calcium phosphate
CP:	Cross polarisation
DDE:	Developmental defects of enamel
DEJ:	Dentino-enamel junction
EAPD:	European Academy of Paediatric Dentistry
FD:	Frequency domain
FDI:	World Dental Federation
FPM:	First permanent molar
GA:	General Anaesthesia
GERD:	Gastroesophageal reflux disease
GIC:	Glass ionomer cement
HCA:	Hydroxycarbonate apatite
HSPM:	Hypomineralised second primary molars
LCI:	Low coherence interferometry
mDDE:	Modified DDE index
MFP:	Sodium monofluoride phosphate
MH:	Molar hypomineralisation
MHSI:	Molar Hypomineralisation Severity Index
MIH TNI:	MIH treatment need index
MIH:	Molar Incisor Hypomineralisation
NaF:	Sodium fluoride
OCT:	Optical coherence tomography
OR:	Odd ratio
PEB:	Post-eruptive enamel breakdown
PI:	Permanent incisors
PLM:	Polarising light microscopy

PS:	Polarisation sensitive
SD:	Spectral domain
SEM:	Scanning electron microscopy
SLS:	Sodium lauryl sulphate
SnF_2:	Stannous fluoride
SPM:	Second primary molars
SS:	Swept source
TD:	Time domain
TSL:	Tooth surface loss
TWI:	Tooth wear index
XMT:	X-ray microtomography

Declaration of work

I, Sarah Alfahad declare that the presented thesis has been conducted by myself and has not been presented, in a whole or in part, in any other university, institution, or examination board. If contributions of other are involved, I made my effort to indicate this by referencing from literature and acknowledgment.

Sarah Alfahad

Eastman Dental Institute, University College Hospital

September 2020

Abstract

Background: Molar Incisor Hypomineralisation (MIH) can affect one or more first permanent molars (FPM), with or without the permanent incisors, prevalence ranges from 3-40%. Severity varies, and can be associated with hypersensitivity, post-eruptive breakdown (PEB) and aesthetic concerns. Different toothpastes have been suggested to enhance remineralization and reduce sensitivity, including fluoride or Novamin containing toothpastes.

Aim: To compare tooth surface loss (TSL) from toothbrushing using different toothpastes in MIH affected and sound FPMs using Optical Coherence Tomography (OCT).

Methods: Extracted human FPMs (N=27) Sound or with MIH were collected under ethical approval. Samples were classified using EAPD index 2014, in which type 21 indicates a white/cream opacity and type 22 yellow/brown opacity. Erosion using 1% citric acid was applied, followed by abrasion with an electric toothbrush and (i) saliva, (ii) Sensodyne® complete protection (inc Novamin), & (iii) Sensodyne® children pronamel (inc fluoride) for 100 cycles. A small needle was attached as a reference for calculation of TSL. OCT images were taken every 20 cycles, and the amount of TSL was calculated.

Results: TSL was higher in children pronamel group than complete protection and saliva for MIH (type 22) and control samples, with the highest TSL 100µm and a mean of 85µm. The lowest TSL was 7µm in control group brushed with saliva. In MIH sample (type 21), the highest TSL was with Complete protection (85µm). However, the average mean of TSL for type 21 lesions with both complete protection and children pronamel groups was 45µm.

Conclusion: Children Pronamel toothpaste resulted in more TSL, whereas complete protection resulted in less TSL in MIH type 22. This suggests Novamin may be beneficial in severely affected MIH teeth, but larger sample sizes are needed before a conclusion can be reached.

Acknowledgment

I would like to express my gratitude and special thanks to all people that helped me conduct this study. My deepest gratitude to my supervisors Dr Susan Parekh and Dr Laurent Bozec. They have supported and guided throughout these years.

My special thanks also go to Prof Paul Ashley, my course director, for giving me the time I needed to complete this study. To my friends who supported me with this journey, thank you.

To my mother and sisters, thank you for being all the time with me, thank you for all the support and encouragement, and thank you for travelling overseas and staying with me to help me finish my study.

Finally, my dear husband, Ahmad Alqabandi, thank you for spending time in helping me with the analysis and statistics and supporting me to complete this project.

Impact Statement

Molar incisor hypomineralisation (MIH) prevalence affects approximately 14% of the population worldwide (Dave and Taylor, 2018), with an estimated 878 million people affected in 2015 (Schwendicke et al., 2018). Patients with MIH face multiple problems including hypersensitivity, caries of the affected teeth, and repeated restorative treatment (Leppaniemi et al., 2001). Globally, it is estimated that 5 million new symptomatic cases of MIH seek dental care every year (Schwendicke et al., 2018). MIH has an impact on aesthetics, quality of life, and children's general health (Schwendicke et al., 2018). In addition, diet and toothbrushing habits might contribute to abrasion and erosion leading to tooth wear. MIH affected teeth, especially the yellow/brown lesions, are affected by erosion and abrasion more than sound teeth (Alqahtani, 2017).

Many parents ask us which toothpaste they should use for their child, especially with the sensitivity associated with MIH. There is a need to assess how can different types of toothpastes help in reducing the TSL in teeth affected by MIH compared to control teeth samples and to protect the enamel surface. To measure the tooth surface loss, Optical coherence tomography (OCT) was used, as an non-invasive method. This can help in guiding us toward monitoring the MIH lesions in clinic using a non-invasive tool like the OCT. Also, advice regarding the least abrasive toothpaste can be given to patients with MIH.

Chapter 1
Background

1 Background

1.1 Molar Incisor Hypomineralisation

MIH is a condition, in which one or more first permanent molars (FPM), with or without involvement of the permanent incisors (PI), are affected by demarcated opacities (Silva et al., 2016). The opacities can vary in colour from creamy, yellow to brown (Lygidakis et al., 2010). Recently similar lesions have been described in the second primary molars (SPM), known as hypomineralised second primary molars (HSPM) in the literature (Silva et al., 2016). The severity of the MIH varies, and can be associated with hypersensitivity, post-eruptive enamel breakdown (PEB) and aesthetic concerns (Lygidakis et al., 2010). Development of progressive carious lesions of affected teeth, and the need for repeated restorative treatment, is one of the complications of MIH (Leppaniemi et al., 2001). In addition, fear and behaviour management problems are more pronounced in MIH patients (Jälevik and Klingberg, 2002). To understand the effect of MIH, it is important to review enamel formation in more detail.

1.1.1 Enamel

Throughout its lifetime, enamel is adapted to absorb essential mechanical and abrasive stresses due to its complex mineralised structure (Fincham et al., 1995). The mineral content of enamel accounts for 97% of its weight, with less than 1-2% organic material and the remaining is water. The tightly packed carbonated hydroxyapatite crystals, arranged into an interwoven structure, provide resistance to fracture (Margolis et al., 2006, Ruan and Moradian-Oldak, 2015).

Many studies have investigated enamel formation, and how its regulated by enamel matrix proteins (Simmer and Fincham, 1995, Fincham et al., 1999, Moradian-Oldak, 2001, Margolis et al., 2006). One of the key factors that controls crystal formation is amelogenin, which accounts for over 90% of the enamel matrix (Moradian-Oldak, 2001, Margolis et al., 2006). Amelogenin proteins are tissue specific proteins, synthesised by ameloblast cells and are rich in proline, glutamyl residues, and histidine (Fincham and Simmer, 2007). Amelogenin protein has a unique characteristic, as it can adopt a structure that suits its environment. Evidence shows that amelogenin interacts with apatite crystals as part of crystal growth to form parallel arrays of mineral crystals (Ruan and Moradian-Oldak, 2015). There are two proposed theories of how amelogenin regulates apatite mineralisation in enamel formation (Ruan and Moradian-Oldak, 2015). The classic theory suggests that amelogenin binds to the crystal sides selectively and specifically to prevent ion deposition on these facets. This will allow crystals to grow in length and thickness during secretory stage and maturation stage respectively (Fincham et al., 1999, Iijima and Moradian-Oldak, 2004). The non-classical theory proposed that amelogenin forms, maintains, and assembles an intermediate prenucleation cluster by interacting with noncrystalline calcium phosphate. The clusters will then convert into organised apatite crystals (Beniash et al., 2009, Yang et al., 2010). Figure 1.1 shows the infrastructure of enamel with the nanoparticle of hydroxyapatite crystals (Kutsch, 2013).

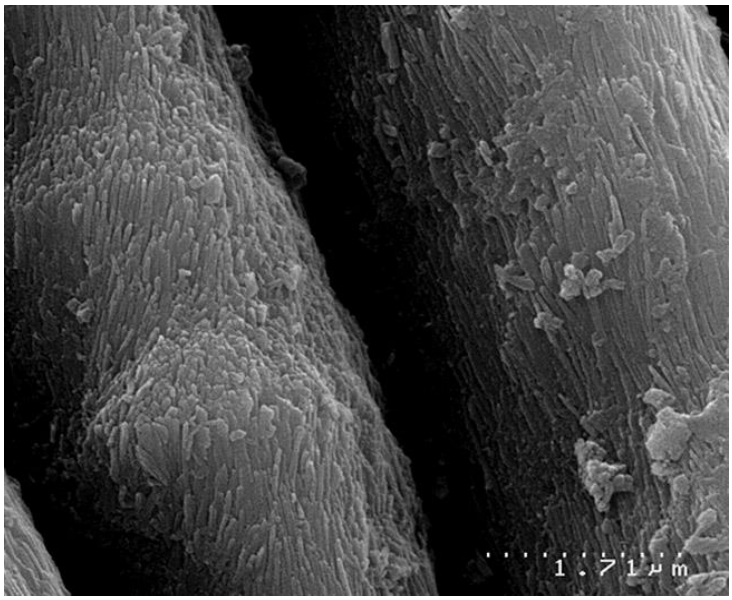

Figure 1.1 Scanning electron microscopy (SEM) micrograph of enamel nanostructure.

Reproduced from (Kutsch, 2013)

Other non-amelogenin proteins and proteinases also identified in the extracellular enamel matrix include enamelin, tuftelins, sulphated enamel proteins and "tuft" proteins. Enamelins are the largest acidic enamel proteins and have high affinity for apatite crystals (Moradian-Oldak, 2001).

Odontogenesis and amelogenesis

Interactions between neural crest-derived ectomesenchyme and oral epithelium results in teeth formation. Stages of tooth formation include development through bud, cap, bell and enamel formation stage (Hu et al., 2007). The development of FPMs starts at about four months of gestation (Alaluusua, 2010). Whereas the enamel formation for the upper central, lower central and lower lateral permanent incisors begins three to four months after birth, and ten to twelve months for the upper permanent lateral incisors (Whatling and Fearne, 2008, Schuurs, 2012).

The major stages of enamel formation are defined by the morphology and function of ameloblasts and these include presecretory, secretory, transitional, and maturation stages (Ruan and Moradian-Oldak, 2015). It takes approximately one thousand days for enamel formation as a whole and of this time, two thirds is devoted to the maturation stage (Alaluusua, 2010). The ameloblasts are responsible for both the enamel composition and its hierarchical structure as they cover the developing enamel forming a single cell layer (Ruan and Moradian-Oldak, 2015). This layer of ameloblasts control crystallite growth by influencing parameters such as pH-value, calcium ion availability, and the re-resorption of fluid and peptides (Reichenmiller and Klein, 2007).

Presecretory stage

Ameloblasts initiate the secretion of enamel proteins on the villous surface of mineralising dentine by sending processes through the degenerating basement membrane (Hu et al., 2007). Following the fenestration and removal of the basement membrane, enamel crystallites initiate at the dentino-enamel junction (DEJ) immediately (Ruan and Moradian-Oldak, 2015). After establishing the DEJ, a novel cell extension called a Tomes' process is formed at the secretory ends of ameloblasts. This extension organizes enamel crystals into rods and interrod enamel as it has secretory and non-secretory regions (Hu et al., 2007).

Secretory stage

During the secretory stage, the ameloblasts secrete enamel proteins that create a mineralisation front, as they concentrate along the ameloblast secretory membrane. The mineralisation front lacks the unmineralised layer that is usually found in dentine and bone as predentine and osteoid. As the ameloblasts continue to secrete enamel proteins, enamel crystals grow primarily in length and thickness (Hu et al., 2007). At this stage, the mineral content of secretory enamel is about 10-20% by volume, and the remaining portions are matrix protein and water (Margolis et al., 2006). The first signs of mineralisation of FPM are seen in the cusp tips which is around or soon after birth. Moreover, the deposition of enamel matrix is completed in the occlusal half of the crown at the end of the first year (Alaluusua, 2010). Disturbances that occur at this stage leads to a thinner or hypoplastic final enamel layer. Horizontal bands of enamel hypoplasia may result from systemic or environmental disturbances that are related to the time of disturbance as shown in figure 1.2 below (Hu et al., 2007, Simratvir, 2011).

Figure 1.2 Intraoral photograph shows hypoplastic lower permanent incisors.

Reproduced from (Simratvir, 2011)

Transitional and maturation stages

Transition and maturation begins after the full thickness of the enamel layer is established (Ruan and Moradian-Oldak, 2015). In the transition stage, the ameloblasts reduce their enamel proteins secretion, and produce a protease that degrades and facilitates the removal of the organic matrix from the extracellular compartment. These changes accelerate the growth of enamel crystallites in width and thickness, and terminate their growth in length as part of the maturation stage. The maturation stage is directed by modulating ameloblasts, and this process is important to harden the enamel layer until the enamel crystallites thicken and press against one another (Hu et al., 2007). Fluoride has an important role at this stage as it incorporates into crystal structure (Hu et al., 2007). It provides enamel with increased resistance to fracture and erosion and increased hardness (Fan et al., 2011). Ameloblasts are highly sensitive during the early stage of the maturation especially to environmental factors (Alaluusua, 2010). Enamel hypomineralisation, a pathologically soft enamel that has normal thickness, occurs as a result of disturbances during the calcification phase, known as hypocalcification, or at maturation phase, known as hypomaturation (Suga, 1989, Hu et al., 2007, Garg et al., 2012). Figure 1.3 illustrates the stages of enamel development (Hu et al., 2007).

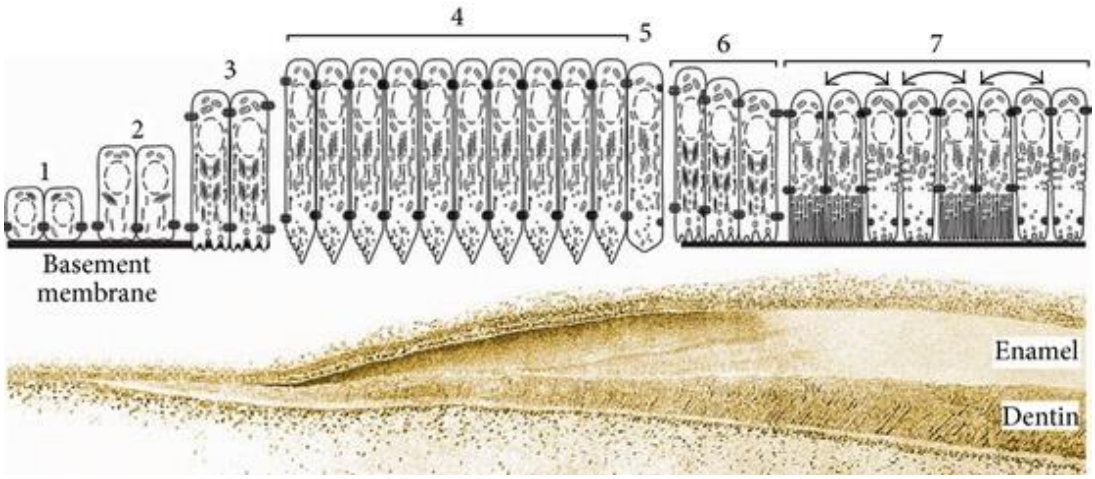

Figure 1.3 Stages of enamel development.

(1) Inner enamel epithelium resting on a basement membrane containing laminin. (2) Increase in the length of these cells as they differentiate to ameloblasts. (3) presecretory ameloblasts sending processes through the degenerating basement membrane. (4) The secretory ameloblasts secrete proteins at a mineralising font through developing Tomes' process to establish the DEJ. The enamel crystals grow in length. (5) Ameloblasts lose their precess at the end of the secretory stage. (6) The transition stage in which enamel achieved its final thickness and the secretory activity of ameloblasts diminishes. (7) The maturation stage shows ameloblasts modulating between ruffled and smooth-ended phase to promote the deposition of mineral on the sides of enamel crystals. Reproduced from (Hu et al., 2007).

1.2 Aetiology of MIH

Although tooth development is genetically controlled, environmental factors may disturb its development. The most critical period for enamel defects that affects FPM and incisors is the first year of life. However, hypomineralisation might develop later as enamel maturation takes several years in the FPM (Alaluusua, 2010). The aetiology of MIH and the exact nature of systemic insults are unclear and poorly defined (Whatling and Fearne, 2008, Alaluusua, 2010). That is because one insult at low threshold might not cause MIH, but two or more factors acting synergistically may lead to enamel defects (Whatling and Fearne, 2008, Alaluusua, 2010). The aetiolgy of MIH is divided into prenatal, perinatal and postnatal exposures.

Prenatal exposures

There is little evidence to suggest a causative factor during the prenatal period (Silva et al., 2016). A non-significant association was found between maternal smoking during pregnancy and MIH in several studies (Arrow, 2009, Fagrell et al., 2011, Souza et al., 2012, Kühnisch et al., 2014, Pitiphat et al., 2014). Medical problems during pregnancy were variable including maternal diabetes, hypertension, medications, infections, and hypercalcaemia (Whatling and Fearne, 2008, Alaluusua, 2010, Souza et al., 2012, Silva et al., 2016). Some studies found significant association between problems with pregnancy and MIH (Whatling and Fearne, 2008, Souza et al., 2012). Hypotension-related anaemia was significantly associated with MIH with an odd ratio of 2.5 (Ghanim et al., 2013a). No association was found between the number of ultrasound scans during pregnancy and MIH (Whatling and Fearne, 2008). However, Ghanim et al. found a significant association if the ultrasound taken more than three times during the last trimester (Ghanim et al., 2013a). Seven studies investigated the use of medication during pregnancy and failed to find an association with MIH (Arrow, 2009, Fagrell et al., 2011, Souza et al., 2012, Durmus et al., 2013, Ghanim et al., 2013a, Allazzam et al., 2014). One study found higher odds (OR 3.24, 95% CI 1.33-7.88) of MIH with maternal stress (Ghanim et al., 2013a). Table 1.1 provides a summary of the prenatal factors.

Authors	Year	Method	Sample size	Exposure	Outcome
Kühnisch et al.	2014	Prospective	5991	Smoking	Non-significant association (P-value > 0.05)
Fagrell et al.	2011	Retrospective	1076	Smoking Medication Gestational diabetes and infectious diseases	Non-significant association (P-value >0.2)
Pitiphat et al.	2014	Retrospective	282	Smoking	Non-significant association (P-value = 1)
Souza et al.,	2012	Retrospective	1126	Smoking Medication Maternal health	Non-significant association (P-value = 1) Non-significant association (P-value = 1) Significant association (P-value <0.05)
Arrow	2009	Retrospective	550	Smoking Medication	Non-significant association (P-value = 0.75) Non-significant association (P-value = 0.09)
Whatling and Fearne	2008	Retrospective	109	Maternal health Number of ultrasound scans	Significant association (P-value = 0.025) Non-significant association
Allazzam et al.	2014	Retrospective	267	Medication	Non-significant association (P-value = 0.9)

Ghanim et al.	2013	Retrospective	823	Medication Maternal stress Hypotension-related anaemia Number of ultrasound scans	Non-significant association (P-value = 0.1) Significant association (P-value = 0) Significant association (P-value = 0) Significant association (P-value = 0)
Durmus et al.	2013	Retrospective	228	Medication	Non-significant association (P-value >0.05)
Jälevik et al.	2001	Retrospective	516	Medication	Non-significant association (OR 1, 95% CI 0.4-2.4)

Table 1.1 Prenatal factors

Perinatal exposures

Prematurity, mode of delivery, delivery and birth complications and delivery requiring induction were not associated with MIH (Whatling and Fearne, 2008). However, Ghanim et al. found higher odds (OR 3.87, 95% CI 2.42-6.17) of MIH with low birthweight of less than 2.5 kg (Ghanim et al., 2013a). Lack of oxygen in active ameloblasts has been suggested as a causative factor of MIH or opacities in molars and incisors (Lygidakis et al., 2008). This is known as hypoxia and can be associated with medical problems related to birth such as prematurity or respiratory distress (Alaluusua, 2010). As MIH lesions have been found to be very low in calcium, it has been suggested that impaired metabolism of calcium by ameloblasts might cause these lesions (Jälevik et al., 2001). Enamel hypoplasia rather than hypomineralisation has been a finding in children with nutritional rickets associated with hypocalcaemia (Grahnen and Selander, 1954). Table 1.2 summarizes the perinatal factors.

Authors	Year	Method	Sample size	Exposure	Outcome
Whatling and Fearne	2008	Retrospective	109	Prematurity Mode of delivery Delivery and birth complications	Non-significant association (P-value = 0.6) Non-significant association (P-value = 0.2) Non-significant association (P-value = 0.1)
Ghanim et al.	2013	Retrospective	823	Low birth weight	Significant association (P-value = 0)
Lygidakis et al.	2008	Retrospective	3518	Hypoxia due to prematurity or respiratory distress	Significant association (P-value <0.001)

Table 1.2 Perinatal factors

Postnatal exposures

Several early childhood illnesses, up to three or four years of age, have been investigated to assess their relationships with MIH (Alaluusua, 2010, Silva et al., 2016). These include asthma (Jälevik et al., 2001), otitis media (Jälevik et al., 2001, Beentjes et al., 2002), pneumonia (Jälevik et al., 2001, Beentjes et al., 2002, Ghanim et al., 2013a), chickenpox (Whatling and Fearne, 2008, Ghanim et al., 2013a), Tonsillitis (Ghanim et al., 2013a) and urinary tract infections (Tapias-Ledesma et al., 2003). Most of these illnesses have been positively associated with MIH, although with some specific diseases, controversial results exist such as respiratory infections, asthma, unexplained high fever and ear infections (Jälevik et al., 2001, Whatling and Fearne, 2008). A combination of fever with other symptoms such as chest and/or ear infections has a significant association (OR 3.27, 95% CI 1.09–9.82) with MIH (Ghanim et al., 2013a). The odds of MIH have been found to increase (OR 9.37, 95% CI 2.71-32.34) in relation with pneumonia (Ghanim et al., 2013a). A significant association with MIH has been found in children who had chickenpox between ages of 3 and 3.99 (Whatling and Fearne, 2008). This is opposite to another study that found a non-significant association between MIH and chickenpox (Ghanim et al., 2013a).

Medications, particularly antibiotics, used in the first year of life have been significantly associated with MIH and fluoride like defects in the permanent incisors and FPMs (Jälevik et al., 2001, Ghanim et al., 2013a). In children who used amoxicillin as the only antibiotic during the first four years, MIH was more common than in children with mixed antibiotic use (Whatling and Fearne, 2008). Also, a higher intake of macrolides during the first three years was significantly associated with enamel defects in FPM (Tapias-Ledesma et al., 2003). One study failed to find an association between MIH and asthma medication (Arrow, 2009).

One study failed to report an association between prolonged breastfeeding and MIH (Laisi et al., 2008), while another study found a significant correlation between MIH and breastfeeding due to the high levels of dioxin pollution in mother's milk (Alaluusua et al., 1996). Demarcated opacity and/or hypoplasia have been reported in children who are exposed to high levels of dioxins or polychlorinated biphenyls (PCBs) in early years of life (Jan et al., 2007). In Slovenia, children living in areas contaminated with PCB had a high prevalence of enamel defects (Jan and Vrbič, 2000). However, children living in urban areas polluted by dioxins had a similar prevalence of MIH as those living in an area with low pollution according to a Turkish study (Kuscu et al., 2009). Diffuse opacities are reported to be significantly related to fluoride exposure by drinking water or supplementation that affect enamel formation during maturation stage (Alaluusua, 2010). As for demarcated opacities related to MIH, no association has been found between those opacities and fluoride exposure (Whatling and Fearne, 2008). Table 1.3 shows the postnatal exposures in summary.

Authors	Year	Method	Sample size	Exposure	Outcome
Beentjes et al.	2002	Retrospective	45	Otitis media Pneumonia	Significant association (P-value = 0.019) Significant association (P-value = 0.027)
Jälevik et al.	2001	Retrospective	516	Asthma Otitis media Pneumonia Medications (Antibiotics)	Significant association (OR 24, 95% CI 5.2-110) Significant association (OR 1.5, 95% CI 0.9-2.5) Significant association (OR 2.5, 95% CI 1-6) Significant association (P-value<0.05)
Ghanim et al.	2013	Retrospective	823	Pneumonia Chickenpox Tonsillitis High fever with other infections Medications (Antibiotics)	Significant association (P-value = 0) Non-significant association (P-value = 0.25) Significant association (P-value = 0.01) Significant association (P-value = 0) Significant association (P-value = 0)

Whatling and Fearne	2008	Retrospective	109	Amoxicillin Chickenpox Fluoride Exposure	Significant association (P-value = 0.028) Significant association (P-value = 0.047) Non-significant association (P-value = 0.6)
Tapias-Ledesma et al.	2003	Retrospective	196	Urinary tract infections Macrolides	Significant association (OR 6.68, 95% CI 1.01-54) Significant association (OR 2.3, 95% CI 1-5)
Arrow	2009	Retrospective	550	Asthma Medication	Non-significant association (P-value = 0.9) Non-significant association (P-value = 0.7)
Laisi et al.	2008	Prospective	167	Breast Feeding	Non-significant association (P-value = 0.05)
Alaluusua et al.	1996	Retrospective	96	Breast Feeding	Significant association (P-value = 0.026)
Jan et al.	2007	Retrospective	432	High levels of dioxins or PCBs	Significant association (P-value = 0.005)
Jan and Vrbič	2000	Retrospective	202	PCBs	Significant association (P-value = 0.0001)
Kuscu et al.	2009	Retrospective	153	Dioxins Pollution	Non-significant association (P-value = 0.001)

Table 1.3 Postnatal exposures.

1.3 Prevalence of MIH

The prevalence of MIH varies between region, country and the indices and criteria used for diagnosis (Mast et al., 2013). The incidence of MIH appears to be increasing worldwide (Jälevik, 2010). A study found that prevalence of MIH around the world is 14.2% (Dave and Taylor, 2018). The overall prevalence of MIH in Northern England was 15.9% (Balmer et al., 2012). In Germany and Bulgaria, the prevalence of MIH has been reported to be 5.6% and 3.5% respectively (Dietrich et al., 2003, Kukleva, 2008). Whereas a prevalence of 40.2% has been reported in Brazil (Soviero et al., 2009) and 13.7% in Kenya (Kemoli, 2008). In Iraq, 18% of children were considered to have MIH with at least one first molar or first molars and incisors affected (Ghanim et al., 2011). Table 1.4 presents the prevalence of MIH with details of each study.

Authors	Year	Country	Sample size	Index/method	Prevalence
Dave and Taylor	2018	Worldwide	89,520	Meta-analysis	14.2%
Balmer et al.	2012	Northern England	4795	mDDE	15.9%
Dietrich et al.	2003	Germany	2408	mDDE	5.6%
Kukleva	2008	Bulgaria	2960	mDDE	3.5%
Soviero et al.	2009	Brazil	292	EAPD	40.2%
Kemoli	2008	Kenya	3591	Simple criteria developed by author	13.7%
Ghanim et al.	2011	Iraq	823	EAPD	18%

Table 1.4 Prevalence of MIH in different countries

1.4 Diagnosis and classification of MIH

A variety of terms have been developed and used to describe developmental enamel defects (DDE) throughout the years (Jälevik, 2010). An index is needed to diagnose and classify MIH correctly using a simple and reproducible scoring system (Weerheijm et al., 2003).

Examination of MIH should be carried out at age of 8 years old. Reasons for that is the eruption of all permanent first molars and incisors will be completed at that age and the PEB is minimal (Garg et al., 2012).

The following sections describe the MIH indexes in detail.

1.4.1 The mDDE index

In 1982, the DDE index was published by the World Dental Federation (FDI) and due to its complexity, a modified DDE index (mDDE) was presented in 1992 by the FDI. A working group was formed to critically review and outline the deficiencies in the DDE index (Clarkson, 1992). Table 1.5 shows the classification of enamel defects according to the DDE index. The problems and deficiencies associated with the DDE index with the modifications applied are summarized in table 1.6 (Clarkson, 1992).

The mDDE index has two forms, one is the simple form, for screening surveys, and the other form is more detailed for epidemiological studies. The simple screening form records three basic types of defects as shown in table 1.7. The more detailed form records the same defects as the simple form but in more detailed information. Table 1.8 summarize the different codes given for the type of the defect for use in general epidemiological studies. Once the type of the defect is recorded, the extent of the defect should be also given a scores illustrated in table 1.9 (Clarkson, 1992). Using the mDDE criteria, a phenodent form has been developed and used in Eastman Dental Hospital in collaboration with Strasburg University to record the enamel defects. The form describes the defect in terms of the location, extent of lesion, demarcation, and type of defect. Figure 1.4 shows the phenodent form applying the mDDE criteria.

Classification	Permanent teeth	Primary teeth
1.Type of defect		
Normal	0	A
Opacity (white/cream)	1	B
Opacity (yellow/brown)	2	C
Hypoplasia (pits)	3	D
Hypoplasia (grooves: horizontal)	4	E
Hypoplasia (grooves: vertical)	5	F
Hypoplasia (missing enamel)	6	G
Discoloured enamel (not associated with opacity)	7	H
Other defects	8	J
Combination of defects		
2.Number and demarcation of defects		
Single	1	A
Multiple	2	B
Diffuse, fine white lines	3	C
Diffuse, patchy	4	D
3.Location of defects		
Gingival one half	1	A
Incisal one half	2	B
Occlusal	3	C
Cuspal	4	D

Table 1.5 The DDE index

DDE index deficiencies	mDDE index modifications
Examination criteria	
Teeth could be examined either wet or dry.	Teeth should be examined wet.
Difficult to decide whether a defect is present or absent.	Any defect less than 1 mm in diameter should not be recorded.
Many conditions such as white spot lesions, white cuspal ridges, de-mineralised areas… etc, were not mentioned.	If in doubt, classify as 'normal'. Any defect not in the criteria, reported as 'other'.
Some opacities could not be seen with bright light.	Chose the type of light carefully. Natural or minimized intensity artificial lights.
Position of the examiner.	Should be from different examining.
Recording of data	
Difficult to distinguish between diffuse and demarcated opacities.	Categorized and clarified.
Difficult to understand 'discoloured enamel'.	Discolouration is a secondary factor.
Various scores need to be recorded, multicoding system.	Record the type and extent of defect.
Analysis and interpretation of results	
Complicated to analyze due to multicoding system.	Adjusted by having less codes.
Present data as number or percentage of persons and the teeth affected.	Simplified the presentation of data. Grouped the results into demarcated opacities, diffuse opacities, and hypoplastic defects.
Type of defect does not refer to the demarcation of the opacities and only refers to the colour of them.	Distinction between the opacities whether diffuse or demarcated is more important.
The extent of the defects could not be recorded.	The extent of the defects applied.

Table 1.6 The main differences between DDE and mDDE indexes

Type of Defect	Code
Normal	0
Demarcated opacities	1
Diffuse opacities	2
Hypoplasia	3
Other defects	4
Combinations	Code
Demarcated and diffuse	5
Demarcated and hypoplasia	6
Diffuse and hypoplasia	7
All three defects	8

Table 1.7 mDDE index for screening surveys.

Type of Defect	Code
Normal	0
Demarcated opacities	
white/cream	1
yellow/brown	2
Diffuse opacities	
Diffuse-lines	3
Diffuse-patchy	4
Diffuse-confluent	5
Confluent/patchy + staining + loss of enamel	6
Hypoplasia	
Pits	7
Missing enamel	8
Any other defects	9
Combinations	Code
Demarcated and diffuse	A
Demarcated and hypoplasia	B
Diffuse and hypoplasia	C
All three defects	D

Table 1.8 mDDE index for epidemiological studies

Type of defect	Code
Normal	0
Less than 1/3	1
At least 1/3 – 2/3	2
At least 2/3	3

Table 1.9 Extent of defect

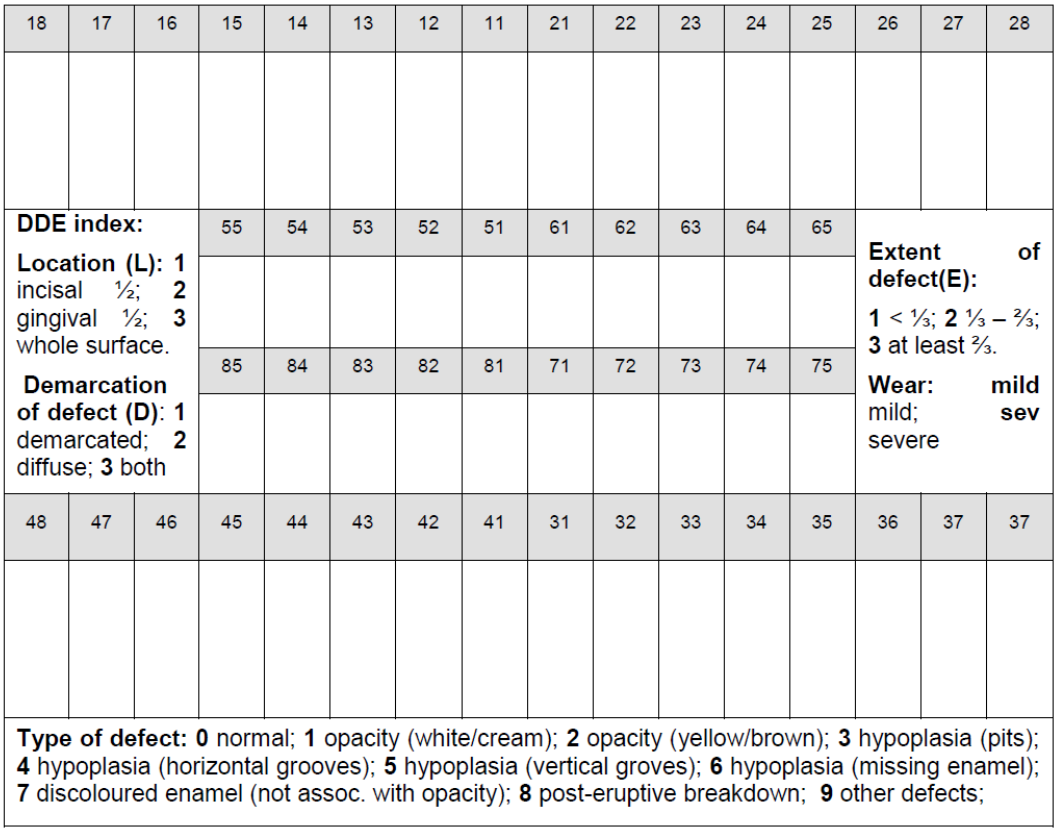

Figure 1.4 The phenodent form of mDDE

1.4.2 The MHSI

Molar Hypomineralisation Severity Index (MHSI), was developed in 2008. This index includes sensitivity associated with MIH as a subjective measure. Also, it helps in guidance toward the best treatment required for MIH affected teeth (Chawla et al., 2008). Some studies classified the severity of MIH into mild, moderate, and severe. The mild defect includes the demarcated opacities without colour differentiation. Whereas the defects presenting with PEB are considered moderate. The severe forms of defects include the presence of atypical restorations with or without PEB or teeth extracted due to hypomineralisation (Leppaniemi et al., 2001, Ghanim et al., 2011). These classifications do not describe the location or colour of the defect (Oliver et al., 2014).

The MHSI describes both the MIH and the Molar hypomineralisation (MH) as generalized hypomineralisations have been observed in primary and permanent dentition. Also, the enamel breakdown and hypersensitivity occur in the molar region rather than the inscisor region which mainly has opacities (Chawla et al., 2008).

The MHSI is based on severity weightings, which are summed to give a score. The colour, location, and previous restorations scores indicate an increased severity. Whereas the other characteristics have dichotomous scores. The summation of the scores determine the best treatment to be provided. The values of the whole dentition range between 1-52 and for individual teeth between 1-13. As the scores of MHSI increase, the treatment needs of restorations and extractions increase, and the use of fissure sealants decrease. Table 1.10 describes the different characteristics of hypomineralised defects of FPMs and PIs based on the MHSI. (Chawla et al., 2008).

Characteristics of molar hypomineralised defects	Severity of characteristic	Weighting assigned
Eruption status	Unerupted	0
	Erupted	1
Colour of most severe defects	None	0
	White/cream	1
	Yellow	2
	Brown	3
Location of most severe defect	None	0
	Smooth surface	1
	Occlusal surface (FPMs)	2
	Incisal edge (PIs)	2
	Cuspal involvement	3
Restorations placed/replaced	None	0
	One	1
	Two	2
Atypical restorations	None	0
	Present	1
Post eruptive breakdown	None	0
	Present	1
Sensitive to temperature (child report)	None	0
	Sensitive	1
Sensitive to tooth brushing (child report)	None	0
	Sensitive	1

Table 1.10 The MHSI

1.4.3 The EAPD index

In 2003, the European Academy of Paediatric Dentistry (EAPD) established a clinical evaluation guidance for MIH (Weerheijm et al., 2003). This evaluation criteria was used extensively in epidemiological studies reporting prevalence rates of MIH, but the results differed considerably. Socio-behavioural, genetic, and environmental factors of the populations studied could attribute to these differences (Elfrink et al., 2015).

In 2014, the 12th EAPD Congress in Sopot, Poland, was held and an MIH workshop was associated with the Congress. Suggestions were given on how to improve the use of the established EAPD guidelines in epidemiological studies for MIH. An agreement on the need to develop a data collection instrument for summarizing clinical data collected from the examination fields was reached by the workshop experts and participants (Elfrink et al., 2015). The new charting method combines the elements of the EAPD criteria and the mDDE index for classifying the clinical status of MIH and its extent on the involved tooth surface as well as other enamel defects (Ghanim et al., 2015).

The EAPD index has two forms, the short form for surveys with simple screening and the long form for more detailed, clinic-based or community-based studies. The key elements in both forms emerged from the EAPD criteria reflecting the theme of charting. The short form grades only index teeth that are mentioned in the MIH and HSPM definition, including FPM, PI, and SPM (Ghanim et al., 2015). The long form helps to diagnose all teeth available at time of examination in addition to MIH/HSPM-specific index, as evidence showed the involvement of other teeth with demarcated hypomineralisation defects (Soviero et al., 2009).

The charting format has two main sections, a section that assess the clinical presentation of enamel lesions (clinical status criteria) and the other section is related to the size of the tooth surface area affected by the lesion (lesion extension criteria), and minor section for the tooth eruption status (eruption status criteria). Figure 1.5 and 1.6 illustrate the short and long forms of the charting sheet. Table 1.11 explains and defines the codes of the clinical status criteria for both forms (Ghanim et al., 2015). Also, reference photographs have been used for both the short and long forms as in figure 1.7.

The information for the lesion status will not be obtained fully if less than 1/3 of the crown erupted (Fteita et al., 2006). Therefore, including teeth with at least 1/3 or more of the crown erupted will lead to more appropriate results rather than recording the fully erupted teeth only, in which the prevalence rates will be overestimated (Ghanim et al., 2015). In addition, only teeth with more than 1 mm lesion extent are recommended to be included (Lygidakis et al., 2010).

An increased number of affected FPMs, carious lesion severity, and enamel break down has been significantly associated with the increased extent of the lesion (Ghanim et al., 2011). In most of the epidemiological studies for MIH, dental caries has hardly been highlighted (Elfrink et al., 2008, Ghanim et al., 2013b). Therefore, it is required to assess the caries experience with a full mouth assessment to

avoid confusion between children with severe carious that have hypomineralisation defect as the primary cause of enamel loss and those with severe caries as the primary loss, and to determine the best treatment required. Also, assessment of dental caries simultaneously with MIH is encouraged in future research (Ghanim et al., 2015).

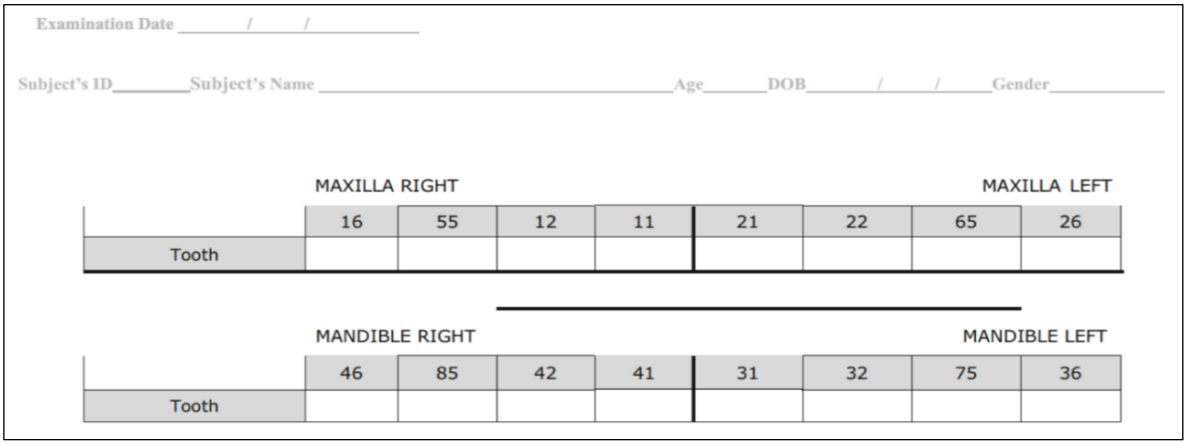

Charting Criteria Notes	**Notes**
Eruption status criteria A = not visible or less than 1/3 of the occlusal surface or of the crown length of incisor is visible.	Score a tooth on MIH/HSPM if at least 1/3 or more of the tooth is visible, otherwise, use Code A and no need to score the clinical status or the extent.
Clinical status criteria 0 = No visible enamel defect. 1 = Enamel defect, non-MIH/HSPM. 2 = White, creamy demarcated, yellow or brown demarcated opacities. 3 = Post-eruptive enamel breakdown (PEB). 4 = Atypical restoration. 5 = Atypical caries. 6 = Missing due to MIH/HSPM. 7 = Cannot be scored*.	Record the clinical status first and lesion extent as second (if required). Use punctuation mark "," to separate between digits. An enamel defect of one millimetre or less in diameter is considered as sound. If non MIH/HSPM lesions diagnosed together with MIH/HSPM, score the non MIH/HSPM first. When uncertainty exists regarding rating of the lesion the less severe rating is to be recorded.
Lesion extension criteria (only after diagnosing MIH/HSPM, i.e. scores 2 to 6) I = less than one third of the tooth affected. II = at least one third but less than two thirds of the tooth affected. III = at least two thirds of the tooth affected.	When more than one MIH/HSPM lesion exists per tooth, visually combine all areas affected by the lesion and score the more severe presentation. *Index tooth with extensive coronal breakdown and where the potential cause of breakdown is impossible to determine.

Figure 1.5 EAPD short form.

Reproduced from (Ghanim et al., 2015)

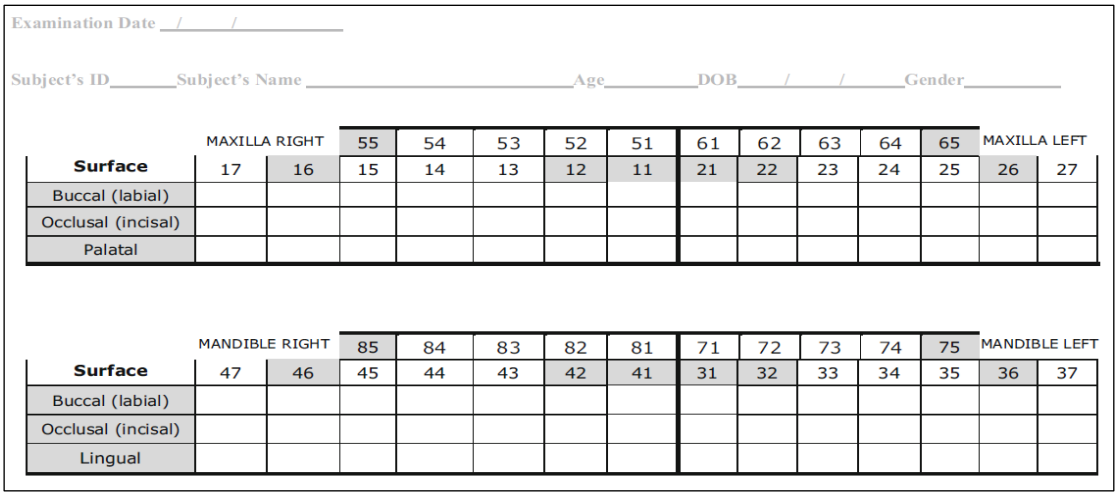

Examination Date __/____/_____

Subject's ID_____Subject's Name _____Age_____DOB____/____/_____Gender_____

	MAXILLA RIGHT		55	54	53	52	51	61	62	63	64	65	MAXILLA LEFT	
Surface	17	16	15	14	13	12	11	21	22	23	24	25	26	27
Buccal (labial)														
Occlusal (incisal)														
Palatal														

	MANDIBLE RIGHT		85	84	83	82	81	71	72	73	74	75	MANDIBLE LEFT	
Surface	47	46	45	44	43	42	41	31	32	33	34	35	36	37
Buccal (labial)														
Occlusal (incisal)														
Lingual														

Charting Criteria Notes

Eruption status criteria

A = not visible or less than 1/3 of the occlusal surface or of the crown length of incisor is visible.

Clinical status criteria

0 = No visible enamel defect.

1 = Enamel defect, non-MIH/HSPM

11 = diffuse opacities

12= hypoplasia

13 = amelogenesis imperfecta

14= hypomineralisation defect (not MIH/HSPM)

2 = demarcated opacities

21 = White or creamy demarcated opacities

22 = Yellow or brown demarcated opacities

3 = Post-eruptive enamel breakdown (PEB)

4 = Atypical restoration

5 = Atypical caries

6 = Missing due to MIH/HSPM

7 = Cannot be scored*

Lesion extension criteria (only after diagnosing MIH/HSPM, i.e. scores 2 to 6)

I = less than one third of the tooth surface affected.

II = at least one third but less than two thirds of the surface affected.

III = at least two thirds of the tooth surface affected.

Notes

Score a tooth surface on MIH/HSPM if at least 1/3 or more of the tooth surface is visible, otherwise, use Code A and no need to score the clinical status or the extent.

In the charting sheet place a circle around the tooth number you score.

Record the clinical status first and lesion extent as second (if required). Use punctuation mark "," to separate between digits.

An enamel defect of one millimetre or less in diameter is considered as sound.

Use codes 2 to 6 for MIH/HSPM index teeth only (i.e. FPM, PIs and SPM). Codes (0, 11, 12, 13) are applicable on all teeth including index teeth. Code 14 should be assigned to any tooth other than index teeth when MIH/HSPM-like opacities are diagnosed.

If non MIH/HSPM lesions diagnosed together with MIH/HSPM, score the non MIH/HSPM first.

When uncertainty exists regarding rating of the lesion the less severe rating is to be recorded.

When more than one MIH/HSPM lesion exists per surface, visually combine all areas affected by the lesion and score the more severe presentation.

For MIH/HSPM lesion involving the incisal surface only, score the labio-incisal (labial) and palato/lingual-incisal (palatal/lingual) surfaces as normal and assign the incisal surface the most severe score.

If the main code is not to be chosen then there is no need to look at the sub-codes that belong to that main code, the examiner can proceed to the next main code.

*Index tooth with extensive coronal breakdown and where the potential cause of breakdown is impossible to determine.

Figure 1.6 EAPD long form.

Reproduced from (Ghanim et al., 2015).

Code	Definition
0	**No visible enamel defect:** Tooth/surface is apparently free of enamel lesions represented by diffuse opacities, hypoplasia, demarcated hypomineralisation and amelogenesis imperfecta.
1	**Enamel defect, non-MIH/HSPM:** Quantitative or qualitative defects that are not comply with the characteristic features mentioned in the MIH/HSPM definitions. These defects include the following;
11	**Diffuse opacities:** These defects can have a linear, patchy or patchy confluent distribution with indistinct borders with the surrounding normal enamel exists. Also includes opacities due to fluorosis.
12	**Hypoplasia:** Defect can present as pit, groove and areas of partial or total enamel missing with rounded smooth borders adjacent to the intact enamel.
13	**Amelogenesis imperfect:** Includes a range of enamel malformations, genomic in origin, and include variations in thickness (hypoplastic malformation), smoothness and hardness (hypocalcified and hypomatured malformation) or a combination of these.
14	**Hypomineralisation defect (not MIH/HSPM):** Includes MIH/HSPM-like demarcated defects diagnosed in primary or permanent teeth other than MIH/HSPM index teeth.
2	**Demarcated opacities:** A demarcated defect involving an alteration in the translucency of the enamel, variable in degree from white/creamy to yellow/brown in colour. The defective enamel is of normal thickness with a smooth surface and a clear defined boundary from adjacent, apparently sound, enamel.
21	**White or creamy opacities:** Demarcated opacity, white or creamy in colour.
22	**Yellow or brown opacities:** Demarcated opacity yellow or brown in colour.
3	**Post-eruptive enamel breakdown (PEB):** Is a defect that indicates loss of initially formed surface enamel subsequent to tooth eruption that it appears clinically as if the enamel has not formed at all. The loss is often associated with a pre-existing demarcated opacity. PEB exists on surfaces traditionally considered at low caries risk (i.e. cuspal ridges and smooth surfaces) and its areas are rough and have uneven margins.
4	**Atypical restorations:** The size and shape of restorations do not conform to the usual picture of plaque related caries. In most cases in posterior teeth there will be restorations extended to the buccal or palatal smooth surfaces. The restorations may have residual affected enamel visible at the margins. In anterior teeth the buccal restoration is not related to trauma. It is often seen in otherwise caries-free mouths.
5	**Atypical caries:** The size and form of the caries lesion do not match the present caries distribution in the patient's mouth. The unusual pattern of caries can be further confirmed as associated to MIH/HSPM if signs of MIH/HSPM are seen in other teeth in the same mouth.
6	**Atypical extraction (Missing due to MIH/HSPM):** Suspect when absence of a FPM or SPM in an otherwise sound dentition and associated with opacities, PEB, atypical restorations or atypical caries in at least one of the FPM or SPM. It is unlikely that PIs will be extracted due to MIH.
7	**Cannot be scored:** Index tooth with extensive coronal breakdown and where the potential cause of breakdown is impossible to determine.

Table 1.11 Codes and definitions of the clinical status criteria.

Codes marked in grey are related to the long form only.

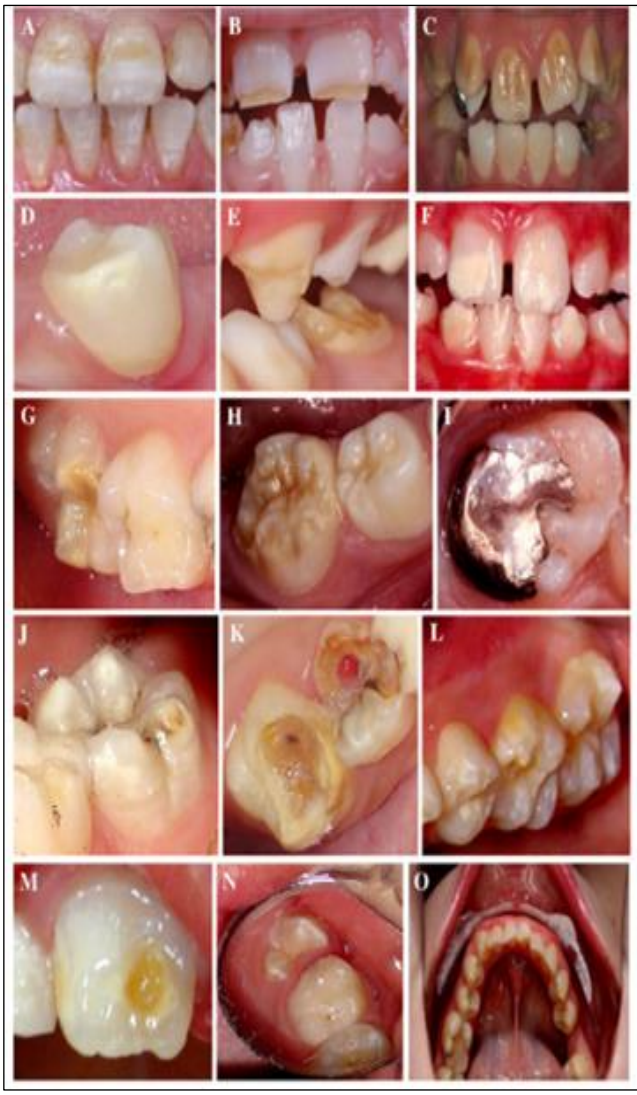

Image description

Image	Tooth No	Surface examined†	Eruption status	Clinical status *(code) **(code)	MIH/HSPM lesion extent††
A	11	Labial		1 11	
B	11	Labial		1 12	
C	11	Labial		1 13	
D & E	34 & 63	Buccal & Labial		1 14	
F	11	Labial		2 21	II
G	26	Occlusal		2 22	I
H	85	Buccal		3††	III
I	16	Occlusal		4††	II
J	36	Buccal		5††	I
K	65	Palatal		7††	
L	16	Buccal		1,2 11,22	I
M	21	labial		1,2 12,21	II
N	14	Palatal	A		
O	36	Buccal		6††	III

*Short form; ** Long form; †Long form only; ††both forms

Figure 1.7 Reference photographs for the short and long forms.

Reproduced from (Ghanim et al., 2015).

1.4.4 The MIH-TNI

The Wurzburg MIH concept, the MIH treatment need index (MIH TNI), was created for the treatment of MIH in 2017. The index includes hypersensitivity and enamel disintegration mainly (Steffen et al., 2017).

The evaluation criteria of the MIH-TNI is used for both primary and permanent teeth. First, a decision must be made as "MIH yes" or "MIH NO" to eliminate other developmental defects. Yes decisions have to be made according to following characteristics:

- Clearly defined opacity on the affected teeth either on the buccal or occlusal surfaces.
- Variation in size, shape, and pattern of the defects.
- Colour deviations are recognizable including white, cream or yellow-brown colour.
- Variation in the size of the defects (defects < 1 mm excluded).
- Hypersensitivity associated with the affected teeth.
- Atypical restoration as shown in figure 1.8.
- Missing of the affected teeth due to MIH reasons.
- Combination of the above characteristics.

A further grading should then be made, if the decision is yes to MIH with any of the above characteristics.

An index values from 1-4 are used for grading which is based on hypersensitivity and disintegration mainly. Table 1.12 demonstrates the index values of MIH-TNI. The MIH-TNI can be applied to individual MIH diagnosis and treatment decisions or for epidemiological studies. Measurements for epidemiological studies can be taken in sextants as shown in figure 1.9. (Steffen et al., 2017).

Figure 1.8 Atypical restoration of MIH affected tooth.

Reproduced from (Steffen et al., 2017).

Index	Definition
Index 0	No MIH, Clinically free of MIH
Index 1	MIH without hypersensitivity, without defect
Index 2	MIH without hypersensitivity, with defect
2a	<1/3 defect extension
2b	>1/3 <2/3 defect extension
2c	>2/3 defect extension or/and defect close to the pulp or extraction or atypical restoration
Index 3	MIH with hypersensitivity, without defect
Index 4	MIH with hypersensitivity, with defect
4a	<1/3 defect extension
4b	>1/3 <2/3 defect extension
4c	>2/3 defect extension or/and defect close to the pulp or extraction or atypical restoration

Table 1.12 The MIH-TNI.

Maxillary right	Maxillary front	Maxillary left
Mandibular right	Mandibular front	Mandibular left

Figure 1.9 The measurements in sextants (Steffen et al., 2017).

From the above-mentioned indices, the EAPD will be used in this study due to multiple advantages. First, the charting method using both forms provide better accuracy of the diagnosis and prognosis of the enamel defects. Also, the subcategories of the MIH lesions and specifying the affected tooth surface area provide information regarding the pattern of MIH defects between individuals. Moreover, measuring the extent of the defect is useful in reflecting the severity of the defect. In addition, distinguishing other defects (non-MIH) and registering them saves time and reduce misdiagnosis. The flexibility in having both short form and long form is another advantage (Ghanim et al., 2015).

1.5 Differential Diagnosis of MIH

It is essential to differentiate demarcated hypomineralisation from other enamel defects to ensure that the best management of MIH is delivered (Ghanim et al., 2015). Patient's medical history is important to obtain the aetiologies of the defects including acquired, environmental, or genetic aetiologies (Mast et al., 2013). Differential diagnosis of MIH include:

- Amelogenesis imperfecta (AI): a hereditary condition in which the structure of tooth enamel is disturbed giving rise to hypoplastic, hypocalcified, or hypomature enamel affecting the clinical appearance of enamel (Nanci, 2014). Severe forms of MIH might be confused with AI. The difference is that all teeth might be affected in AI, whereas the defect is asymmetrical in MIH (Garg et al., 2012, Mast et al., 2013, Ghanim et al., 2015). In addition, a positive family history is an indication of AI (Ghanim et al., 2015).
- Hypoplasia: a reduction in enamel quantity that results from a damage during the secretory phase of amelogenesis (Mast et al., 2013). The PEB that results from MIH can resemble enamel hypoplasia (Mast et al., 2013, Ghanim et al., 2015). However, borders around the healthy enamel in hypoplastic teeth are smooth and regular, whereas in MIH, the edges around the lost enamel are irregular and sharp (Garg et al., 2012, Mast et al., 2013, Ghanim et al., 2015). To confirm the visual assessment, a periodontal probe can be used gently across the borders of the defect (Ghanim et al., 2015).
- Dental fluorosis: hypomineralisation due to excessive fluoride during tooth formation (Mast et al., 2013). With fluorosis, the opacities are diffuse and irregular in contrast to the demarcated opacities observed with MIH (Garg et al., 2012, Mast et al., 2013, Ghanim et al., 2015). In addition, the demarcated opacities are caries prone and they occur in isolated teeth, while teeth with diffuse opacities are relatively caries resistant and may affect all teeth bilaterally (Garg et al., 2012, Mast et al., 2013, Ghanim et al., 2015)
- White spot lesions: clinically, they represent the early stages of dental caries. Can be distinguished from demarcated enamel by its opaque, chalky appearance and irregular surface in areas where plaque accumulates (Ghanim et al., 2015).

1.6 Characteristics of MIH-affected enamel

Structural, chemical, and mechanical properties of MIH-affected enamel compared to normal enamel are different (Elhennawy et al., 2017). In several studies, MIH-affected enamel showed less dense prism structure, loosely packed crystals, partial loss of prismatic pattern, less distinct prism borders, wider sheath regions, and more marked inter-prismatic space (Jälevik et al., 2005, Xie et al., 2008, Chan et al., 2010, Fagrell et al., 2010, Crombie et al., 2013, Bozal et al., 2015). Using the SEM to examine the enamel

structure of MIH affected teeth, the enamel rods and the surface ultrastructure were defective (Crombie et al., 2013).

The mineral density is significantly less in MIH-affected enamel compared to normal enamel (Crombie et al., 2013). Moreover, as shown in a study using the X-ray microtomography (XMT) to assess the ultrastructure of enamel, the area of low mineral content varies from affecting the whole thickness in enamel to only affecting the enamel that is closer to the DEJ (Fearne et al., 2004). Mineral content was less, while the protein content was higher in the MIH-affected teeth compared to normal enamel (Fagrell et al., 2010, Bozal et al., 2015). A 15 to 21- fold and 8 -fold more protein content were found in brown and yellow lesions, respectively, compared to normal enamel (Farah et al., 2010). Higher serum albumin, antitrypsin, and serum antithrombin were found in yellow and brown enamel lesions than normal enamel (Farah et al., 2010). The crystal growth is inhibited by the presence of albumin and the proteolytic activity is inhibited by antitrypsin and antithrombin (Farah et al., 2010).

The modulus of elasticity and the hardness of MIH-affected enamel were also significantly less than the normal enamel (Mahoney et al., 2004, Chan et al., 2010, Fagrell et al., 2010, Crombie et al., 2013). Figure 1.10 shows the lower values of hardness of MIH teeth compared to normal and AI teeth (Mohd Noor, 2014). In addition, the affected enamel had higher porosity and carbonate content than sound enamel when examined with polarising light microscopy (PLM) and carbon dioxide release from acidic dissolution (Crombie et al., 2013).

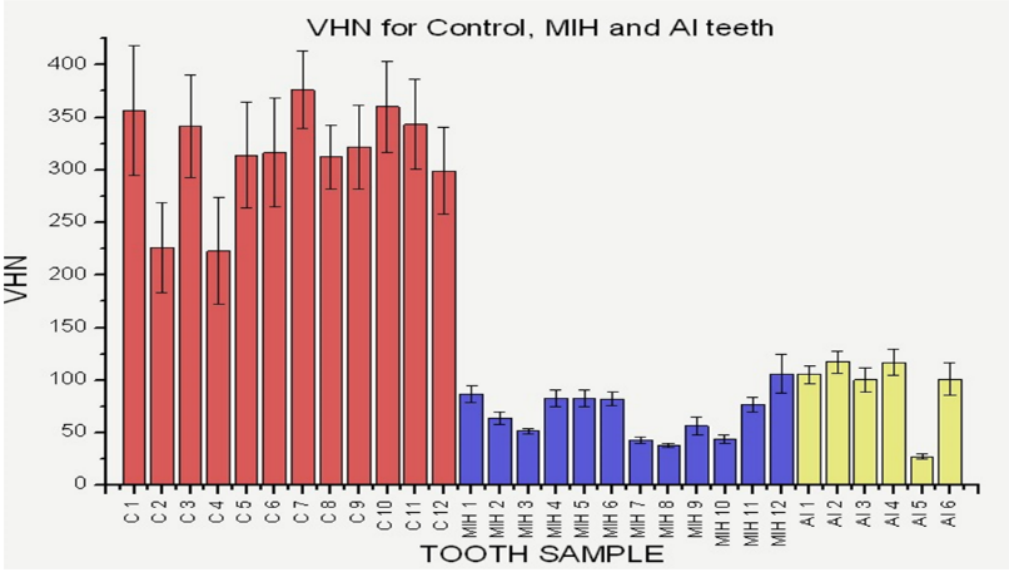

Figure 1.10 Hardness of control, MIH, and AI affected teeth.

Reproduced from (Mohd Noor, 2014).

The surface area, measuring about 25 Mm in thickness, and the cervical area of MIH affected teeth were unaffected and had the properties of normal enamel when examined using the PLM (Crombie et al., 2013).

1.7 Management of MIH

The management of MIH could be by prevention, restoration, or extraction, in the case of poor prognosis FPMs (Lygidakis et al., 2010). Selection of the best treatment option depends on many factors including the patient's age, the severity of the condition, the patient's social background and expectations (Lygidakis et al., 2010, Garg et al., 2012). Other factors that could make the treatment challenging are the sensitivity, difficulty in achieving anaesthesia, rapid development of caries, limited cooperation of the young patients, and repeated failure of restoration by marginal breakdown (Garg et al., 2012). A case control study revealed that patients with MIH had more fear and behaviour management problems compared to the controls due to the repeated experiences of pain and discomfort (Jälevik and Klingberg, 2002).

A fluoridated toothpaste with a minimum of 1000 ppm F must be recommended (Willmott et al., 2008). In addition, to enhance remineralization, Casein Phosphopepetide-Amorphus Calcium Phosphate (CPP-ACP) has been recommended as it provides a super saturated amount of calcium and phosphate on the enamel surface (Lygidakis et al., 2010). Although the effectiveness of CPP-ACP has insufficient evidence (Azarpazhooh and Limeback, 2008), one study found that the inclusion of CPP-ACP in sugar-free gum significantly increase the remineralization of enamel (Shen et al., 2001). A professional application of fluoride varnish and the use of 0.4% stannous fluoride gel might help patients with spontaneous hypersensitivity (Lygidakis et al., 2010). For the affected teeth, fissure sealants (FS) can be applied before the enamel breakdown as a protection (Lygidakis et al., 2010). The retention rate of the applied FS can be increased using the 5th generation bonding adhesive (Lygidakis et al., 2009). A summary of 6 steps clinical management of MIH affected molars is shown in table 1.13 (William et al., 2006).

Steps	Recommended procedures
Risk identification	Assess medical history for putative etiological factors
Early diagnosis	Examine at-risk molars on radiographs if available Monitor these teeth during eruption
Remineralization and desensitization	Apply localized topical fluoride
Prevention of dental caries and PEB	Institute thorough oral hygiene home care program Reduce cariogenicity and erosivity of diet Place pit and fissure sealants
Restorations or extractions	Place intracoronal (resin composite) bonded with a self-etching primer adhesive or extracoronal restorations (stainless steel crowns) Consider orthodontic outcomes post-extraction
Maintenance	Monitor margins of restorations for PEB Consider full coronal coverage restorations in the long term

Table 1.13 A clinical management approach for FPMs affected by MIH (William et al., 2006).

Patients who present with or without MIH may have other dental problems as well. Tooth wear is one factor that, if present, might increase the severity of PEB and sensitivity in patients with MIH. This might occur through brushing or having acidic beverages, which leads to abrasion or erosion. The following section will discuss tooth wear in more details.

1.8 Tooth wear

The loss of dental hard tissue, known as tooth wear, includes abrasion, erosion, attrition, and abfraction (Karan et al., 2009), with each of these lesions having different characteristics and aetiologies (Levrini et al., 2014). A more generic name of dental wear lesions, non-carious cervical lesions (NCCLs), has been favoured over abrasion, erosion, attrition, and abrasion due to the difficulty in identifying each type (Levrini et al., 2014). Moreover, tooth surface loss (TSL) is another term that describes tooth wear (Kelleher and Bishop, 1999).

Abrasion is the loss of dental hard tissues through a mechanical process of interaction between teeth and other materials (Shellis and Addy, 2014). Attrition also involves a mechanical process, but the dental hard

tissue loss is through tooth to tooth contact (Shellis and Addy, 2014). The main result of both attrition and abrasion is occlusal wear (Kaidonis, 2008). The demineralisation of hard tissue by acidic substances is the process of erosion. This demineralisation may lead to tissue loss if combined with mechanical wear, abrasion and attrition (Shellis and Addy, 2014). An abnormal occlusal loading predisposes cervical enamel to mechanical and chemical wear and this process known as abfraction (Grippo, 1991).

1.8.1 Erosion

Erosion is multifactorial, the susceptibility is variable from one individual to another (Litonjua et al., 2003). When the PH of saliva decreases below 5.5 due to an acidic exposure that is intermittent and lengthy, this may lead to erosion (Meurman and Ten Gate, 1996). In early stages of erosion, enamel is smooth and glazed with lack in developmental ridges (Litonjua et al., 2003). Concavities and cupping appear at advanced stages of erosion (Litonjua et al., 2003). Figure 1.11 shows an example of erosion of affecting posterior teeth.

Figure 1.11 Example of erosion on posterior teeth.

Reproduced from dentodontics.files.wordpress.com.

Aetiological classification of erosion is divided into three categories: extrinsic (exogenous), intrinsic (endogenous), or idiopathic (unknown) (Imfeld, 1996). Environmental, diet, medication, and lifestyle are further subdivisions to extrinsic factors (Zero, 1996).

1.8.1.1 Environmental

Environmental erosion related to people who are exposed to acids in their work place or during leisure activities, although this risk is most likely reduced due to health and safety laws (Kelleher and Bishop, 1999). The labial surfaces of maxillary or mandibular incisors are mainly affected by this process (Bishop et al., 1997). Examples of industrial environments are battery factory workers as they are exposed to

hydrochloric acid, workers in cleaning and etching processes, laboratory workers, munitions manufacturing, and commercial printing (Litonjua et al., 2003).

1.8.1.2 Diet

There is a strong evidence that links the dental erosion to acidic food and beverages (Zero, 1996). The PH, acidity, and phosphate and fluoride contents of food and beverages are significantly associated with their erosive potential (Lussi et al., 1993). Carbonated soft drinks, sports drinks, diet drinks, acidic and citrus fruits and their juices, and vinegar conserves are some of the erosive food and beverages (Grobler et al., 1989, Johansson et al., 1996, Zero, 1996). Saliva has an important role in protecting against mineral loss by erosion and this depends on the quantity of saliva, chemical composition of saliva, and the effect fluoride content (Hall et al., 1999).

1.8.1.3 Medications

As some medications and over-the-counter dental products have low PH, their marked effect on dental erosion appear upon frequent or/and sustained contact with the dentition (Zero, 1996). Aspirin, vitamin C ,and oral hygiene products with calcium chelators are examples of some erosive medications (Zero, 1996).

1.8.1.4 Lifestyle

Lifestyle and behaviour factors modify the quantity and frequency of how acidic foods and beverages are ingested (Zero, 1996). Obsession for a healthier lifestyle and dieting may contribute to ingestion of more fruits and diet drinks (Litonjua et al., 2003). In addition, bleaching agents and toothbrushing immediately after an acidic attack may raise the risk of dental erosion (Zero, 1996).

1.8.1.5 Intrinsic

Gastric acid that reaches the oral cavity frequently and consistently is the main intrinsic factor in dental erosion (Litonjua et al., 2003). The source of this acid could be from chronic vomiting, persistent gastroesophageal reflux disease (GERD), rumination, or regurgitation (Milosevic et al., 1997). In most cases, bulimic eating disorder is the underlying cause of vomiting that leads to dental erosion (Milosevic et al., 1997).

1.8.2 Attrition

Attrition is an age-related process that in addition to the occlusal surfaces, it can sometimes occur on the proximal surfaces (Litonjua et al., 2003). Parafunctional habits ,such as bruxism and clenching, may lead to attrition (Bishop et al., 1997, Bartlett et al., 1999). Attrition is considered a physiologic process, if not contributing to excessive destruction of tooth structure (Litonjua et al., 2003).

1.8.3 Abrasion

The major abrasive factor contributing to abrasion is toothpaste (Bartlett and Smith, 2000). Clinically, there was no effect on enamel and a small effect on dentine when brushing performed without toothpaste (Absi

et al., 1992). However, the texture, density, and arrangement of the filaments of the toothbrush can modulate the abrasivity of the toothpaste (Dyer et al., 2000, Wiegand et al., 2009). In addition, the duration, frequency, and force of brushing affect the toothbrushing wear (Addy and Hunter, 2003). Also, the sites, teeth and sides that receive most attention during brushing are at most risk for wear (Shellis and Addy, 2014). Regarding the filament stiffness of different brushes and their effect on abrasion using standard toothpaste, evidence show that the differences are clinically insignificant (Dyer et al., 2000). Figure 1.12 is an example of abrasion provoked by tooth brushing (Lopez Frias et al., 2012).

Figure 1.12 Abrasion provoked by tooth brushing.

Reproduced from (Lopez Frias et al., 2012)

Comparing between abrasion in primary teeth to permanent teeth, there seems to be no difference as studies showed (Attin et al., 2007, Wegehaupt et al., 2008). Abrasion could be caused by other factors like pipe smoking, nail biting, nut and seed cracking, and hairpin biting. These factors will lead to notching of incisal edges (Litonjua et al., 2003).

1.8.4 Epidemiology of tooth wear

The Children's Dental Health Survey 2013 has published a report regarding the amount of TSL among UK children. In Wales, 51% of 5-year-olds had no TSL into enamel or dentine, when the upper primary incisors were examined. This percentage drops to 42% in England and 32% in Northern Ireland indicating more children having TSL. The TSL of the primary incisors among the 5-year-olds was higher on the lingual surfaces than the buccal surfaces accounting for 67%, 57%, and 47% in Northern Ireland, England, and Wales respectively.

In the permanent dentition, the upper incisors, upper and lower permanent molars were examined for TSL. In Northern Ireland, three fifths (59%) of children had no TSL into enamel and most children (97%) had no TSL into dentine. Compared to Northern Ireland, in England, 55% of children had no TSL into enamel

and 96% had no TSL into dentine. Children in Wales had less TSL compared to Northern Ireland and England, with two thirds of children (67%) having no TSL into enamel and 97% no TSL into dentine.

A systematic review has shown that prevalence of wear into dentine ranged from 0 to 82% in primary dentition of children up to age 6.5 years and 0 to 54% in permanent dentition of children aged 7 years and older (Kreulen et al., 2010). The study also concluded that tooth wear into dentine increases with age in primary dentition, whereas no definitive relation in the permanent dentition could be drawn (Kreulen et al., 2010).

Oral health is maintained by toothbrushing and using toothpaste to deliver fluoride that protects the teeth against caries and erosion (Magalhaes et al., 2014). However, a side effect of toothbrushing is the abrasive wear of both the sound and eroded enamel (Addy and Hunter, 2003). The following section will discuss different types of toothpastes' ingredients and how they affect TSL.

1.8.5 Toothpastes and abrasion

Studies showed that increasing the abrasivity of the toothpaste, increases the abrasion of demineralised and sound dentine (Wiegand et al., 2006, Wiegand et al., 2009). To avoid the abrasive wear in patients with severe erosion, it is advisable to brush before an erosive attack to protect the softened tissue (Wiegand et al., 2008).

Fluoride is one of the most active ingredients in the toothpastes (Magalhaes et al., 2014). Triclosan is an antiplaque and antimicrobial agent that is compatible with other toothpaste components such as fluoride (Davies et al., 2010). Moreover, a toothpaste that contains triclosan and copolymer is effective in decreasing calculus (Volpe et al., 1996, Panagakos et al., 2005). Sodium lauryl sulphate (SLS) is a detergent agent that solubilizes triclosan and flavours (Davies, 2004). Toothpastes also contain silica as an abrasive agent (Davies, 2004). Silica varies in particle size and usually combined with different fluoride salts (Davies, 2004). The abrasive agents are the main ingredients in whitening toothpastes that reduce stain, in addition to other chemical agents (Davies et al., 2010). The consistency and stability of the toothpaste are controlled by the gelling or binding agents such as carboxymethyl cellulose and hydroxyethyl cellulose (Davies, 2004).

Other toothpastes are used to treat sensitivity either by inhibiting the transmission of neural impulses or by blocking the dentinal tubules (Davies et al., 2010). Example of components that block the neural transmission are 5% potassium nitrate, 5.5% potassium citrate, and 3.75% potassium chloride (Davies et al., 2010). All these forms of potassium are effective in reducing sensitivity within a period of two to four weeks of twice daily (Tarbet et al., 1980, Salvato et al., 1992, Nagata et al., 1994, Schiff et al., 1998, Hu et al., 2004). In addition, Strontium chloride and stannous fluoride reduce sensitivity by occluding dentinal

tubules and are effective after four weeks of twice daily use (Blong et al., 1985, Thrash et al., 1994, Schiff et al., 2005). Bioglass also occludes the dentinal tubules, thus reducing hypersensitivity (Curtis et al., 2010, Mitchell et al., 2011).

Some of the ingredients in the toothpaste will be discussed in more details below.

1.8.5.1 Fluoride

It has been concluded that fluoride in toothpaste is effective in reducing caries (Marinho et al., 2003, Twetman et al., 2003). It protects and repairs enamel by reducing the acid solubility of both enamel and dentine (Shannon and Trodahl, 1977). Fluoride levels in saliva are highest during brushing and are deposited on the surface of the tooth as CaF_2 –like material. This deposit inhibits demineralisation as it is released as free fluoride at low pH (Li et al., 2014).

There are different compounds of fluoride that have been used in toothpastes, such as sodium fluoride (NaF), sodium monofluoride phosphate (MFP), amine fluoride (AmF), and stannous fluoride (SnF_2) (Magalhaes et al., 2014). Comparing NaF toothpaste to SnF_2-containing toothpaste, evidence suggest that SnF_2 is better in preventing erosive and abrasive wear (Faller et al., 2011, Ganss et al., 2011, Cassimiro-Silva et al., 2016). Typical concentrations of fluoride in toothpastes vary between 450 and 1450 ppm F (Magalhaes et al., 2014). Studies showed that high concentrations of fluoride applications help in preventing erosion and increase abrasion resistance (Tezel et al., 2002, Wiegand and Attin, 2003, Ganss et al., 2004). In addition, toothpastes with 2200 ppm F and 2800 ppm F have higher efficacy to prevent caries initiation and progression than the 1100 ppm F toothpastes (Biesbrock et al., 2001).

Casein phosphopeptide-amorphous calcium phosphate (CPP-ACP) has also been used in toothpastes to enhance remineralization of enamel and to reduce erosive wear (Soares et al., 2017). It helps in delivering calcium and phosphate to the tooth surface by acting like a carrier (Rees et al., 2007). One study showed that using CPP-ACP as a mousse significantly reduces erosion and abrasion tooth wear by remineralising tooth surfaces (Ranjitkar et al., 2009).

1.8.5.2 Bioglass

Bioglass belongs to a group called bioactive materials, which are defined as materials that bind to host bone tissue to stimulate a beneficial response including formation of a calcium phosphate layer (Jones, 2013). The trade name for bioactive glass used in oral health care is Novamin® (Burwell et al., 2009). The bioglass composition includes calcium, sodium, phosphate, and silicate. They deposit calcium phosphate on the surface, when are reactive, by being exposed to body fluids (Andersson and Kangasniemi, 1991).

In Vitro studies found that bioglass, using SEM imaging, transforms into hydroxyapatite-like material occluding the dentinal tubules and reducing dentinal hypersensitivity (Gillam et al., 2002, Earl et al., 2011).

In addition, a clinical trial showed that toothpaste containing 5% calcium sodium phosphosilicate had a significant reduction in dentinal hypersensitivity compared to 5% potassium nitrate at 2 weeks and 6 weeks (Pradeep and Sharma, 2010).

The formation of an Hdroxycarbonate apatite HCA layer by Novamin® is not only useful for treatment of dentinal hypersensitivity, but also useful in treating demineralised tooth structure (Burwell et al., 2009). In a study, bioglass combined with a 5000 ppm F toothpaste showed significantly greater remineralisation than a 5000 ppm F alone on white-spot lesions after 10 days (Burwell et al., 2009). Novamin® also protects dentin from the repeated acidic and mechanical challenges by creating a tenacious surface layer, which was not provided by the use of CPP-ACP as shown in a vitro study (Burwell et al., 2009). Moreover, in 28 days of in situ application, Novamin-containing toothpaste treated enamel surface abrasions by the deposition of the material onto the defected areas (Burwell et al., 2009). Oral formulations containing 7.5% Novamin, 5% potassium nitrate, and 0.4% stannous fluoride has been compared in one study. After 2 and 4 weeks of duration, the Novamin provided more significant improvements in reducing sensitivity compared to other formulations (Sharma et al., 2010).

1.8.6 Measurement of tooth wear

The measurements of tooth wear are divided into quantitative and qualitative methods (Lopez Frias et al., 2012). Clinical descriptions of the wear by intraoral examinations are mainly related to qualitative measurements, in which the wear is graded using different tooth wear indices (Lopez Frias et al., 2012). Examples of these indices include Smith and Knight tooth wear index (TWI), Modified TWI, and Basic Erosive Wear Examination (BEWE).

The TWI measures the tooth wear irrespective of the cause and assigns a score from 0-4, table 1.14 (Smith, 1984). The modified TWI was developed to include cupping of molar cusps as shown in table 1.15 (Bardsley et al., 2004). The BEWE is a validated and standardised index that measures the most affected tooth in each sextant and assigns it a score from 0-3, then the sum of scores is added from the six sextants and classified in a risk level as shown in table 1.16 (Bartlett et al., 2008).

Score	Surface	Criteria
0	B/L/O/I C	No loss of enamel surface characteristics No loss of contour
1	B/L/O/I C	Loss of enamel surface characteristics Minimal loss of contour
2	B/L/O I C	Loss of enamel exposing dentine for less than one third of surface Loss of enamel just exposing dentine Defect less than 1 mm deep
3	B/L/O I C	Loss of enamel exposing dentine for more than one third of surface Loss of enamel and substantial loss of dentine Defect less than 1-2 mm deep
4	B/L/O I C	Complete enamel loss - pulp exposure – secondary dentine exposure Pulp exposure or exposure of secondary dentine Defect more than 2mm deep – pulp exposure – secondary dentine exposure

B: buccal; L: lingual; O: occlusal; I: incisal; C: cervical

Table 1.14 TWI.

Reproduced from (Smith, 1984)

Score	Criteria
0	No wear into dentine
1	Dentine just visible (including cupping) or dentine exposed for less than 1/3 of surface
2	Dentine exposure greater than 1/3 of surface
3	Exposure of pulp or secondary dentine

Table 1.15 Modified TWI.

Reproduced from (Bardsley et al., 2004)

Risk level	Cumulative score of all sextants	Management
None	Less than or equal to 2	Routine maintenance and observation Repeat at 3-year intervals
Low	Between 3 and 8	Oral hygiene and dietary assessment, and advice, routine maintenance, and observation Repeat at 2-year intervals
Medium	Between 9 and 13	Oral hygiene and dietary assessment, and advice, identify the main etiological factor(s) for tissue loss and develop strategies to eliminate respective impacts Consider fluoridation measures or other strategies to increase the resistance of tooth surfaces Ideally, avoid the placement of restorations and monitor erosive wear with study casts, photographs, or silicone impressions Repeat at 6-12-month intervals
High	14 and over	Oral hygiene and dietary assessment, and advice, identify the main etiological factor(s) for tissue loss and develop strategies to eliminate respective impacts Consider fluoridation measures or other strategies to increase the resistance of tooth surfaces Ideally, avoid the placement of restorations and monitor erosive wear with study casts, photographs, or silicone impressions Especially in cases of severe progression consider special care that may involve restorations Repeat at 6-12-month intervals

Table 1.16 The BEWE index.

Reproduced from (Bartlett et al., 2008)

Quantitative method is the physical measurement of the height of crown or depth of groove, which is easily performed on a model or in the laboratory (Lopez Frias et al., 2012). One clinical study has used Optical coherence tomography (OCT) for dental erosion quantification (Wilder Smith et al., 2009). The following section will discuss the OCT tool in more details and its applications in dentistry.

1.8.7 Optical coherence tomography

The OCT imaging was first demonstrated in 1991, displaying images of the retina and human coronary artery (Huang et al., 1991). Then, the OCT has been available for several years as an accepted clinical device to be used in the field of ophthalmology for diagnosing retinal diseases (Marschall et al., 2011).

Research groups worldwide are exploring and applying the OCT in the biology and medicine fields (Marschall et al., 2011).

OCT measures echoes of backscattered light of the microstructure of biological tissues to perform a high-resolution cross-sectional image (Huang et al., 1991). OCT uses nonionizing near-infrared light that is safe and considered inexpensive imaging system (Marschall et al., 2011).

1.8.7.1 OCT and other imaging techniques

The OCT has common features with both ultrasound and microscopy (Fujimoto and Drexler, 2008). The ultrasound uses sound instead of light to image deep structures in the body but with a limited resolution (Fujimoto and Drexler, 2008). In contrast, a higher resolution image with a limited depth can be obtained with microscopy and confocal microscopy (Fujimoto and Drexler, 2008). OCT provides an image with an axial resolution that ranges between 1 to 15 µm, which is when compared with ultrasound, 10-100 finer (Fujimoto and Drexler, 2008). Figure 1.13 demonstrates a comparison between different imaging techniques in relation to resolution and penetration.

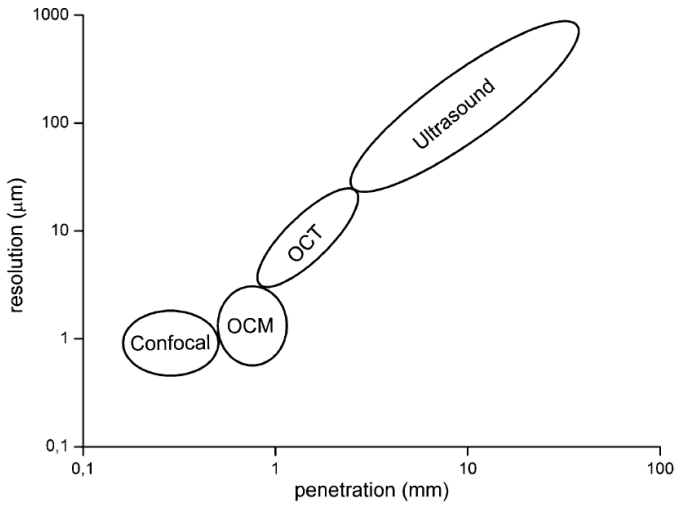

Figure 1.13 Comparing OCT with ultrasound and microscopy.

Image reproduced from (Marschall et al., 2011).

The speed of light is faster than sound and that is the difference between ultrasound and OCT (Fujimoto and Drexler, 2008). The speed of light is approximately 3 X 10^8 m/s, whereas the speed of sound is approximately 1500 m/s (Fujimoto and Drexler, 2008). Due to that, a higher time resolution is required to detect echo of time delays that cannot be detected with direct electronic detection (Fujimoto and Drexler, 2008).

1.8.7.2 Principle of OCT

The OCT is a device that has a software and five components including an imaging apparatus, a partially coherent light source, a measurement head, a data processing module, and an image generator (Machoy et al., 2017). The central element of the device is the imaging apparatus. In addition, the axial resolution and penetration depth are determined by the light source. Also, depending on the field of which the OCT device is used, the measuring head and the probe beam system have different forms and shapes. Moreover, an important part of the OCT imaging is how the values that are obtained from the images are analysed, processed, and presented. This can be accomplished by different techniques, for example, segmentation, image resolution enhancement, noise reduction algorithms, and visualisation correction algorithms (Machoy et al., 2017).

The synchronisation of all the components and the control of scanning of the reference arm of the interferometer are enabled by the computer system of the OCT scanner. In addition, the computer system permits the display of the results by allowing the communication between the apparatus and the imaging processor block (Bouma, 2001, Machoy et al., 2017). Figure 1.14 shows the components of the OCT scanner and how they are connected and processed.

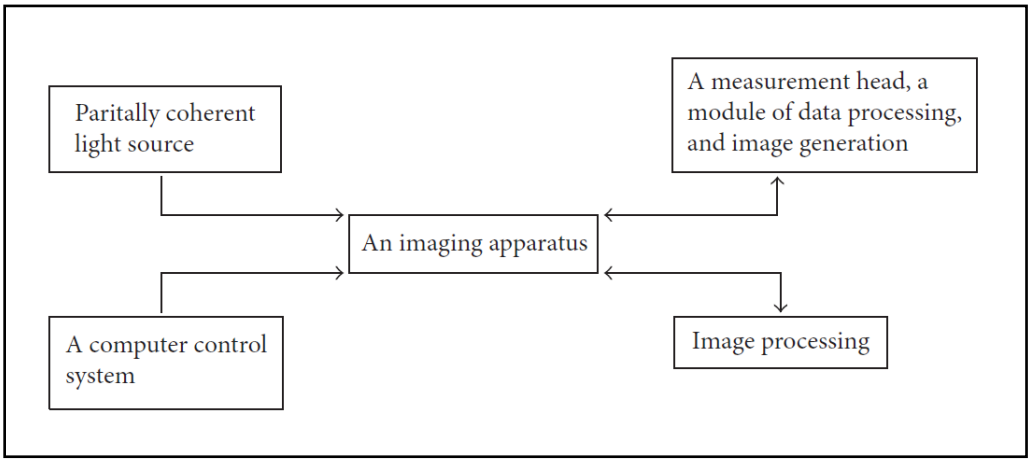

Figure 1.14 The operating principle of the OCT with details of the components.

Reproduced from (Marschall et al., 2011)

OCT detects reflected or backscattered light to measure the depth-resolved reflectivity of scattering material. The OCT system uses a broadband light source to probe the sample with a beam of light, then the reflections of the beam of light will interfere with the reference beam that originates from the same light source. The reflectivity profile can be derived from the resulting interference signal along the beam axis. This will provide with what is known as an A scan, which is a one-dimensional depth scan that is similar

to ultrasound. Then two or three-dimensional images of the sample are created by performing many adjacent A-scans using the OCT system (Marschall et al., 2011).

A-scans are acquired in the time domain (TD), the first OCT system to be implemented by a group of researchers in the United States from Massachusetts Institute of Technology (Huang et al., 1991, Marschall et al., 2011). However, due to the increased time in taking the measurements, the TD-OCT provides images of low quality; and production of three-dimensional images of objects is not allowed (Machoy et al., 2017) In addition to the TD-OCT, the A-scans can be acquired in the frequency domain (FD). Also, it can produce images in three-dimensions in a reduced, by more than a hundred times, capture time (Marschall et al., 2011, Machoy et al., 2017). The TD-OCT system is based on low coherence interferometry (LCI) to perform the depth scan (Marschall et al., 2011). However, the FD-OCT system measures the spectral response of the interferometer with a fixed reference path to acquire A-scans (Fercher et al., 1995).

The FD-OCT has two methods of detection of light source (Machoy et al., 2017). The first method is termed spectral domain (SD-OCT) method, which has a system that can perform the depth scan sampling the interference pattern with a spectrometer and a broadband light source. The other method is known as the swept source OCT (SS-OCT), which uses a tunable narrowed light source and a photodetector (Marschall et al., 2011). Figure 1.15 represents these two methods of the FD-OCT system. The two methods have a fixed reference mirror as a common element between them (Machoy et al., 2017). The SS-OCT has an improved image scan speed of 100,000 per second and a faster scan rate of more than 400,000 scans per second can be reached with the prototype models (Potsaid et al., 2010, Mohler et al., 2015).

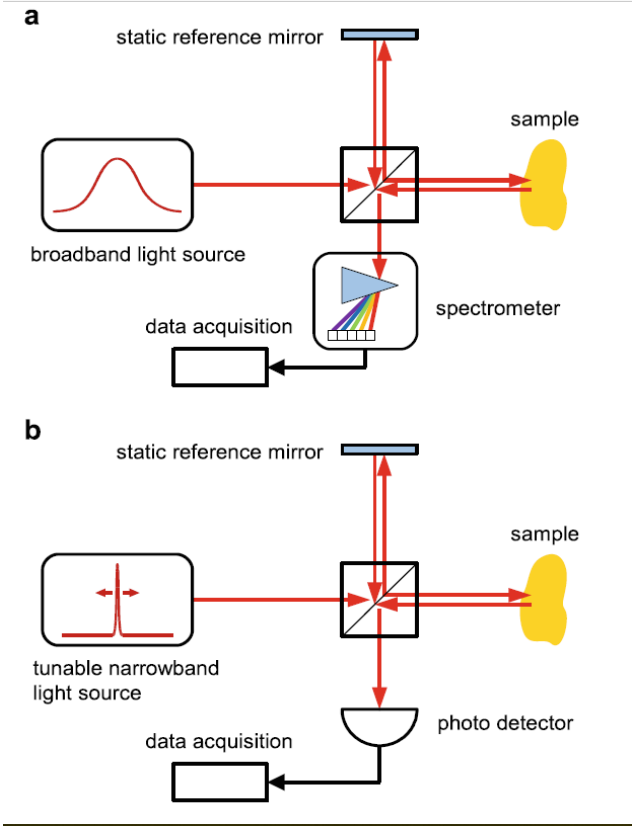

Figure 1.15 The FD-OCT system (a) SD-OCT, (b) SS-OCT.

Reproduced from (Marschall et al., 2011)

The FD-OCT has a significantly higher imaging speed and has been applied in research and medical applications. It requires no mechanical scanning of the reference path length (Marschall et al., 2011). However, it has a limited dynamic range and a complex data processing (Liu and Brezinski, 2007).

1.8.7.3 Applications of OCT

OCT has many applications in Biology and medical fields as well as in technical applications (Marschall et al., 2011). The OCT has been accepted in ophthalmology as a clinical standard to perform direct imaging of the ocular structure (Marschall et al., 2011). A cross-sectional image of the retina, similar in resolution to a histological section in light microscopy, can be obtained with OCT (Marschall et al., 2011). Monitoring and treatment of some retinal diseases has been performed by the use of OCT such as age-related macular degeneration, diabetic retinopathy and glaucoma (Kaiser et al., 2007, Soliman et al., 2008, Tan et al., 2008).

Intravascular OCT has been implemented in visualising and diagnosing atherosclerotic plaques, the most prevalent cause of myocardial infarctions (Low et al., 2006). In addition to its use in cardiological fields, OCT has been used in examining dermatological diseases (Marschall et al., 2011). With the use of OCT in diagnosing non-melanoma skin cancer, the number of invasive skin biopsies can be reduced (Mogensen et

al., 2009). Hollow organs like the bronchi, the gastrointestinal tract, and the urinary bladder can by examined with the OCT as it is endoscopic-compatible (Tearney et al., 1997, Jesser et al., 1999, Wang et al., 2001, Tsuboi et al., 2005).

1.8.7.4 OCT in Dentistry

Most of the clinical studies that have used OCT are undertaken with research based system rather than using equipment systems that can be applied within the dental practice (Clarkson, 2014). The OCT can help to develop remineralisation products and also monitor the mineralisation properties of individuals in future (Clarkson, 2014).

As a result of tooth demineralisation that is associated with caries progression, the optical properties of enamel and dentine change (Shi et al., 2000). These optical properties are important in selecting the optimum wavelength for OCT in dentistry (Clarkson, 2014). The scattering characteristics rather than the absorption characteristics of both enamel and dentine dominate the transmission characteristics (Clarkson, 2014). The scattering coefficient for enamel is inversely proportional to the cube of the wavelength, while dentine shows insignificant wavelength dependence (Clarkson, 2014). The refractive index of enamel is 1.63 and for dentine is 1.45 (Vaarkamp et al., 1995). Darling et al. measured the optical characteristics of several samples of natural and artificially demineralised dental enamel. These were then compared with values of mineral density obtained from a high resolution digital micro radiology system. The results indicated an increase in the optical scattering coefficient that is significantly related to the increase in mineral loss (Darling et al., 2006).

The SS-OCT has been used to detect caries in one of the studies. In this study, excised teeth were compared using visual inspection without magnification, confocal laser scanning microscope, and SS-OCT. With the microscopy used as a reference, results showed that the SS-OCT is superior to visual inspection without magnification (Shimada et al., 2010). Chen et al. conducted a study that used a fibre OCT probe for three-dimensional dental imaging. The probe was interfaced with SS-OCT in which the teeth samples were scanned form occlusal, mesial, distal, buccal, and lingual surfaces. The study concluded that OCT imaging, compared to gold standard dental radiography (x-ray), offers better contrast and resolution and that the lesion area showed stronger back scattered signal intensity. Moreover, the study found that the OCT is particularly suited for detecting occlusal caries as it can provide the 3D topology of occlusal surfaces and the DEJ surface can be also visualised (Chen et al., 2011). In addition, an ex vivo study has combined the OCT with deep learning conventional neural network (CNN) to detect and analyse caries and concluded that this combination can be very useful in caries diagnosis (Salehi et al., 2019).

The MIH lesions have been also investigated using the OCT. One study used the OCT to compare different types of MIH lesions with sound teeth and found that more details of the ultrastructure of enamel and extent

of MIH defects obtained using OCT than clinical examination and radiographs (Al-Azri et al., 2016). In addition, an in vitro study concluded that the OCT is a safe tool in investigating MIH lesions in terms of depth and extent and providing a three dimensional images (Alsabah, 2018). Another study utilized the OCT to measure the enamel loss of MIH affected teeth compared to sound teeth after erosion and abrasion. The study found that MIH teeth with brown discolouration showed more evidence of enamel loss than the sound teeth (Alqahtani, 2017).

Other lesions and pathologies have also been investigated using OCT. One study measured early stages of demineralisation using phosphoric acid for 2 minutes; and compared the OCT results with SEM (Tsai et al., 2019). In addition, tooth cracks can be identified using the SS-OCT with different positions and types of cracks including split lines, craze lines, and structural ones (Kim et al., 2017). Tooth cracks on the OCT are shown as bright line and patterns of vertical, horizontal, or complicated can be identified (Segarra et al., 2017).

1.8.7.5 Examples of application methods of OCT

Different ways have been reported in the literature on how to implement the use of OCT and the type of the OCT machine for quality or quantity measurements.

A study compared polarisation sensitive OCT (PS-OCT) with microcomputed tomography and histology to measure the thickness of enamel using human enamel samples. In their study, the PS-OCT, which is a functional development of OCT, has been selected due to its properties in examining polarisation properties of tissues including optical rotation, birefringence, and depolarisation (Algarni et al., 2016). Moreover, the microcomputed tomography can be used as a gold standard in comparison studies as it has a good accuracy and provide high resolution for enamel thickness measurements (Swain and Xue, 2009). In addition, the microcomputed tomography creates tomographic images comparable to OCT and provides 2 dimensional images to be displayed on any plane from a 3 dimensional images (Alghilan et al., 2019). The enamel thickness studied by creating different enamel thicknesses on the enamel samples without demineralisation (Algarni et al., 2016). It has been concluded that the PS-OCT is comparable to microcomputed tomography and histology in measuring enamel thickness and that the DEJ on the b-scans can be outlined clearly (Algarni et al., 2016). Another study found similar results of good correlation between PS-OCT and microcomputed tomography when compared together for the measurement of remaining dentine thickness above the pulp chamber after caries excavation (Majkut et al., 2015). However, the accuracy of the PS-OCT and its light penetration might be affected by the interference of acquired pellicle, dental plaque, and the diverse anatomical structures including pits and fissures, cusps, and occlusal surfaces (Algarni et al., 2016).

The gold standard microcomputed tomography has also been compared with cross-polarisation OCT (CP-OCT) to measure tooth wear (Alghilan et al., 2019). In their study, human dental enamel was subjected to 5 wear stages and in each stage, the samples' thickness measurements were observed by a micrometre. They concluded that CP-OCT is comparable to microcomputed tomography with a strong correlation between the two methods (Alghilan et al., 2019). In addition, the CP-OCT showed that the small changes in wear depth between wear stages can be detected. However, changes that are less than 0.1 mm are difficult to be quantified by the OCT (Alghilan et al., 2019).

One study measured the depth of white spot lesions and the surface layer thickness of enamel using the SS-OCT and compared it with microcomputed tomography (Espigares et al., 2015). The SS-OCT had a good results by matching the high scattered zones of the demineralised area of the lesion with the microcomputed tomography (Espigares et al., 2015). The SS-OCT identifies the enamel lesion appearance because the demineralised area has a higher backscatter intensity and the more the demineralisation, the more the backscattered intensity (Natsume et al., 2011, Nakagawa et al., 2013). In addition, the dissolution of mineral from demineralisation creates numerous micro interfaces in the enamel structure that results in a higher backscattered signal (Natsume et al., 2011, Nakagawa et al., 2013).

The microcomputed tomography has advantages in quantifying the mineral densities of bone and teeth and different methods have been developed for that (Espigares et al., 2015). Moreover, the enamel and dentine carious lesions, mineral densities of enamel and dentine, and demineralisation and remineralisation can be quantified by microcomputed tomography (Clementino-Luedemann and Kunzelmann, 2006). Although the microcomputed tomography has a high resolution, its application clinically is difficult due to its setup nature (Espigares et al., 2015). If the cone beam computed tomography, which is available clinically, is used instead of microcomputed tomography, its resolution will not allow the detection of early demineralised lesions (Haiter-Neto et al., 2008). In addition, the cone beam computed tomography has a high radiation dose (35 to 652 µSv) compared to a single intraoral x-ray (1 to 8 µSv) and a panoramic radiograph (4 to 30 µSv); which makes it not the safest option for studying enamel and dentine lesions (Roberts et al., 2009, Zhang et al., 2011, Espigares et al., 2015).

The SS-OCT has been investigated in an ex vivo study to measure tooth wear (attrition and abfraction) using mandibular incisors and premolars samples (Marcauteanu et al., 2013). The lesions were created on the samples according to the TWI to mimic a clinical situation of tooth wear; and b scans were taken after every level of tooth wear to construct a 3-dimensional image. The volume difference between the baseline b scan image and the artificially created defect image was measured. The SS-OCT proved to be a good tool in measuring the different level of attrition and abfraction and this can help in monitoring different types of tooth wear, if applied clinically (Marcauteanu et al., 2013).

An in vitro study compared the SS-OCT with quantitative light-induced fluorescence (QLF) in detecting the progression of initial enamel erosion lesions (Chew et al., 2014). Human upper or lower central incisors samples were used; and enamel erosion was artificially created to mimic a level of surface softening without leading to surface loss. This was achieved by placing the samples in orange juice as an erosive medium, which was replaced after each cycle. The total number of cycles were 60 minutes and after each 10 minutes an image was taken using OCT or QLF and the sample is rinsed under running water for 1 minute. By comparing the baseline image with the image from each cycle, the demineralisation was calculated for each sample. For the QLF, significant differences ($P < 0.05$) were detected between the baseline and the 10 minutes image and this was also observed with every 20 minutes of the other cycles. However, the OCT results only showed a significant increase in mean after 50 minutes of erosion. In addition, at the end of the erosion cycles, no more than 10 µm of surface softening was observed from the b scans obtained using the OCT; with no surface loss noted (Chew et al., 2014).

The discoloured area absorbs light more than the lighter areas when light fluorescence is applied (Van der Veen and de Jong, 2000). This is a disadvantage as the demineralised area might look similar to a discoloured area when the QLF is used (Chew et al., 2014). However, The backscattered signal of the OCT is not affected by discolouration compared to QLF (Chew et al., 2014). In addition, a significant correlation between the OCT and QLF was found in quantifying initial erosion, with a higher detection of demineralised area with QLF (Chew et al., 2014).

One study studied enamel loss due to erosion and how different types of toothpastes affected the amount of TSL (Cassimiro-Silva et al., 2016). Bovine teeth were selected in their study and a nail varnish was used as a reference. A total of 7 days of erosion applied to each sample and in each day, a 3 minutes immersion in 0.5% citric acid for 5 times was performed. The samples were then placed in a toothpaste slurry for 2 minutes after the first and last cycle of each day. Different types of toothpastes were selected including toothpastes containing NaF, CPP-ACP/ NaF, and SnF_2. OCT and profilometry were used to calculate the depth of enamel loss. The OCT method that was used in their study is by comparing the difference between the height of the reference point and the eroded surface and the average was calculated and analysed. Figure 1.16 shows the cross-sectional image of OCT with the interface of the varnish and the enamel surface and the difference between them (Cassimiro-Silva et al., 2016). It was concluded that the mineral loss was the least with the toothpaste containing SnF_2 compared to other toothpastes (Cassimiro-Silva et al., 2016).

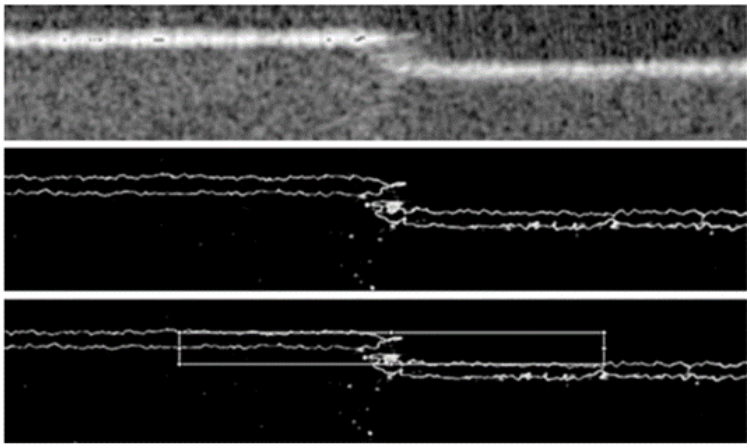

Figure 1.16 The OCT cross sectional image showing the interface of the varnish and enamel surface.

Image reproduced from (Cassimiro-Silva et al., 2016)

The next chapter will discuss the research problem and how the OCT will be used to measure TSL created by brushing with toothpastes.

Chapter 2
Research problem

2 Research problem

Toothbrush abrasion may contribute to further post-eruptive breakdown of molar teeth with MIH. Understanding the effect of toothbrushing on different types of MIH may help to develop better oral care products.

2.1 Aims

To compare tooth wear as result of toothbrushing using different toothpastes in MIH affected molars vs control teeth using OCT.

2.2 Research question

Is there any difference in tooth wear measurements in MIH affected teeth compared to control teeth in an abrasion model?

Chapter 3

Materials and methods

3 Materials and Methods

This in vitro study was planned and conducted in the paediatric department of Eastman Dental Hospital. An ethical approval obtained, with a registration reference number 11/0223, from the National Health Services Research Ethic Committee. Human enamel specimens were used by collecting extracted teeth.

Inclusion criteria included patients who needed extraction of FPM under general anaesthesia (GA) in Eastman Dental Hospital. Exclusion criteria included patients who had the FPM extracted due to caries, as per the diagnosis in notes. The GA list was checked one day before the surgery, diagnosis checked from records, and patients selected. On GA day, a leaflet explaining the research study was handed to the parents (appendix 1), of patients diagnosed with MIH, to read. Then a written consent obtained from the parents who agreed to participate (appendix 2). Both MIH and sound (control) teeth were collected. The control teeth were obtained from the same patients who had MIH, in which the sound FPM were extracted for compensating purposes to prevent their overeruption.

A total number of (25) MIH teeth samples and (12) sound samples of first permanent molars were collected from 34 patients aged between (8-10 years old), prepared and divided into three groups. The first group was with artificial saliva, then the Sensodyne® complete protection group, and finally the Sensodyne® pronamel for kids. Appendix 3 show a list of the three groups with the teeth samples in each group.

All the extracted teeth were stored in labelled pots with an anonymous ID number. In the first 7 days, 95% ethanol was used to store the teeth in. The samples were then cleaned, and any soft tissue attached was removed with a scalpel. Then 0.1% thymol was used to store the teeth in a locked refrigerator at 4C° until needed. Photos and radiographs (periapical radiographs) were taken for each tooth to keep a full record of all the teeth after they were cleaned and before mounting them in resin.

The long form of the EAPD index was used in classifying each tooth. An example of an MIH lesion is shown in figure 3.1.

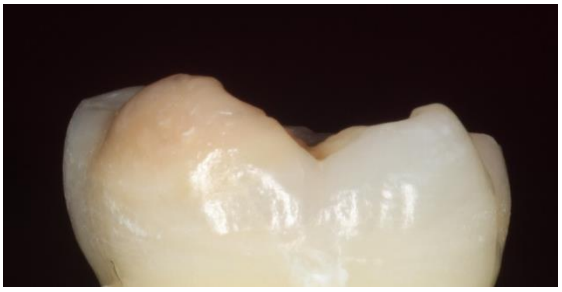

Figure 3.1 Example of MIH affected molar.

The tooth shows an example of yellow demarcated opacity affecting less than 1/3 of tooth surface, using the EAPD classification, this tooth is classified as 22, I. In this study type 11 (white or cream opacities) and type 22 (yellow or brown opacities) were selected to be compared with the control teeth.

3.1 Preparation of tooth sample

The tooth sample was placed into a plastic mounting cup then the cup poured with epoxy resin (Specifix 20 – StruersTM, Denmark), which was mixed according to the manufacturer's instructions. The tooth was left overnight until the resin was fully cured. The resin plate was then removed from the plastic cup. The resin plate was sectioned using a slow speed sectioning machine with a diamond saw, shown in figure 3.2, to slice the tooth horizontally separating the crown from the root.

Figure 3.2 Diamond saw.

The crown was then mounted into a small rectangular mould, 20 X 15 X 5 mm, and poured with epoxy resin (Specifix 20 – StruersTM, Denmark) around it. A small stainless-steel needle was used as reference point on the tooth sample (figure 3.3) and secured using Araldite® adhesive (Huntsman international, India).

Figure 3.3 Prepared tooth sample.

Stainless-steel needle attached using araldite adhesive (Huntsman international, India) to keep the measurements of TSL accurate as the needle will not be affected by the abrasion or erosion. The needle also helped in comparing the OCT images as they can be reproduced easily.

3.2 Toothpastes

Two types of toothpastes were selected and compared with no toothpaste's category. Table 3.1 illustrates the two types of toothpastes and their ingredients.

Toothpastes	Manufacturer	Ingredients
Sensodyne pronamel for children	GlaxoSmithKline	Aqua, Sorbitol, Hydrated Silica, Glycerin, PEG-6, Cocamidopropyl Betaine, Xanthan Gum, Aroma, Sodium Fluoride, Sodium Saccharin, Sucralose, Titanium Dioxide, Sodium Hydroxide, Limonene Contains: Sodium Fluoride 0.315% w/w (1450 ppm fluoride)
Sensodyne complete protection	GlaxoSmithKline	Glycerin, PEG-8, Hydrated Silica 5% Calcium Sodium Phosphosilicate (Novamin), Aroma Sodium Lauryl Sulfate, Sodium Monofluorophosphate, Titanium Dioxide, Carbomer, Sodium Saccharin Eugenol, Limonene Contains: Sodium Monofluorophosphate 1.08% w/w (1450 ppm Fluoride)

Table 3.1 Toothpastes and their ingredients

The first type is Sensodyne pronamel for children toothpaste with 1450 ppm F, has been chosen due to remineralisation effect of fluoride and as marketed in strengthening weakened enamel. The second type of toothpaste was selected based on the active ingredient Novamin®, which helps in reducing sensitivity. The toothpaste slurry with artificial saliva was prepared in a ratio of 3:1.

3.3 Preparation of artifical saliva

A formula that was initially described by (McKnight-Hanes and Whitford, 1992) was used to prepare artificial saliva. One litre of distilled water was mixed with the constituents listed in table 3.2.

Methyly-p-hydroxybezoate	2.3 g
Sodium Carboxymethyle Cellulose	10.00 g
KCl	0.625 g
MgCl2.6H2O	0.059 g
CaCl2.2H2O	0.166 g
K2HPO4.3H2O	1.05 g
KH2PO4	0.326 g

Table 3.2 Artificial saliva constituents

The PH of saliva was then titrated to 6.75 using PH metre and potassium hydroxide (KOH). The saliva was then stored in a glass container and kept in the lab, under room temperature, until needed.

3.4 OCT imaging

3.4.1 OCT scanner

Vivosight OCT scanner was used in this study. It is a multi-beam swept source frequency domain scanner that is manufactured by Michelson diagnostics, Kent, United Kingdom. The laser centre wavelength is 1305 nm with a 1.0 mm depth of focus. The scan area is 6 mm X 6 mm with a depth of between 1.0 mm and 2.0 mm. The scanner presents different images including vertical B-scan, En-face, and 3D. The image formats vary from TIFF, TIFF stack, or DICOM. The scanner's components are Santec HSL -2000-12-MDL light source, monitor for image display, Dell Precision T3600 processing system, Spectrum M2i.4022 4-channel20 MHz 1-bit data acquisition, and a hand-held scanning probe. An adjustable arm was used to mount the scanning probe as shown in figure 3.4.

Figure 3.4 OCT mounted arm.

The probe was fixed and only the vertical distance of the platform was adjusted until the optimum quality of the image is obtained.

3.4.2 Protocol of scanning

The following protocol for imaging the samples using OCT was selected based on a previous study done by (Alqahtani, 2017):

- Before imaging, the excess moisture was wiped off as the moisture affects the image quality.
- The mounting jack, in which the samples are placed on, was adjusted only in vertical dimension to obtain the best image of the sample.
- The laser on the sample surface was perpendicular.
- The surface of the tooth was always visible on the image viewed on the monitor. Figure 3.5 shows an OCT image of one of the samples.

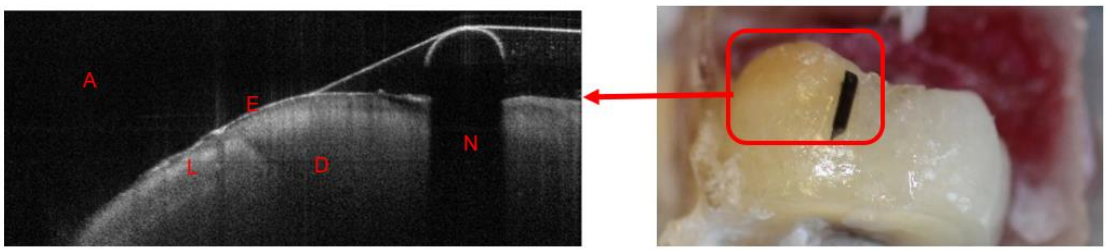

Figure 3.5 An OCT image of a sample tooth

(A: air; E: enamel; D: dentine; L: lesion; N: needle).

The tooth sample was scanned before the experiment to acquire the pre-scan image. Then, the sample was scanned after the 20, 40, 60, 80, and 100 cycles. Each image consisted of 500 slices from a 6mm X 6mm frame. All the frames were exported from the OCT software as a TIFF image.

Once the OCT images are obtained, a software named ImageJ was used to manipulate the image. ImageJ is a java-based image processing program developed at the National institute of health and laboratory (Maryland, USA). The version that was used in this study is 1.52i (2018) with 64-bit Java.

To perform quantitative analysis of the OCT image, the light signal intensity that travels through the depth of enamel was used. The backscattered intensity was plotted against the depth of enamel using the ImageJ by the following process:

- The horizontal intensity profile, the default set, was replaced by the vertical profile.
- Micrometres were used to set the scale instead of pixels.

- The profile was then plotted and transferred to an excel sheet for analysis. Figure 3.6 illustrates an example of a plotted profile.

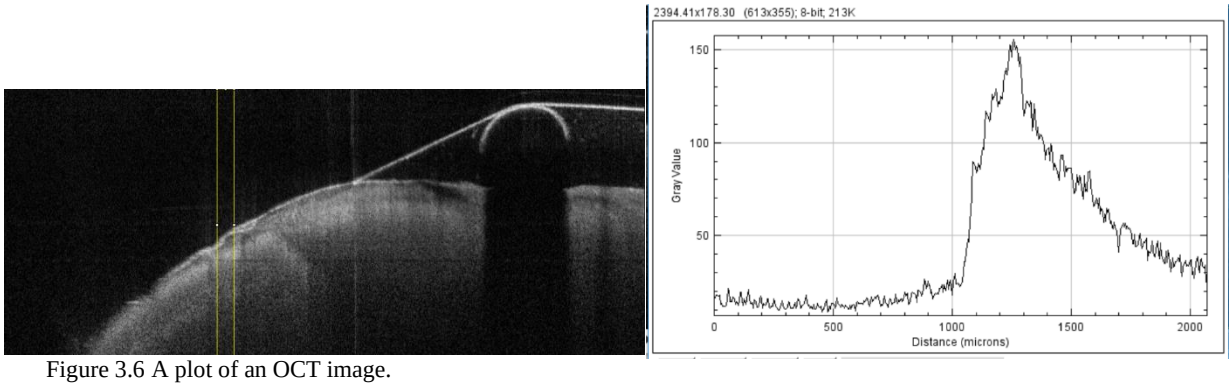

Figure 3.6 A plot of an OCT image.

- Five plots were taken from each image cycle, the highest point was then taken from each A scan point and subtracted from its corresponding point from baseline image to calculate enamel loss.

The next chapter will discuss the development of the protocol and how the three pilots were performed.

Chapter 4
Development of the protocol

4 Development of the protocol

A previous protocol was developed to assess TSL in teeth affected by MIH (Alqahtani, 2017). In her study, MIH affected teeth with white/cream, yellow/brown lesions, and PEB were selected and compared with sound teeth. The study investigated the effect of erosion/abrasion on MIH affected teeth using OCT. The abrasion was performed using a commercial electric toothbrush for 100 cycles. The TSL was calculated after every 20 cycles of brushing. Four toothpastes were used including 1450 ppm F toothpaste, 2800 ppm F toothpaste, 5% Novamin® toothpaste, and 5% potassium nitrate toothpaste. This study concluded that MIH affected teeth had more TSL than control teeth, with the highest tooth wear seen in samples with PEB, however a number of issues were noted:

- The sample size included 14 MIH teeth and sound teeth in total, and it was concluded that a larger sample size was needed.
- A commercial electric toothbrush was used, and the erosion was performed using 0.3% citric acid. It was not clear if the TSL was due to erosion, abrasion or both. Therefore, a decision was made to perform abrasion with and without acid. In addition, it was desirable to standardize the brushing method using a validated brushing machine.
- There was a lack of a reference point (unaffected by abrasion or erosion) to measure TSL on the tooth surface. This reference point was required to reliably compare between the OCT images of each sample.
- The MIH samples selected in the previous protocol included teeth with PEB. In the current protocol, only white/cream and yellow/brown lesions were selected. Samples with PEB were excluded to avoid enamel surface discrepancies, preserve the accuracy of the reference point, and calculate the TSL accurately.

In an effort to further develop the approach designed by Dr Alqahtani, a series of improvements were made to validate and standardise the methods of assessment of tooth surface loss with OCT. In addition, different toothpastes were selected for comparison (as mentioned in section 3.2). Dr Alqahtani selected toothpastes that contain 2800 ppm F, 1450 ppm F, and potassium nitrate containing toothpaste. The two toothpastes selected in this protocol were Sensodyne children pronamel and complete protection toothpastes. The children pronamel was selected as it contains 1450 ppm F and is marketed for children. The complete protection toothpaste was selected as it contains Novamin®, which is said to reduce the sensitivity associated with MIH. Artificial saliva was included as a brushing medium, to compare the TSL using toothpaste vs using saliva alone to assess the potential protective effect of toothpaste in reducing TSL.

Pilot studies were required to reach a final protocol that could be applied in future studies. The pilots assessed different parts of the study design and to standardise the protocol. In the first pilot, the efficacy of

the brushing apparatus using manual toothbrushes was assessed, and the method of calculating TSL from OCT images. The toothbrushing effect was also assessed in the first pilot by performing toothbrushing alone and with erosive challenge. The second pilot followed on from the results of the first pilot, including reverting back to electric toothbrushes to perform abrasion/erosion; and to stabilise the vertical dimension to replicate the OCT images using a jack. The third pilot assessed an accurate method of measuring TSL from the OCT images.

In the next sections of the chapter, the three pilots will be explained in detail.

4.1 Pilot 1

The aim of this pilot was to standardise the brushing technique used to perform abrasion on MIH affected and control teeth. The use of a reference point was also considered in this section. In addition, the effect of abrasion with and without erosion on the enamel surface was investigated.

The brushing apparatus used in this pilot has been validated in multiple studies and is used as a reference model for toothbrushing (Attin et al., 2007, Parry et al., 2008, Wiegand et al., 2013). The benefit of using the brushing apparatus was that it applied a constant and stable movement of the toothbrushes in a specific direction and force. This helped reduce variables between toothbrushes. It also meant that 8 toothbrushes could be used at the same time, increasing the number of samples per experiment.

Manual toothbrushes were selected as most people use manual toothbrushes, due to their low cost. In 2018, The use of manual toothbrushes was estimated to be 31 million vs 23 million people using electric toothbrushes in Great Britain (https://www.statista.com/statistics/303553/toothbrushes-usage-by-type-in-the-uk/, 2019).

4.1.1 Aims

To standardize the brushing technique using the brushing apparatus

4.1.2 Objectives

1. To standardize the brushing method and achieve TSL using brushing apparatus with manual toothbrushes
2. To quantify TSL using OCT

4.1.3 Objective 1

To standardize the brushing method and achieve TSL using brushing apparatus with manual toothbrushes

Methods:

The toothbrushing apparatus used (kindly donated by P&G, Cincinnati, USA), had 8 holders for manual toothbrushes, as shown in figure 4.1. Medium bristled children toothbrushes were used as per the recommendation of Public Health England toolkit for Delivering Better Oral health (https://www.gov.uk/government/publications/delivering-better-oral-health-an-evidence-based-toolkit-for-prevention, 2017). A hole in the handle of the toothbrush was made using a drill (Lomvum Electric Drill Power) in order to stabilize it using a screw (figure 4.1). The movement of the toothbrush was in vertical direction, along the long axis of the brush. The samples were prepared as described in section 3.1 with a reference needle attached using araldite adhesive (Huntsman international, India), mounted on a

rectangular holder, and secured by screw in which the toothbrush bristles were perpendicular to the sample (figure 4.2).

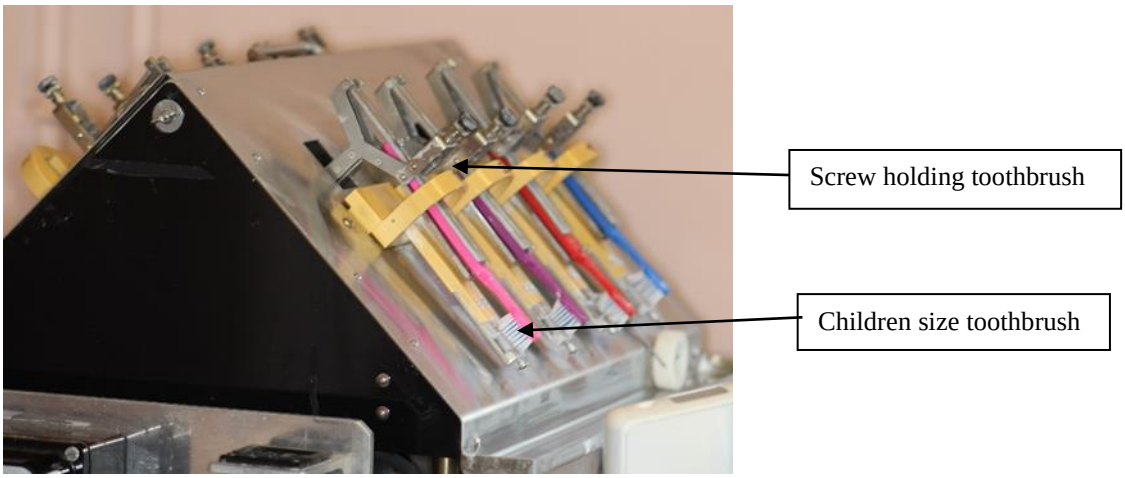

Figure 4.1 Toothbrushing machine.

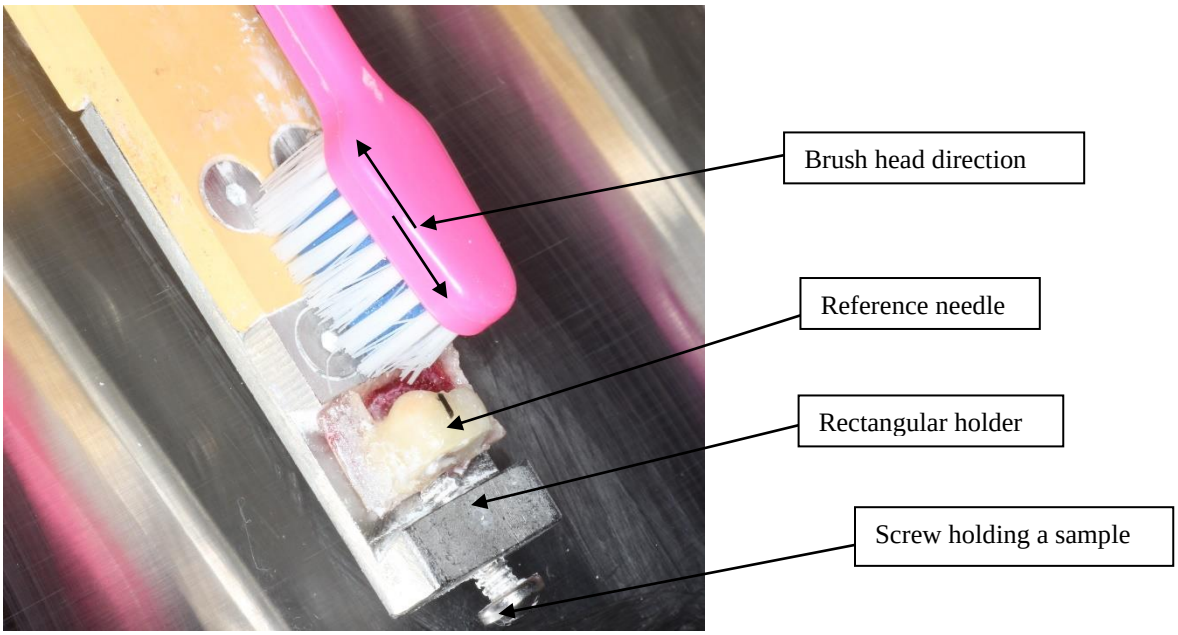

Figure 4.2 A sample placed and secured.

Each toothbrush was designed to work on one sample only, as only one slot was available. The brushing force was 2.5 N (measured with Newton force meter), as the brushing force average varies between 0.2 – 4.5 N with 2.5 N being the most reported clinically (Boyd et al., 1997, McCracken et al., 2001, Wiegand et al., 2007b).

Sensodyne complete protection toothpaste was the first toothpaste selected with 3 samples; a control sample (C13), type 21 (MIH 24) type 22 (MIH 23) teeth. Sensodyne complete protection was selected as it contains

Novamin®, and a toothpaste slurry was prepared as described in section 3.2, A total of one hundred brushing cycles were performed on the three samples using the brushing apparatus, which equals 50 days of two minutes brushing twice per day. The cycles were performed as 20, 40, 60, 80, 100; and an OCT image was taken after every 20 cycles. After each cycle, the brushing apparatus was switched off after every 2 minutes, the sample was washed with distilled water then the apparatus was switched on again. This was repeated every 20 cycles then an OCT image was taken.

For each OCT image, the tooth sample was dismounted from the holder in the toothbrush apparatus and place under the OCT probe. The lack of clearance for the OCT probe prevented recording OCT images whilst the sample remained mounted in the apparatus, as the toothbrush interfered with the OCT probe. If the sample was to be scanned on the brushing apparatus, the toothbrush had to be unscrewed every time the image was taken. Also, even if the toothbrush was unscrewed, scanning the sample on the brushing apparatus resulted in unclear images due to unstable hand movements as the probe needed be held during the scanning. This affected the accuracy of the images and resulted in blurring and distortions.

Results

After the three samples were brushed with the toothpaste slurry, TSL on the OCT images was not detected as seen in the b scans in figure 4.3. The effect of removing the sample from the brushing apparatus, affected the area that was scanned after each cycle, with mismatched OCT images, affecting the accuracy of the TSL. The white arrows (fig 4.3) show the variations between the images and how different areas appeared in the scanned area between the brushing cycles, indicating that the sample had moved.

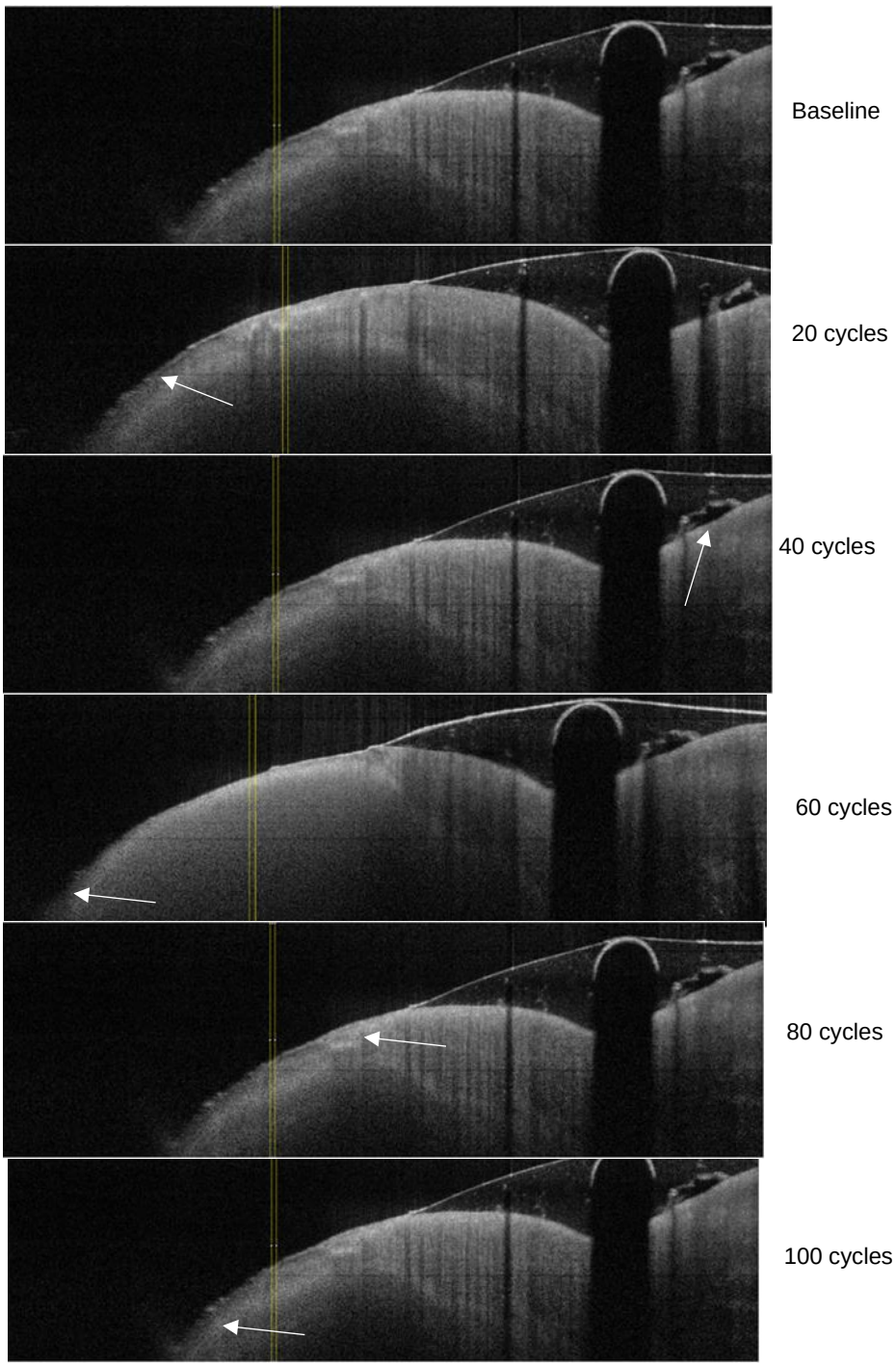

Figure 4.3 OCT images taken before the brushing and after each cycle.

No TSL was noted from baseline to 100 cycle images.

Despite issues highlighted above, the fact that no TSL could be seen on any of the b scans, made it clear that an erosion / abrasion model was required. One sample with type 22 lesion (MIH 25) as shown in figure 4.4, was selected and immersed in 0.3% citric acid for 30 minutes before the brushing cycles performed (Alqahtani, 2017).

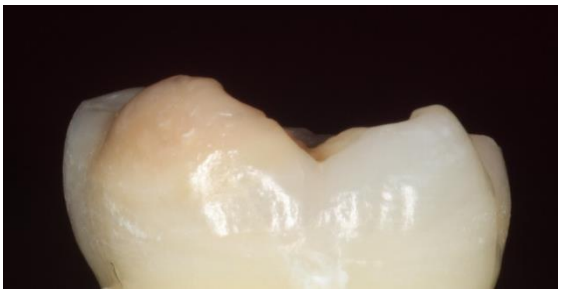

Figure 4.4 Type 22 tooth sample.

Then the sample was brushed with complete protection toothpaste as described above for 20, 40, 60, 80, and 100 cycles.

Results

Despite the use of acid, no TSL could be detected (figure 4.5). TSL always shows as a positive value when the TSL calculated using the method described in section 3.4.2. The figure shows a positive number in microns only in 80 cycles' image, this indicate that TSL only occurred at this cycle. The negative values mean an increase in enamel, which the other cycles showed with a non-linear tooth surface gain. This was an error as no remineralization process was performed and tooth surface gain was not possible in this experiment.

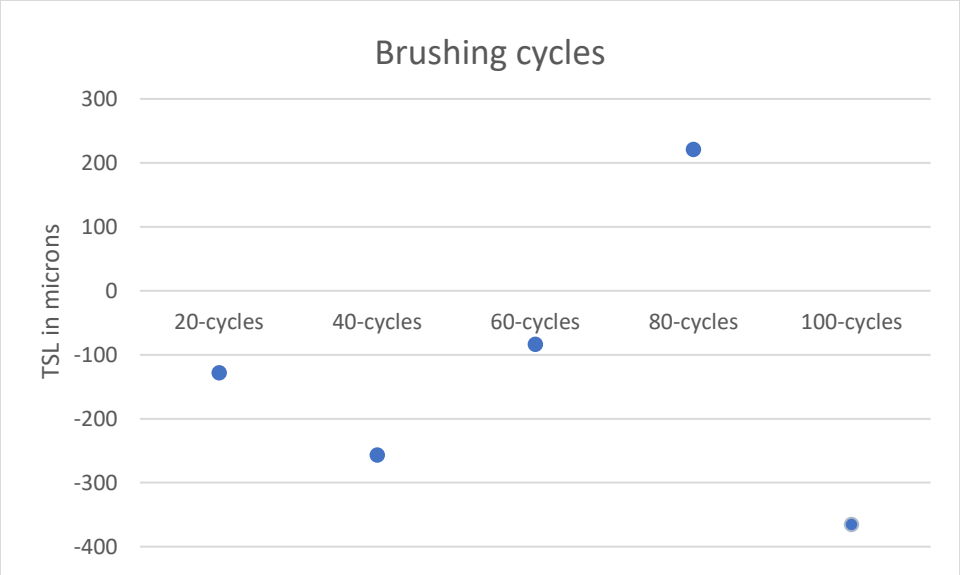

Figure 4.5 TSL of a sample type 22, showing an increase in enamel except in 80 cycles.

The OCT images in figure 4.6 showed variations between the b scans due to rotation of the sample between cycles. The white arrows highlight different features in individual cycle image. For example, the white arrow on the 20-cycle image shows a radiopaque dot on the glue that was not found on the baseline image. At the 40, 60, 80, and 100 cycles, the radiolucent areas were not visible on the baseline image. This indicated changing on the rotation of the sample when placed on the platform for scanning. In addition, the position of the needle was not fixed on all the images, indicating that the position of the sample in relation to the OCT probe was changing between brushing cycles. Red arrow indicates radiopaque area on surface of enamel.

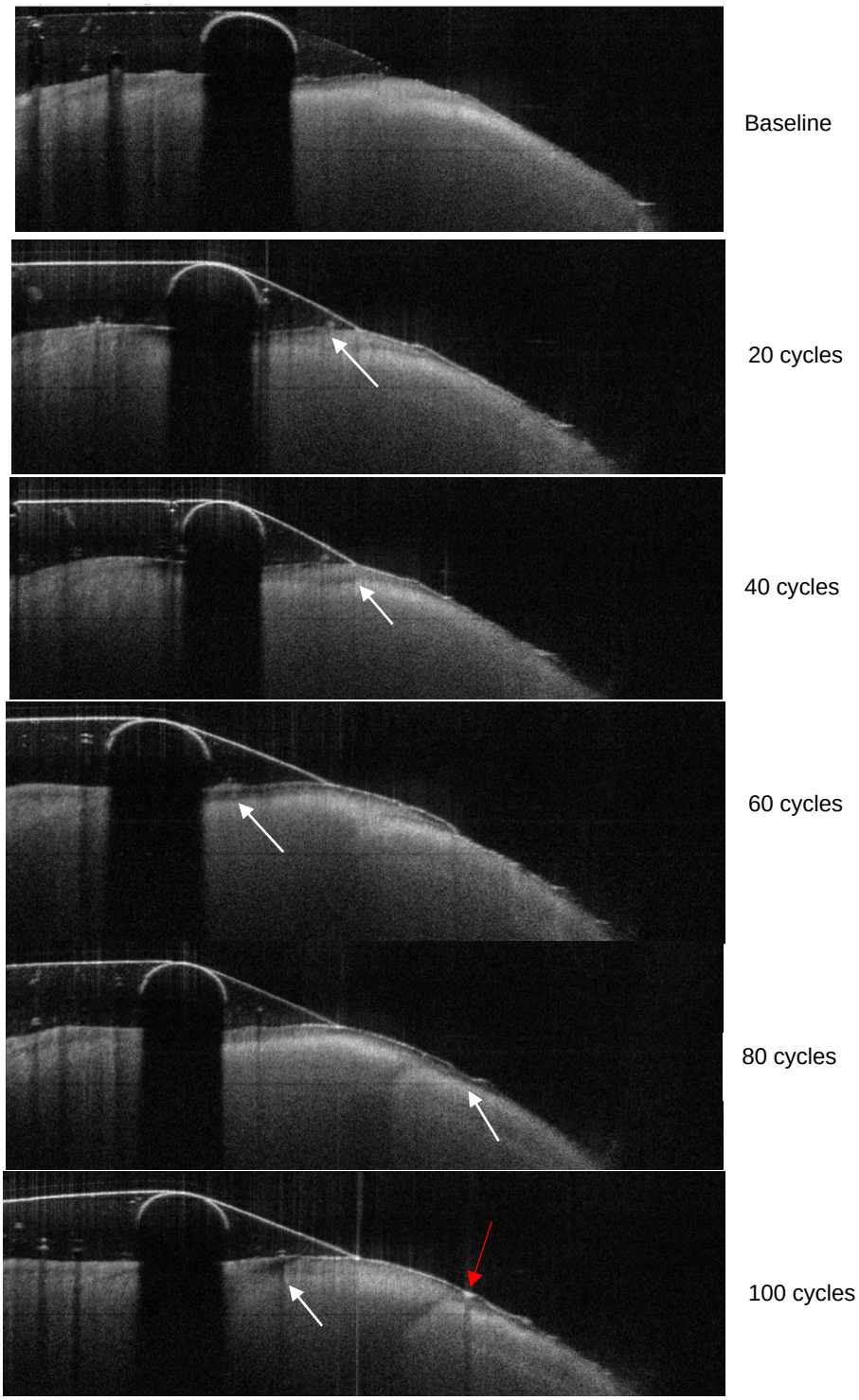

Figure 4.6 OCT images after the erosion/abrasion effect.

Red arrow indicates radiopaque area on surface of enamel

Discussion:

The brushing apparatus was selected as it applies a constant and stable movement of the toothbrushes in a specific direction and force, and is the validated apparatus used in previous brushing experiments (Attin et al., 2007, Parry et al., 2008, Wiegand et al., 2013).

Some difficulties were faced with the brushing apparatus. MIH lesions are never homogeneously present on the tooth surface, i.e. on the occlusal region, buccal or lingual. This means that the samples need to be sectioned and cut to optimise the orientation of the lesion with respect to the brush. This was difficult to achieve as the teeth that were used are molars and the lesions were mostly present around the cusps. Even after carefully sectioning the teeth, it was difficult to create a flat surface that fit in the slot and maintained the toothbrush head in a stable direction. Therefore, the brushing apparatus was not suitable for experiments using MIH affected permanent molar teeth. However, the brushing apparatus may be useful if central incisors are used or bovine teeth in other types of studies. Although central incisors are affected by MIH, they are not subjected to extractions as part of routine treatment.

Another difficulty faced with the brushing apparatus was the need to mount the sample in and out of the holder slot for imaging with OCT. This affected the reproducibility of capturing the same position of the lesion each time the scan taken. Although the OCT probe can be handheld for sample scanning, this affected the accuracy of the scan as the probe was not stable due to hand movements. The toothbrush was dismantled between the cycles as it was in direct contact with the sample and interfered with the OCT probe and the sample when scanning.

When abrasion was performed alone, no TSL was noted. That could be because tooth wear is multifactorial (abrasion, erosion, and attrition) and rarely acts alone and it is usually the interactions of more than one factor that results in TSL (Wiegand and Attin, 2011). This could also be due to the lack of precision in repositioning the tooth sample in and out of the tooth brushing apparatus, exposing slightly different surface of the tooth in contact with the brush every time. Additionally, the efficacy of the brushing combined with erosion to generate sufficient TSL that can be measured from the OCT images was questioned. Citric acid was selected here as it is commonly found in fruit juice drinks (Baker et al., 1998). It is also considered more damaging to the mineral content of enamel as it binds to the calcium stronger thus, eroding the crystals (Featherstone and Lussi, 2006). This is known as chelating action, one of the interactions of citric acid with calcium when it is in the form of anions (Featherstone and Lussi, 2006).

Outcome:

Based upon this pilot, there are significant difficulties in aligning the lesion properly with respect to the brushes and the mounted samples. Also, TSL was difficult to achieve using the brushing apparatus regardless of whether abrasion with/without erosion was applied.

4.1.4 Objective 2

To quantify TSL using OCT

Methods:

The samples were removed from the slot holder and placed on an adjustable jack then the OCT image was taken. TSL was then quantified, using the method described in section 3.4.2.

Results:

When the obtained OCT images were analysed using ImageJ, the results showed an increase in mean difference of the measurements, without TSL, from the baseline OCT image compared with 20, 40, 60, and 100 cycles' image, using complete protection toothpaste. Figures 4.6 and 4.5 show the OCT images of two samples, one brushed with toothpaste and the other one immersed in acid then brushed with the same toothpaste. The images show how the scans from the same sample were not repetitive and there was a parallax issue.

Discussion:

Using OCT to measure the TSL on MIH affected teeth and control teeth showed difficulties, including moving the sample from the rectangular holder to a stable flat surface so that the OCT image could be taken. This movement of the sample after every 20 cycles resulted in changes in the stability of the location of the lesion and made the reproducibility of the OCT images more challenging and difficult.

Outcome:

Based on this objective, quantifying TSL using OCT can be difficult when the samples are not placed in a fixed position.

4.1.5 Overall review of pilot 1

It can be concluded from this pilot that the brushing apparatus was not suitable for assessing TSL using the OCT machine due to the disadvantages described above.

Next Steps: to address the deficiencies described above using the brushing apparatus, another method of brushing will be applied in the next pilot using electric toothbrushes.

4.2 Pilot 2

The toothbrushing apparatus in the previous pilot study was not sufficient for this study on MIH teeth as the mounting and dismounting of the sample, combined with discrete location of the lesion, reduced the efficiency and repeatability of the method.

This second pilot focused on standardising the method of scanning the samples using OCT. As the sample transfer from the brushing machine to the OCT affected the results in the first pilot, the brushing apparatus from Dr Alqatani's study was used. However, controlling and handling the samples were adjusted to achieve more accurate results.

4.2.1 Aims

To improve the stabilisation of the sample for the accuracy of scanning with OCT

4.2.2 Objectives

1. To perform brushing using another brushing apparatus
2. To achieve and quantify TSL using an OCT and a chemistry lab jack for scanning

4.2.3 Objective 1

Methods:

The brushing machine was changed to an electric toothbrush mounted by a chemistry lab stand with 3-prong clamp, the electric toothbrush was the Oral B with trizone 2000 head (Procter & Gamble, USA). It moves in a vibrating motion from side to side mimicking the manual toothbrush. Also, it has a criss-cross bristles with a 3D movement cleaning system that sweeps back and forth. The toothbrush has 1 speed setting that provides 8,800 rotations and 40,000 pulsations per minute (https://www.electricteeth.com/uk/oral-b-cleaning-modes-explained/, 2020).

The following steps were performed:

1. The sample was mounted in a round pot with epoxy resin (Specifix 20 – StruersTM, Denmark) to fit in the plastic container as shown in Figure 4.7 with the MIH lesion facing upwards to ensure maximum contact with the brush.
2. The tooth sample was placed on a digital scale, which was attached to the jack to preserve the tooth in a fixed position (Figure 4.7). The scale was used to fix the brushing load.

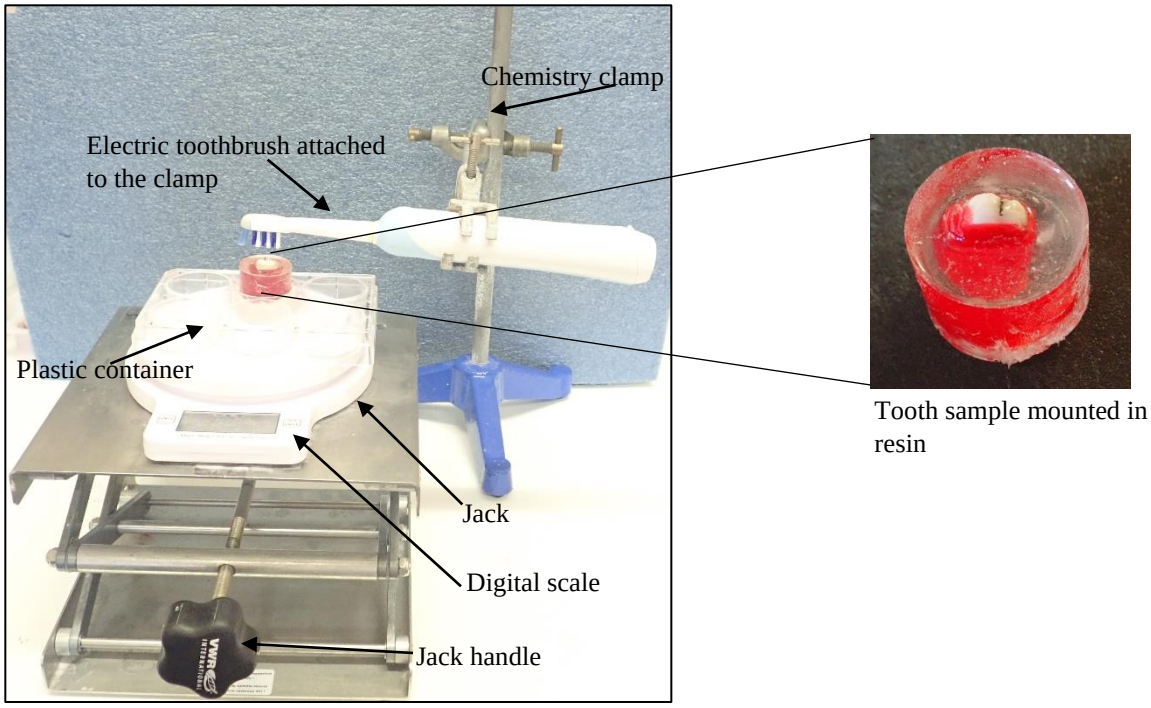

Figure 4.7 The brushing apparatus.

3. A baseline image was taken using the OCT.
4. The sample was immersed in 0.3% citric acid by placing a plastic tube, open from the top and bottom, on the sample; and stabilising the tube with a wax (Orth-care Ltd, UK) to prevent any leakage of the acid. The acid was filled inside the tube covering the tooth surface for 30 minutes (figure 4.8).

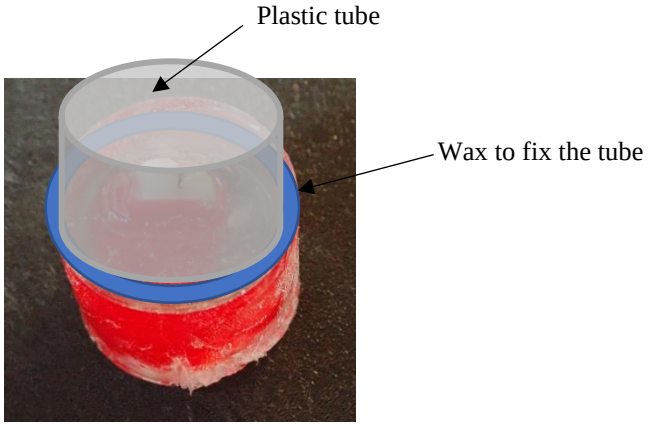

Figure 4.8 Example of a mounted tooth sample and the tube used for acid.

5. Brushing was performed as described in pilot 1.
6. The difference from pilot 1 was that after every 20 cycles, the toothbrush was replaced with a new charged toothbrush to preserve the speed of brushing. Also, the brush head was replaced between samples.

Discussion:

The brushing apparatus with the electric toothbrush helped solve the difficulties faced with toothbrushing apparatus used in pilot 1. The sample was fixed on the container and the jack without the need to remove it and remount it again. This was one limitation faced in pilot 1 using the brushing apparatus with manual toothbrushes. This helped in preserving the sample in a fixed position as the remounting affected the sample direction in relation to the OCT probe.

In addition, the anatomy and the structure of the samples was not a disadvantage, as the samples were in contact with the brush head without the need to mount it in a specific position. This ensured that the lesion was always in contact with the toothbrush during the abrasion cycles. This contrasted with the brushing apparatus in pilot 1, as the anatomy of the tooth sample affected the brush head direction. Moreover, there was no need to trim the sample as it can be mounted in resin directly without the need to match it with a size of a holder as in pilot 1.

The limitation of using the electric toothbrush was that it needed charging between cycles, as the toothbrush cannot turn on while it linked to the charger. This required more than 8 toothbrushes to be fully charged for each sample to be brushed for 100 cycles. This is because each charged toothbrush can brush for 28 minutes maximum and each 20 cycles requires 40 minutes of brushing. Also, the speed of brushing might be affected as the toothbrush is not connected to the charger directly. This might affect the results as the toothbrush might be moving in a slower speed resulting in an inconsistent brushing cycles. For example, it can be faster in beginning of the 20 cycles and then slower toward the end of the 20 cycles.

A disadvantage of using the current apparatus was in using one sample at a time compared to the brushing apparatus used in pilot 1 that held 8 toothbrushes. This affected the number of samples brushed each day, as only one sample could be brushed using the apparatus with electric toothbrush.

Another reason for brushing one sample per day was with the timing of brushing, because a total of 5 hours was needed for each sample to be brushed and scanned. An explanation is that every 20 cycles of brushing take 40 minutes (2 minutes/cycle), so a total of 200 minutes for the 100 cycles of brushing. Adding the erosion time of 30 minutes and scanning of six OCT images between the cycles, with each image taking

around 10 minutes, equal around 5 hours. So, the long time for each sample and the fact that only one sample can be brushed in a day are limitations for the length and the sample size of the study.

Outcome:

Based upon this objective, the brushing apparatus with electric toothbrushes has some limitations, but compared to brushing apparatus in pilot 1, can be used for the current study for its other advantages mentioned above.

4.2.4 Objective 2

Methods:

After every 20 cycles, the sample, which was in a fixed position in relation to the OCT and toothbrush, was taken to the OCT optical table and scanned using the OCT probe.

Rulers were used as stoppers on the optical table to fix the location of the jack (figure 4.9). This was to ensure that the position of the sample and the scanned area were preserved when the sample was moved between brushing and scanning. Also, the OCT probe was in a fixed position during all the cycles of brushing to guarantee that only the focussing distance between the sample and the probe is changed using the jack screw in between each series of brushing cycle for every single sample.

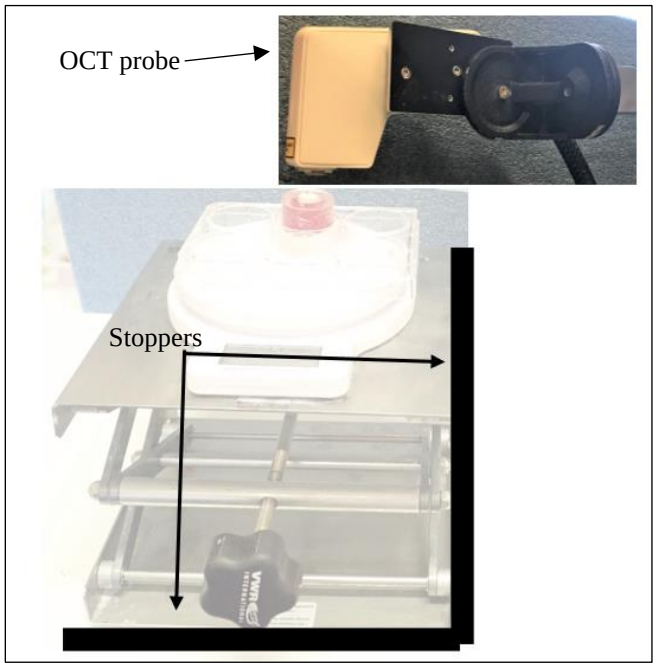

Figure 4.9 Example of stoppers fixed around the jack on the optical table.

Three samples from the saliva group were selected, including one sound tooth (C 1), type 21 (MIH 1), and type 22 (MIH 2) defects. Brushing and scanning was performed on all three samples as described above using the brushing apparatus and stoppers.

The selection of the baseline image was based on the frame that showed the lesion and the needle in the best resolution. Then, the 20, 40, 60, 80, and 100 cycles' b scans were selected by comparing them with the baseline image and matching specific features on the baseline frame, such as a dot on the glue or a radiolucent spot.

The OCT images were taken and analysed as described chapter 3 section 3.4.2.

Results:

The results of the samples brushed with saliva did not show TSL. Figure 4.10 shows how the TSL measurements (sample type 21, white/cream lesion) did not result in TSL. The TSL should be a positive value, which was not the case in here. The negative values in figure 4.10 indicate a tooth surface gain, which is considered odd as no remineralisation process has been performed for the sample. The values also show a non-linear and inconsistent readings between the cycles. For example, it shows that the 20 cycles resulted in surface gain by 260 microns, then on the 40 cycles image there was a TSL of 100 microns. This was again back to tooth surface gain at 60 cycles image.

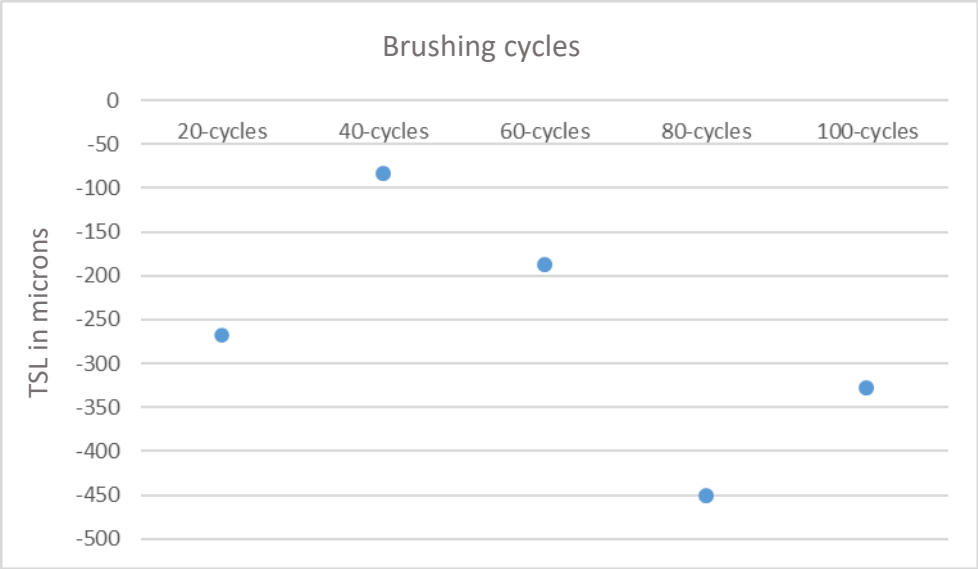

Figure 4.10 A tooth sample showing an increased number of microns on the enamel surface.

Also, figure 4.11 illustrates the b scans of same sample with no TSL between the cycles. In addition, the scanned area and the features on the images of cycles 20 to 100, were not similar to the baseline image

(white arrows), as the features on the b scans were not consistent as described above in methods. For example, the 20 cycles image has a radiopaque circle shown on the glue that is not found on the baseline image. The white arrow on the 40 cycles image points at the glue indicating a different area of the sample has been scanned. The 60, 80, and 100 cycles images also have a demineralised area that is not scanned in the baseline image. The red curves show the variation between the baseline image and the other images, when the baseline image was superimposed on them. This indicates an in-plane variation between the cycles as the tooth has a certain degree of rotation that needs to be maintained throughout the scanning process

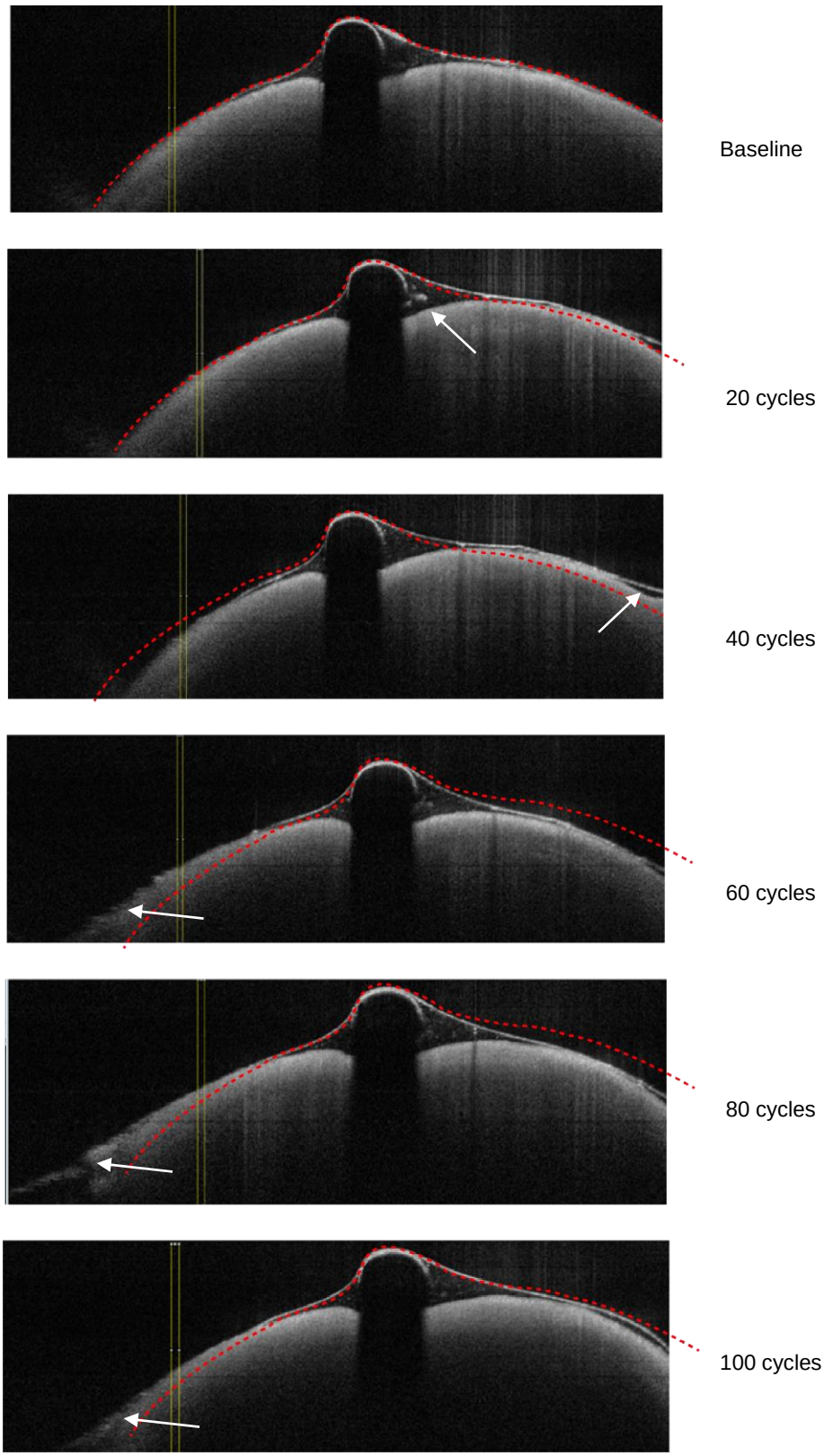

Figure 4.11 The OCT images of type 22 defect in saliva group.

Discussion:

Scanning the same area after every 20 cycles was achieved using the jack and stabilising the position of the probe. However, the jack that was used in this pilot was not stable. This has resulted in an in-plane variation and the focal distance between the OCT probe and the sample was not fixed. In addition, it resulted in scanning different areas on the sample through the cycles, which affected the selection of the 20, 40, 60, 80, and 100 b scans, as the features on the frames could not be matched to the baseline b scan.

Also, the method of measuring TSL that has been used here and in pilot 1 might be inaccurate. This is because the calculation of the TSL was based on using five points on the same b scan for each 20, 40, 60, 80, and 100 cycles' image without comparing the results with the baseline image directly as described in chapter 3 section 3.4.2.

Outcome:

Based on this objective, the jack and the calculation method need to be adjusted to have a more stable jack and a better measurement method of TSL.

4.2.5 Overall review of pilot 2

The use of brushing apparatus is recommended with the adjustments of the jack and calculation method of TSL.

Next steps: A new jack will be used in pilot 3 with an adjustment of the calculation method.

4.3 Pilot 3

At the end of pilot 2, the use of the brushing apparatus with electric toothbrushes was recommended. However, the reproducibility of the OCT images with the jack used and the method of calculation were not recommended as the jack was not stable and the TSL was in positive values.

The aim of this pilot was to use a more stable optical jack (Thorlabs, Inc), and as 0.3% citric acid did not show any TSL, the percentage of the acid and its erosive effect was raised to 37% phosphoric acid. In addition, a new method of measuring TSL was implemented by comparing the baseline image with the other b scans after brushing.

4.3.1 Aims

To standardise a calculation method for TSL

4.3.2 Objectives

1. To address the stability of the new platform
2. To achieve TSL using a high percentage acid (37% phosphoric acid)
3. To develop a method to accurately and reproducibly measure TSL

4.3.3 Objective 1

Methods:

As noted in pilot 2 the jack was not stable, a more stable optical jack (Thorlabs, Inc) was used as shown in figure 4.12.

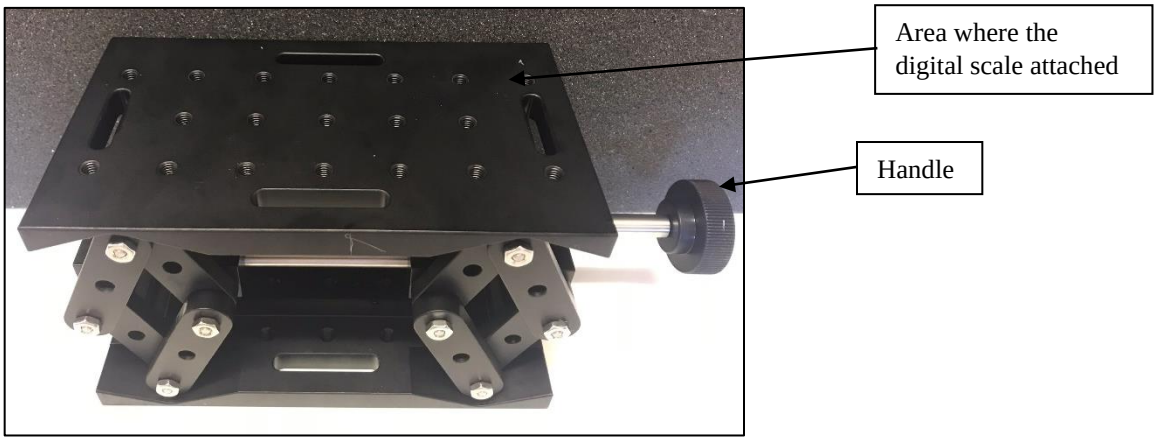

Figure 4.12 The Thorlabs Jack

The advantages of the optical jack include the more precise movements as the images were reproducible, when the jack was tested. Also, the jack moved slower vertically, which make capturing the b scan on the OCT more accurate as the samples will be stable and will not be affected by the fast movements. The digital scale was attached on the jack as described in pilot 2 as in figure 4.13.

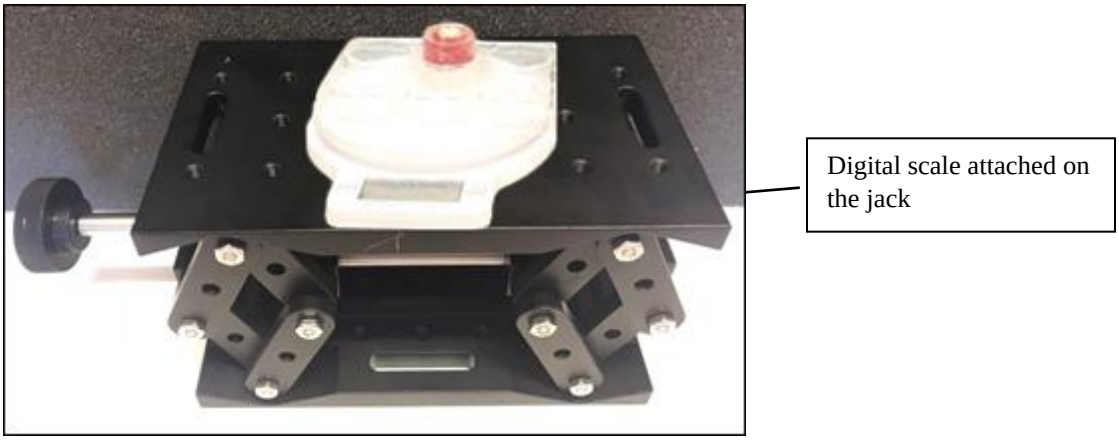

Figure 4.13 Digital scale attached on the jack

Results:

Using the new optical jack, the OCT images between the cycles were successfully captured without the movement of the tooth sample (MIH 22, yellow/brown lesion), as the images were reproducible and the same frame of the image was captured at the 20, 40, 60, 80, and 100 cycles when compared with the baseline image. Figure 4.14 shows the baseline image and the 20 cycles image and how the two images matched for sample MIH 22 (yellow/brown lesion), where only the focal distance between the sample and the OCT probe was adjusted. The red arrow shows the lesion and how the location of the lesion was reproduced on the second image.

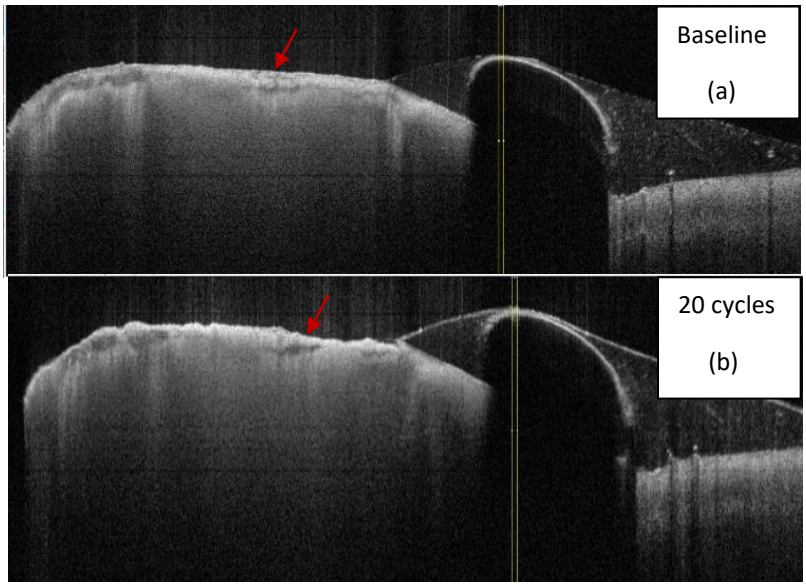

Figure 4.14 An example of TSL

the baseline image (a) was compared to 20 cycle's images (b)

Discussion:

The Thorlabs jack was more stable and prevented any distortion or variation. The only adjustments that were performed were on the focal distance between the OCT probe and the sample.

Outcome:

The jack can be used successfully in this experiment as it proved its stability.

4.3.4 Objective 2:

Methods:

As TSL was not observed with 0.3% citric acid, a decision was made to use 37% phosphoric acid to soften the enamel. The reason of selecting this high percentage was to confirm the ability of the OCT to show the TSL on eroded samples. That is because after pilot 1 and 2, a question raised whether OCT could show TSL or not. The phosphoric acid was applied for 10 minutes (instead of 0.3% citric acid for 30 minutes). The 10 minutes application of 37% phosphoric acid was chosen to ensure TSL was visible as there were no comparable studies for the application time. The brushing was then performed as in pilot 2 using electric toothbrushes.

Results:

Using 37% phosphoric acid resulted in TSL visible on the OCT images. Figure 4.15 shows the TSL sample MIH 22 (yellow/brown lesion) and the difference between the reference needle and enamel surface is severe. It showed how the demineralised area (white arrow) has reduced throughout the cycles. Also, the yellow circles show how the enamel surface has been affected by the erosion/abrasion process in comparison with the needle and the glue.

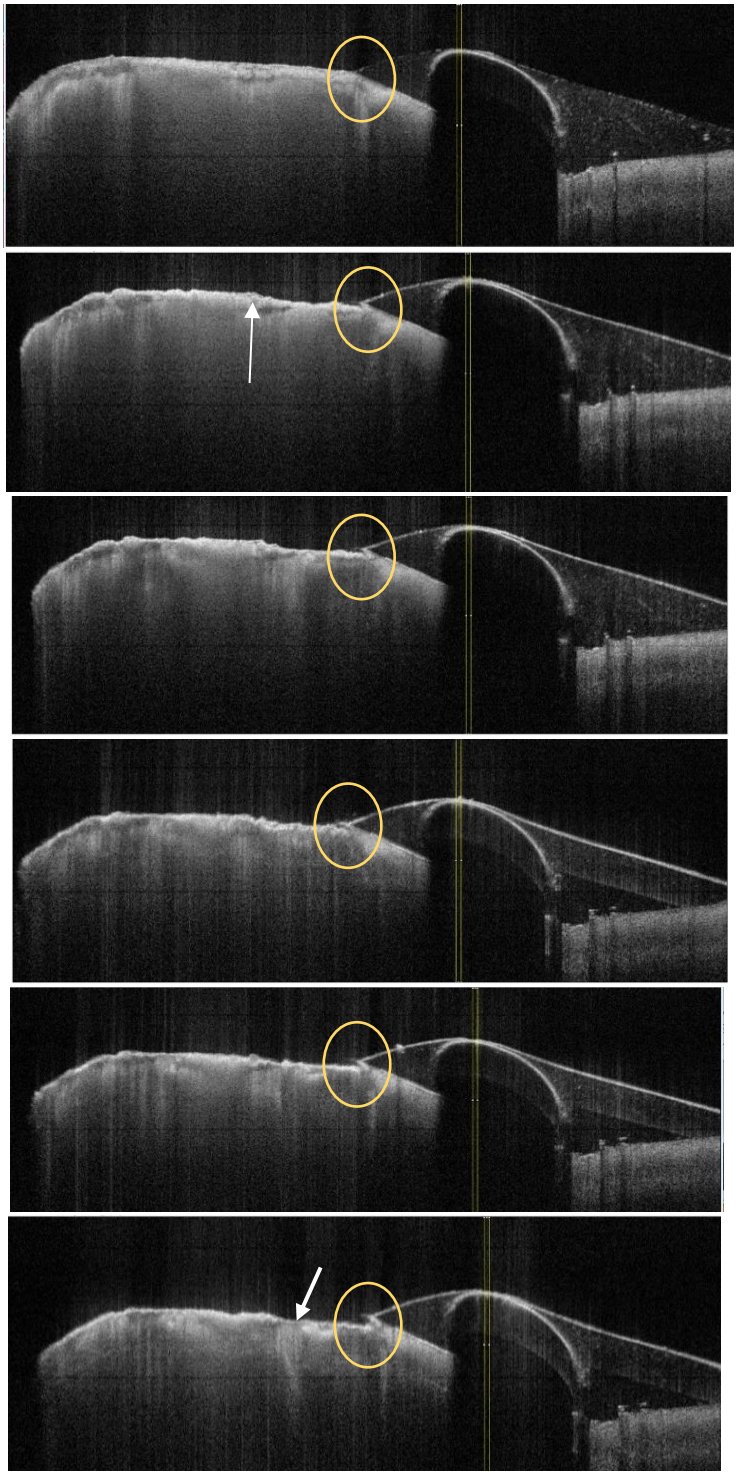

Figure 4.15 The OCT images of Type 22 tooth with Phosphoric acid.

White arrows present TSL.

A comparison between pilot 2 (citric acid) and pilot 3 (phosphoric acid) using the baseline and 100 cycles images was performed (figure 4.16).

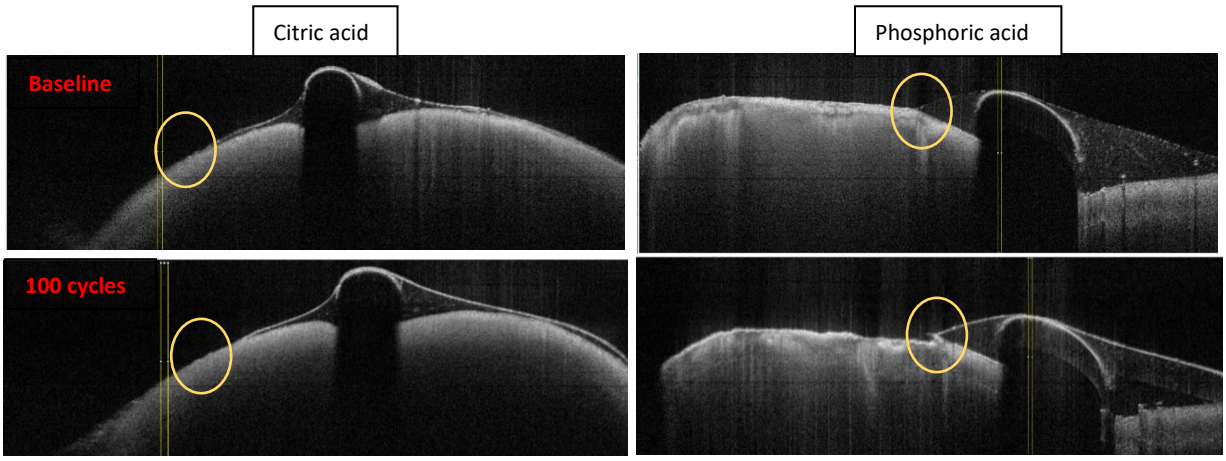

Figure 4.16 Comparison between TSL using citric acid vs phosphoric acid.

Yellow circles represent the TSL area.

The comparison shows that TSL was detectable when phosphoric acid was used compared with citric acid.

Discussion*:*

Although 37% phosphoric acid is used professionally for treatment purposes for less than a minute, its application in this pilot was purely for the purpose of achieving TSL that can be viewed on the OCT images. This has helped in answering the question of whether TSL can be achieved using the current method of brushing and OCT imaging. However, this percentage cannot be applied for the remaining of the study and another percentage that can be found in consumed beverages will be required.

Outcome:

TSL can be achieved using a high percentage of erosive medium but the percentage applied is not clinically relevant.

4.3.5 Objective 3

Methods:

Two teeth from the saliva group were selected, type 21 (MIH 21) and type 22 (MIH 22) defects. Brushing was performed as described in pilot 2 and OCT images were taken after 20, 40, 60, 80, and 100 cycles. The jack area was outlined with its dimensions using rulers, as in pilot 2, to ensure the same area is captured every time the sample is moved from the brushing area to the scanning area.

The method of calculation of TSL implemented in this pilot was by comparing the baseline image with the other images of the cycles. The steps of calculating the TSL are summarised below:

1. The baseline image (selected b scan) was saved from Image J and imported into a PowerPoint programme together with either the 20, 40, 60, 80, or 100 cycles' b scan. The selection of the b scan frame was based on specific features on the image.
2. A line was drawn on the surface profile from the needle to the enamel surface that needed scanning on the baseline image.
3. The line was then copied and pasted on the 20, 40, 60, 80, and 100 cycles' image.
4. The curvature area was avoided as this affected the measurements of the five white points selected as shown in figure 4.17.

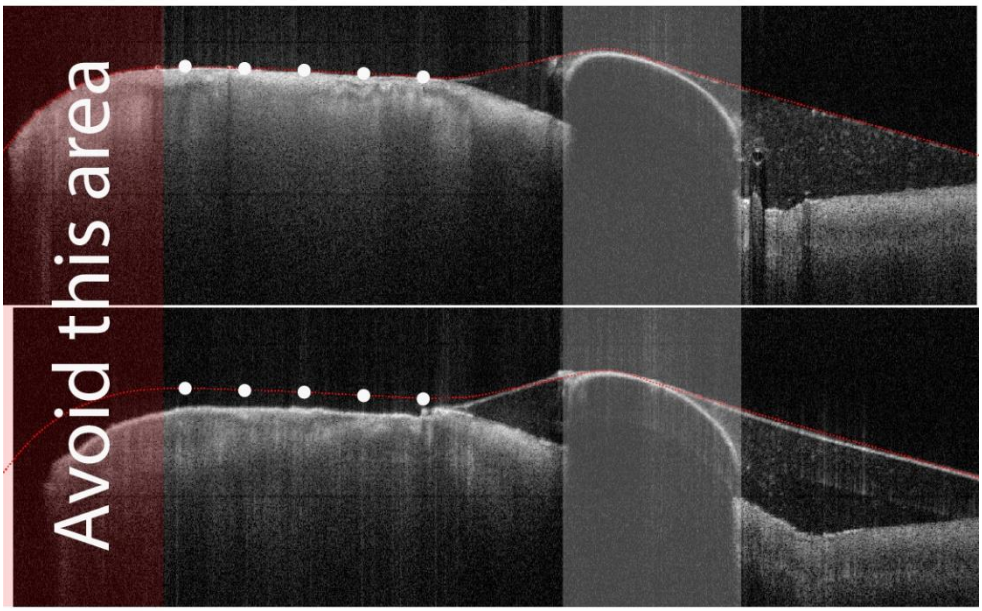

Figure 4.17 An example of lines drawn on the b scans.

5. Both the baseline and one of the cycles images (either 20, 40, 60, 80, or 100) were captured and saved, then imported into the Image J.
6. The scattering plot (figure 4.18) was extracted from both images on image J and transferred into an excel sheet.

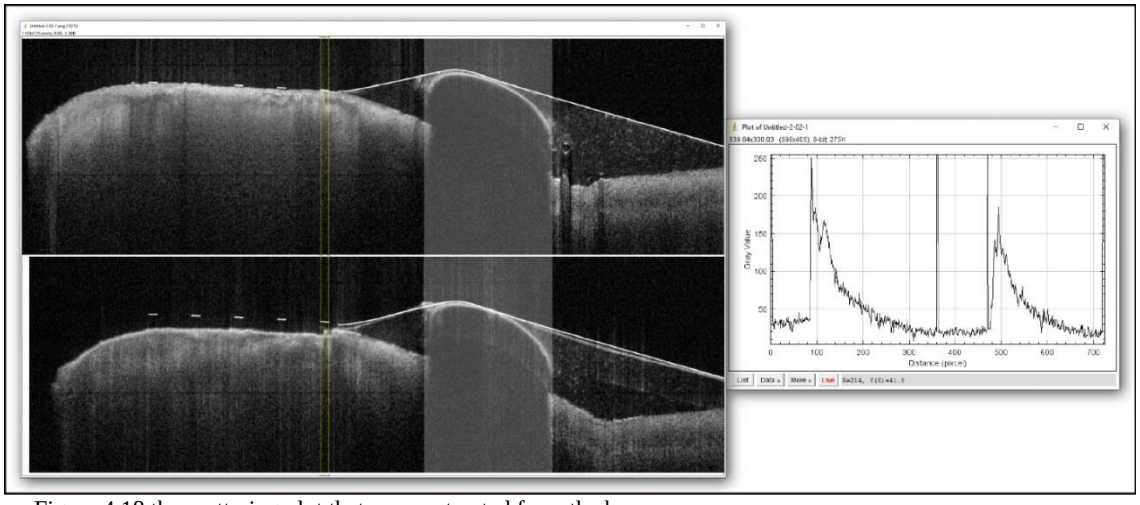

Figure 4.18 the scattering plot that were extracted from the b scans.

7. Two columns were shown on excel sheet. The columns represent the x axis (distance in pixels) and y axis (grey value). Four values of X1, X2, X3, and X4 were extracted from the columns corresponding to the vertical lines on the a scan. Figure 4.19 shows an example of the 4 values and what they present on the b scan. These values were the highest and the lowest on each column that will be used to adjust the pixel values to microns.

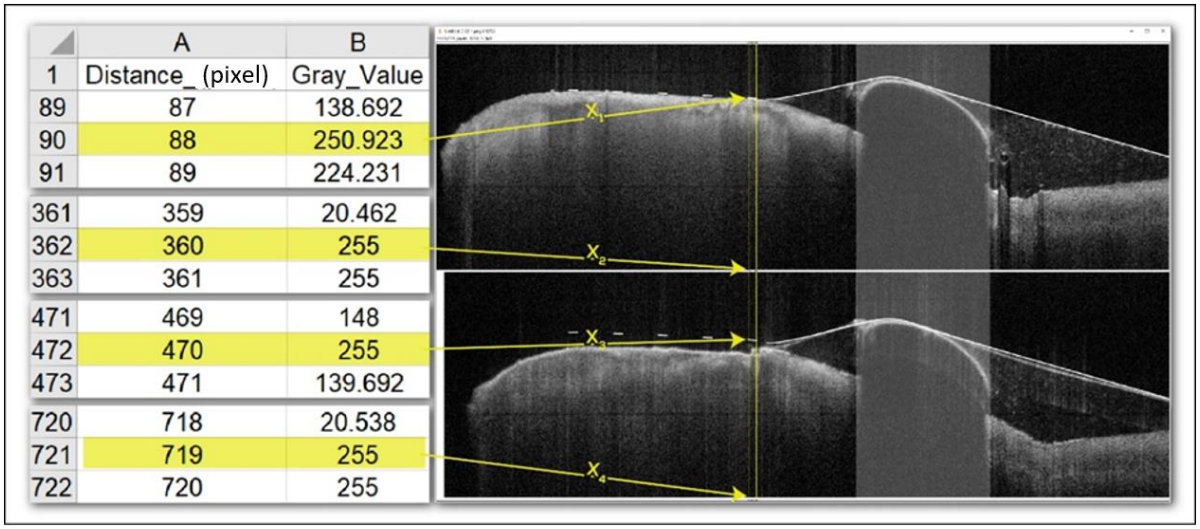

Figure 4.19 The values from excel sheet and what they present on the b scan.

8. The ranges of X2-X1 and X4-X3 were calculated. The average of both ranges was measured. Then the pixel size was adjusted, as it changes when the image is captured affecting the resolution. This was done by multiplying 460 (number of pixels in OCT image) by 4.53 (OCT pixel size) divided by the range (figure 4.20)

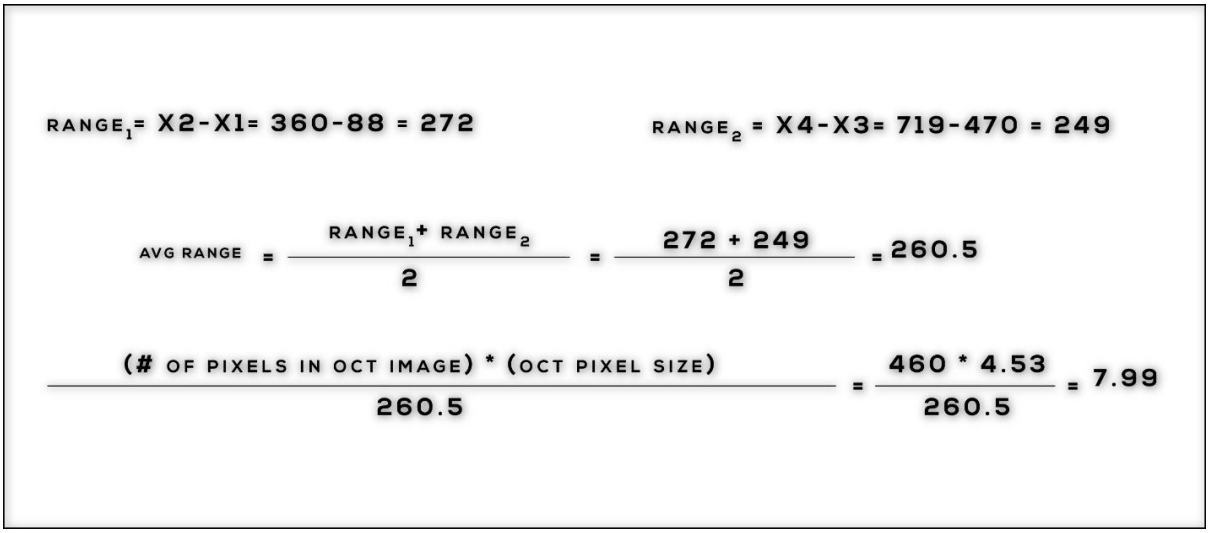

Figure 4.20 The calculation of the range and the number for pixels adjustment.

9. The new adjusted pixel size was then multiplied by the x axis on the excel sheet (from step 7) and the resulting numbers were in microns. A new scattering figure created using excel program (figure 4.21).

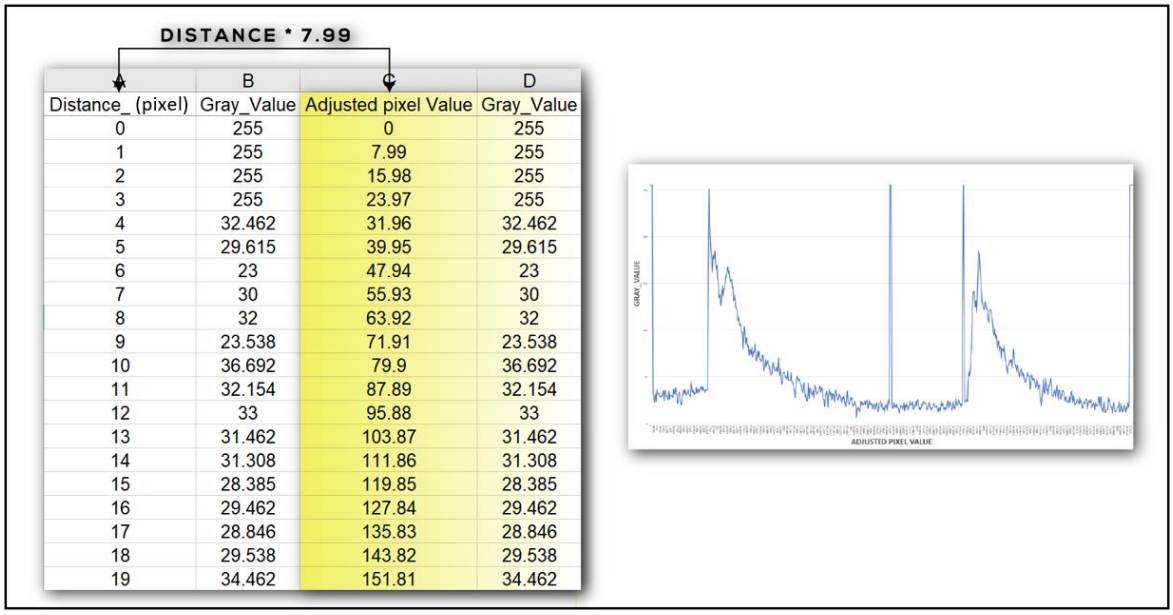

	B	C	D
Distance_ (pixel)	Gray_Value	Adjusted pixel Value	Gray_Value
0	255	0	255
1	255	7.99	255
2	255	15.98	255
3	255	23.97	255
4	32.462	31.96	32.462
5	29.615	39.95	29.615
6	23	47.94	23
7	30	55.93	30
8	32	63.92	32
9	23.538	71.91	23.538
10	36.692	79.9	36.692
11	32.154	87.89	32.154
12	33	95.88	33
13	31.462	103.87	31.462
14	31.308	111.86	31.308
15	28.385	119.85	28.385
16	29.462	127.84	29.462
17	28.846	135.83	28.846
18	29.538	143.82	29.538
19	34.462	151.81	34.462

Figure 4.21 the new numbers in microns with a scattering plot in microns.

10. The TSL was then measured from the distance between the very narrow peak (reference line) and the large scattering peak (enamel surface) as shown in figure 4.22. This measurement will calculate the TSL in one area of the five points presented in figure 4.17.

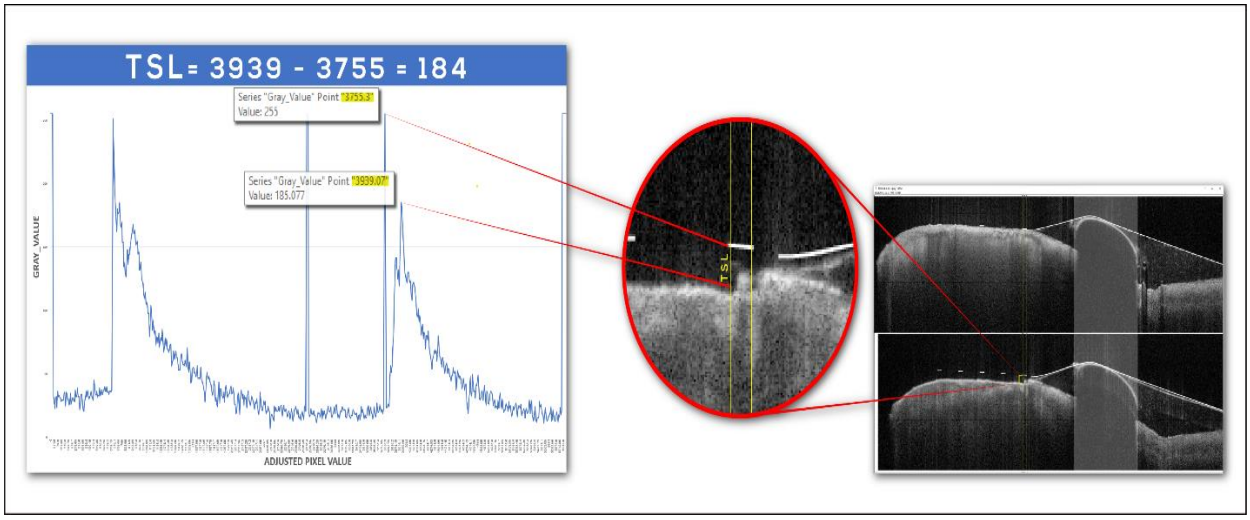

Figure 4.22 the abrasion viewed on the scattering plot.

All the previous steps were followed for each sample used in this pilot. Then the mean of the five points on the b scan was calculated and plotted on the graph for the 20, 40, 60, 80, and 100 cycles (figure 4.23).

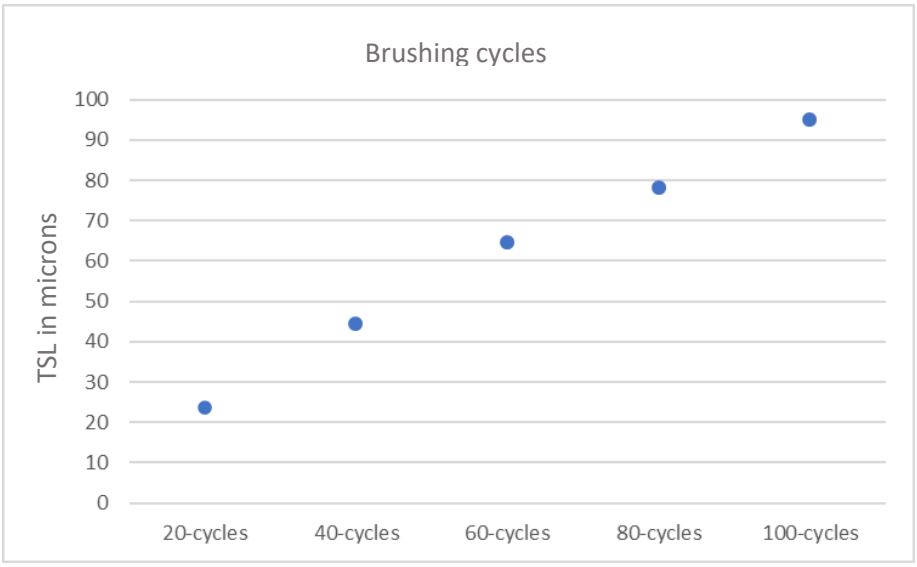

Figure 4.23 An example of the mean of each five points on 20, 40, 60, 80, and 100 image.

Results:

The technique demonstrated increasing TSL from 20 to 100 cycles, as shown in the plotted graph in figure 4.24.

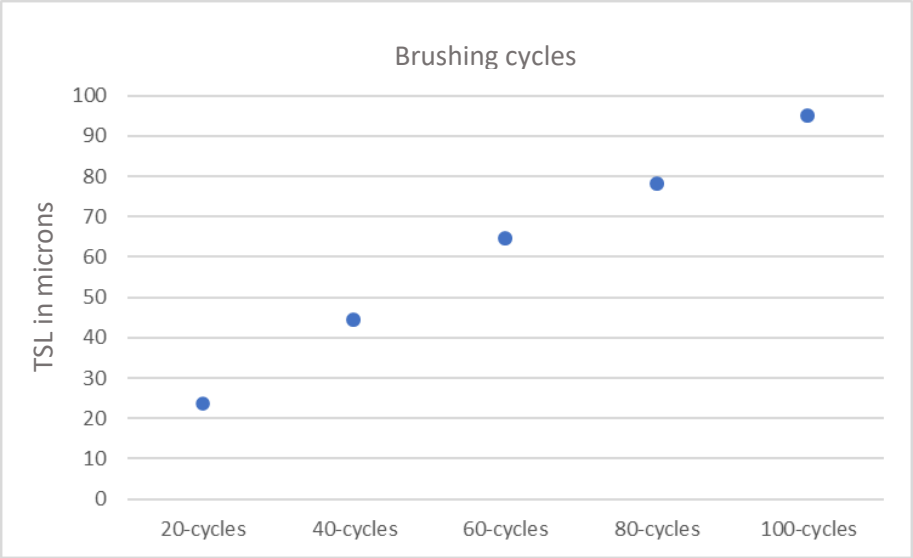

Figure 4.24 gradual increase in TSL on sample MIH 22.

Discussion:

The new method of calculating TSL had an advantage of comparing the baseline image with the other cycles' images. The pixel size can also be adjusted using this method. The most important part that should be avoided include the curvature area of the b scan as it affects the measurements when the intensity profiles were plotted. This is difficult to achieve with most samples as the lesion is on the cusps and the five points selected on b scans will be close to each other on the flat area. Also, this method of measurement depended on the reference needle to compare between the images by matching them on each other. This has shown how important and useful the use of the reference needle.

Outcome:

The calculation method of TSL improved the accuracy in measuring TSL

4.3.6 Overall review of pilot 3

The optical jack and the calculation method successfully measured TSL. However, there were limitations associated with the current methods. These included:

- The selection of the exact b scan from all the cycles might be difficult. This is because the OCT captures a 500 b scans from a selected are of a 6mm.
- The reference needle and the glue could shield some of the lesion area if not mounted perfectly. Alternative method of creating a small hole and fill it with amalgam, next to the lesion, can be used

as a reference. However, amalgam usage has reduced due to its contamination effect to the environment.

Next steps: to implement the use of the brushing apparatus with electric toothbrushes, the jack, and the calculation method in the next part of the study with the adjustment of the acid percentage.

4.4 Discussion of the three pilots

The process of the 3 pilots discussed above was followed to reach a definitive protocol that can be used in this study.

Starting with pilot 1, the efficacy of the brushing apparatus using manual toothbrushes was assessed, and the method of calculating TSL from OCT images. Several disadvantages were found with the use of the brushing apparatus. These include the location of the lesions on the molar teeth samples and how it was difficult to section and mount the sample on the holder slots available on the brushing apparatus. That was because samples with a flatter surface worked better on the apparatus slots compares to curved surfaces. In addition, moving the sample in and out of the holder slots on the brushing apparatus affected the reproducibility of capturing the same image between the brushing cycles.

In pilot 1, the toothbrushing effect was also assessed in the first pilot by performing toothbrushing alone and with erosive challenge. When abrasion was performed alone, no TSL was noted. That could be because tooth wear is multifactorial and it is usually the interactions of more than one factor that results in TSL (Wiegand and Attin, 2011). Additionally, the efficacy of the brushing combined with erosion to generate sufficient TSL that can be measured from the OCT images was questioned. This was seen when the TSL was calculated and an increase in mean difference of the measurements.

The second pilot followed on from the results of the first pilot, including reverting back to electric toothbrushes to perform abrasion/erosion; and to stabilise the vertical dimension to replicate the OCT images using a jack. Using the electric toothbrushes and fixing tooth samples on the platform helped to solve some difficulties faced in pilot 1. These include the ability to brush and scan the samples without the need to remove them between the cycles. In addition, there was no need to section the samples to mount them. The disadvantages found in pilot 2 included the need to replace the electric toothbrush more than one time for each sample to complete the 100 cycle of brushing. Also, only one sample can be brushed and scanned at a time compared to 8 samples using the brushing apparatus in pilot 1.

The TSL in pilot 2 was calculated using the same method of measurement from pilot 1, which revealed no TSL. This indicated that the method of calculation without directly comparing the baseline image with the 20, 40, 60, 80, or 100 cycles' image was not successful. In addition to the calculation method, the OCT images were not reproducible, due to unstable jack that resulted in variation between the images taken between the cycles.

The findings from pilot 1 and 2 led to the initiation of pilot 3. The main issues addressed in pilot 3 included the need for a more stable jack and the need for a new calculation method. Another question that was raised in pilot 3 was that can the TSL be seen on the OCT images. This question was tested by raising the

percentage of the acid to 37% using phosphoric acid to produce TSL. The jack that was used in pilot 3 was the optical jack, which was more stable than the one used in previous pilots. The images taken for one sample proved to be stable and reproducible. This maintained the same frame of the image between the cycles. In addition, the phosphoric acid used in pilot 3 produced a TSL that can be seen on the OCT images. Although the application of the phosphoric acid does not mimic the real-life scenario, it showed that TSL can be seen on the OCT images.

With regards to the calculation method used in pilot3, it helped in calculating the TSL with the adjustment of the pixel size and by directly comparing the baseline image with the other cycles' images for an accurate measurement. This proved that the TSL can be measured in microns for each sample. However, the disadvantage was that the curvature area on the samples must be avoided during the measurement. This was difficult using molar teeth as most of the lesions were on the cusps.

From the three pilots above, it can be concluded that the optical jack, the brushing apparatus with electric toothbrushes, and the calculation method from pilot 3 are recommended to perform the study. The type and percentage of the acid will be 1% citric acid to mimic high acidic beverages. The next section will explain the protocol that was applied for the study.

4.5 Definitive protocol

A definitive protocol was concluded from pilots 1, 2, and 3. The pilots helped in confirming the method of brushing, acid type and percentage, and the measurement protocol. The following steps describes in detail the protocol that will be followed in the next chapter.

1. Nine samples will be allocated in each saliva, complete protection toothpaste, and children pronamel toothpaste group. The nine samples include 3 control samples, 3 white/cream samples, and 3 yellow/brown samples.
2. The tooth sample is mounted in resin in a plastic container and a stainless-steel needle will be placed on the sample using araldite adhesive (Huntsman international, India). The lesion should be facing upward for the brushing.
3. The plastic container is glued on a digital scale. Then, the scale is glued on the Thorlabs jack.
4. A baseline image will be taken using the OCT and the area of the jack is outlined with stoppers.
5. A plastic tube, open from the top and bottom, is placed on the sample and stabilised on the tube with a blue tack to prevent any leakage of the acid. The acid will be poured inside the tube for 30 minutes.
6. The brushing will be performed using the brushing apparatus (chemistry clamp and charged toothbrush). The toothbrush should be facing downward.
7. A 20 cycles of brushing is performed (2 minutes/cycle), in which the sample is rinsed with water every 2 minutes.
8. An OCT image is taken after the 20 cycles.
9. Steps 7 and 8 are repeated to reach 40, 60, 80, and 100 cycles.
10. The method of calculation of TSL will be performed as follows:
    A. The baseline image (selected b scan) is saved from Image J and imported into a PowerPoint programme together with either the 20, 40, 60, 80, or 100 cycles' b scan.
    B. A line is drawn on the surface profile from the needle to the enamel surface that needed scanning on the baseline image.
    C. The line is then copied and pasted on the 20, 40, 60, 80, and 100 cycles' image.
    D. The curvature area will be avoided as this affected the measurements of the five white points selected as shown in figure 4.25.

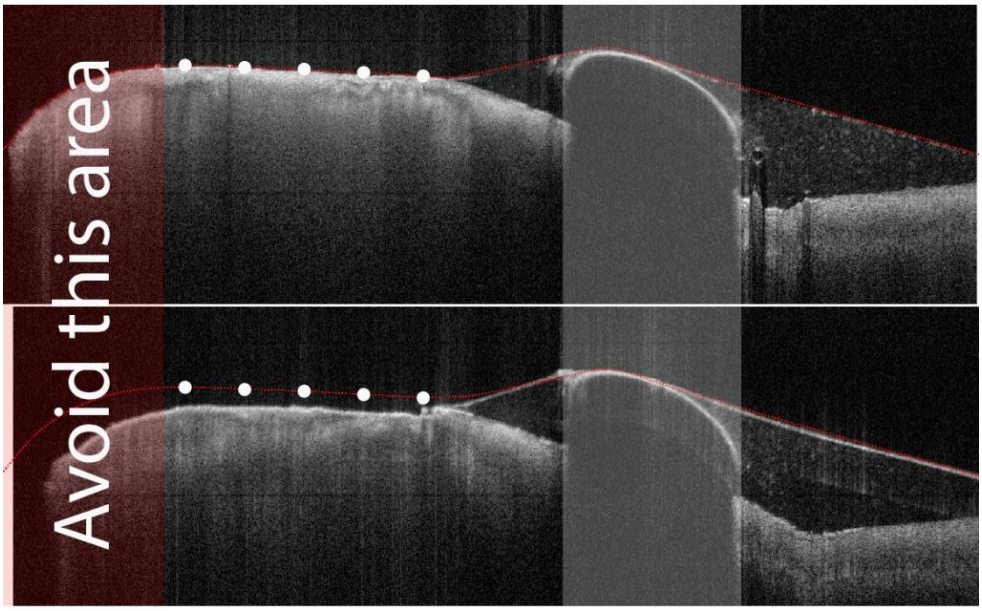

Figure 4.25 An example of lines drawn on the b scans.

E. Both the baseline and one of the cycles images (either 20, 40, 60, 80, or 100) will be captured and saved, then imported into the Image J.

F. The scattering plot (figure 4.26) will be extracted from both images on image J and transferred into an excel sheet.

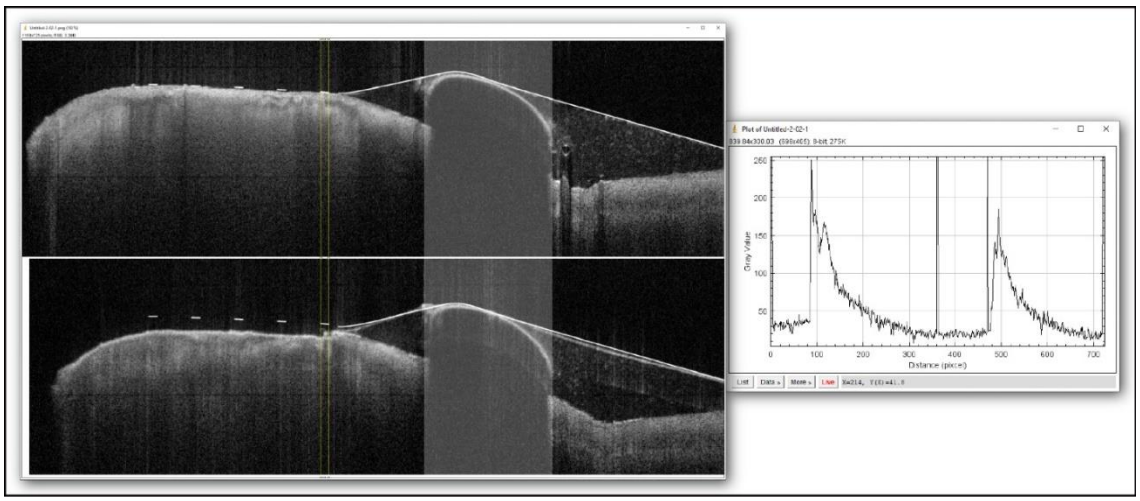

Figure 4.26 the scattering plot extracted from the b scans.

G. Two columns will be shown on excel sheet. The columns represent the x axis (distance in pixels) and y axis (grey value). Four values of X1, X2, X3, and X4 will be extracted from the columns corresponding to the vertical lines on the a scan. Figure 4.27 shows an example of the 4 values and what they present on the b scan.

These values will be the highest and the lowest on each column that will be used to adjust the pixel values to microns.

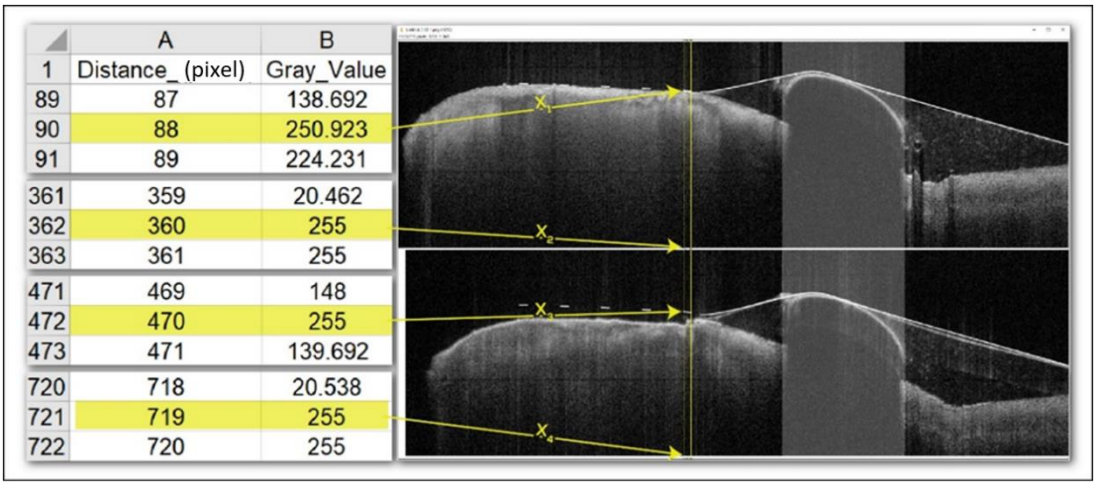

	A	B
1	Distance_ (pixel)	Gray_Value
89	87	138.692
90	88	250.923
91	89	224.231
361	359	20.462
362	360	255
363	361	255
471	469	148
472	470	255
473	471	139.692
720	718	20.538
721	719	255
722	720	255

Figure 4.27 The values from excel sheet and what they present on the b scan.

H. The ranges of X2-X1 and X4-X3 will be calculated. The average of both ranges will be measured. Then the pixel size will be adjusted, as it changes when the image is captured affecting the resolution. This is done by multiplying 460 (number of pixels in OCT image) by 4.53 (OCT pixel size) divided by the range (figure 4.28).

$$RANGE_1 = X2 - X1 = 360 - 88 = 272 \qquad RANGE_2 = X4 - X3 = 719 - 470 = 249$$

$$\text{AVG RANGE} = \frac{RANGE_1 + RANGE_2}{2} = \frac{272 + 249}{2} = 260.5$$

$$\frac{(\#\text{ OF PIXELS IN OCT IMAGE}) * (\text{OCT PIXEL SIZE})}{260.5} = \frac{460 * 4.53}{260.5} = 7.99$$

Figure 4.28 The calculation of the range and the number for pixels adjustment.

I. The new adjusted pixel size will then be multiplied by the x axis on the excel sheet (from step G) and the resulting numbers will be in microns. A new scattering figure will be created using excel program (figure 4.29).

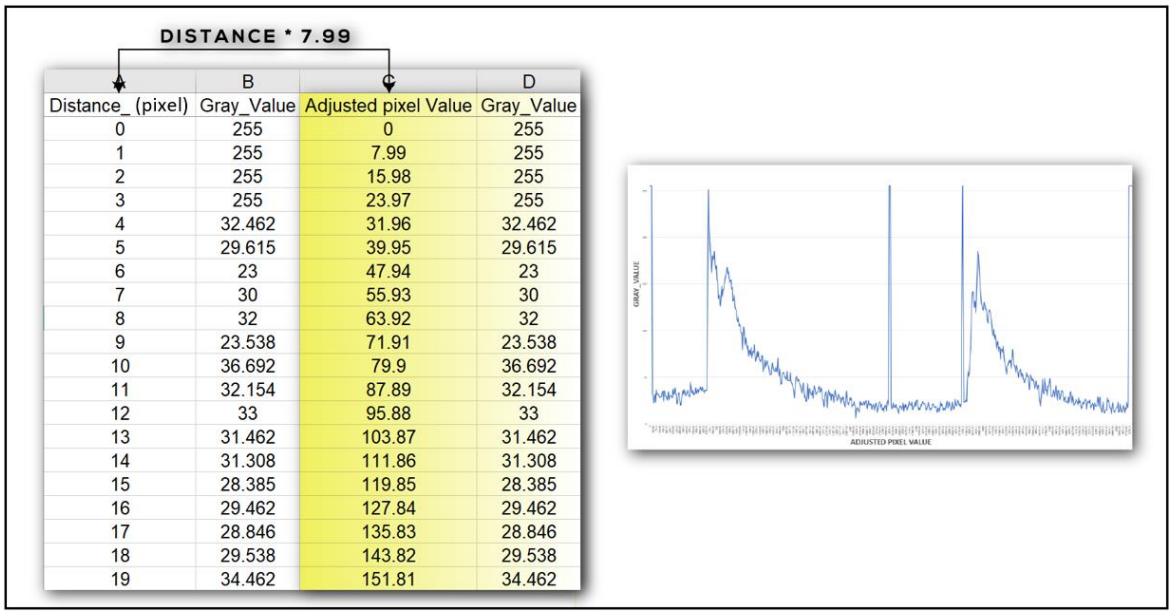

	B	C	D
Distance_ (pixel)	Gray_Value	Adjusted pixel Value	Gray_Value
0	255	0	255
1	255	7.99	255
2	255	15.98	255
3	255	23.97	255
4	32.462	31.96	32.462
5	29.615	39.95	29.615
6	23	47.94	23
7	30	55.93	30
8	32	63.92	32
9	23.538	71.91	23.538
10	36.692	79.9	36.692
11	32.154	87.89	32.154
12	33	95.88	33
13	31.462	103.87	31.462
14	31.308	111.86	31.308
15	28.385	119.85	28.385
16	29.462	127.84	29.462
17	28.846	135.83	28.846
18	29.538	143.82	29.538
19	34.462	151.81	34.462

Figure 4.29 the new numbers in microns with a scattering plot in microns.

J. The TSL will be measured from the distance between the very narrow peak (reference line) and the large scattering peak (enamel surface) as shown in figure 4.30. This measurement will calculate the TSL in one area of the five points presented in figure 4.25.

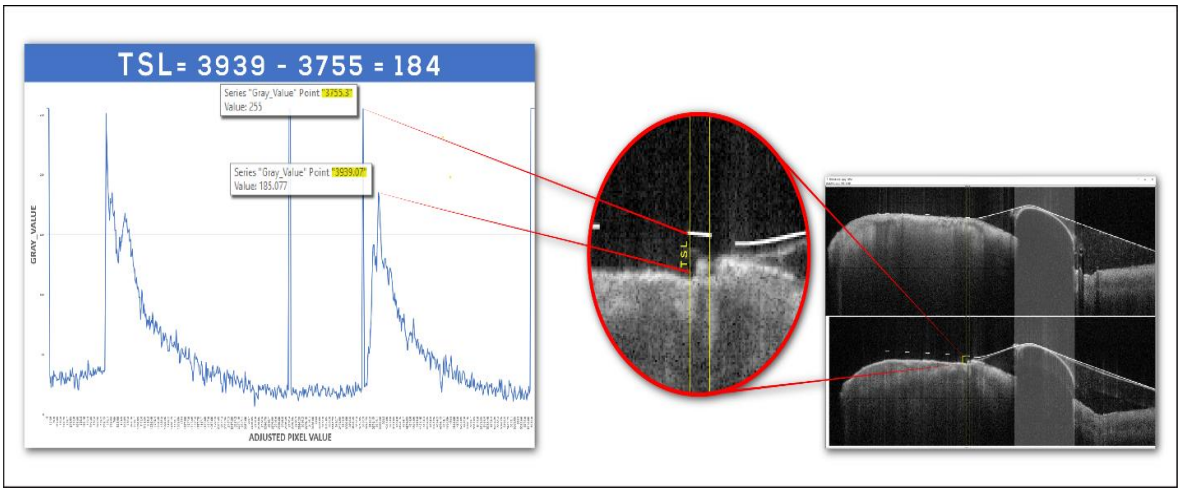

Figure 4.30 the abrasion viewed on the scattering plot.

All the previous steps will be followed for each sample. Then the mean of the five points on the b scan will be calculated and plotted on the graph for the 20, 40, 60, 80, and 100 cycles. The rate of progression of TSL is calculated for each sample and compared with the other samples (figure 4.31).

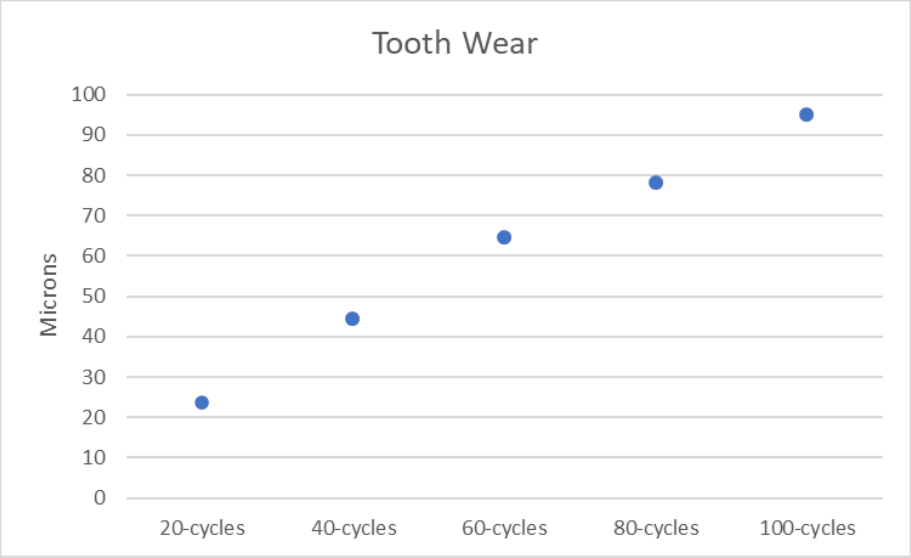

Figure 4.31 An example of the mean of each five points on 20, 40, 60, 80, and 100 images.

In the following chapter, the above protocol was applied for the measurements of TSL using OCT.

Chapter 5

Quantification of TSL on MIH affected teeth using OCT

5 Final model

From the previously described three pilots, it can be summarised that erosion/abrasion performed on MIH affected teeth using the toothbrush model can be achieved and the effect can be demonstrated on the OCT images.

The aim of this chapter was to perform erosion/abrasion using the optical jack, the electric toothbrushes on the brushing apparatus, and the calculation method described in pilot 3. The only difference from pilot 3 was the use of 1% citric acid instead of 37% phosphoric acid as an erosive medium to represent a high acidic beverage (Attin et al., 2003).

5.1 Aims

To quantify TSL on MIH affected teeth using OCT using 1% citric acid as an erosive medium

5.2 Objectives

To perform abrasion/erosion using saliva and two types of toothpastes, and 1% citric acid then calculate TSL on the OCT images

5.3 Methods

For the final model, MIH teeth (18) and sound (9) samples were used, the samples were divided as shown in figure 5.1. The patients' demographics details of each tooth type are shown in Table 5.1. The final protocol from pilot 3 was followed in the final model except that 1% citric acid was used instead than 37% phosphoric acid. The 1% citric acid used to as it represents the acidity of soft beverages (Attin et al., 2003). However, in this study, the sample was immersed in the citric acid rather than rinsing the sample with acid as mentioned in another study (Attin et al., 2003). Attin et al. rinsed the sample for 1 minute only with repeating that every few minutes after brushing and in this study the immersion time was 30 minutes, so placing the sample in acid was a better option than rinsing it with acid. In addition, further statistics were performed to compare samples using regression using SPSS (SPSS®, 2009).

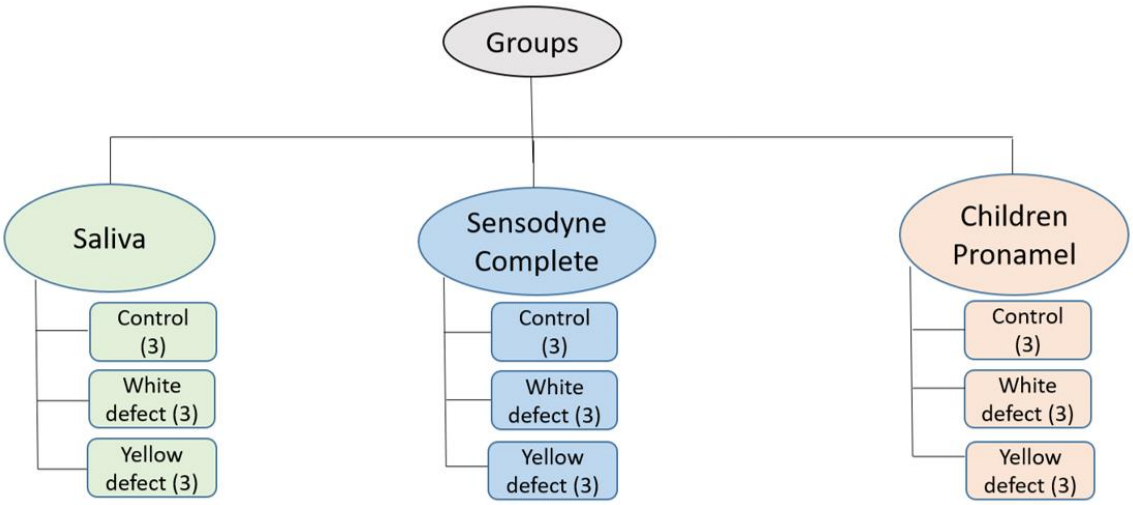

Figure 5.1 Flowchart of the teeth samples used in final model

Patient gender and age	Sample number	Type of sample	Group of brushing
Female, 9 years	C 9	Control	Saliva
Female, 9 years	C 10	Control	Saliva
	C 6	Control	Saliva
Male, 9 years	C 3	Control	Children pronamel
	MIH 3	White/ cream type 21	Children pronamel
Male, 9 years	C 11	Control	Children pronamel
	C 12	Control	Complete protection
	C 8	Control	Complete protection
Male, 8 years	C 7	Control	Children pronamel
Female, 10 years	C 5	Control	Complete protection
Male, 10 years	MIH 16	White/ cream type 21	Saliva
	MIH 7	Yellow/ brown type 22	Complete protection
Female, 9 years	MIH 15	White/ cream type 21	Saliva
	MIH 13	White/ cream type 21	Saliva
	MIH 10	White/ cream type 21	Children pronamel
	MIH 14	White/ cream type 21	Complete protection
Male, 9 years	MIH 12	White/ cream type 21	Children pronamel
	MIH 6	White/ cream type 21	Complete protection
Female, 9 years	MIH 5	White/ cream type 21	Complete protection
Female, 10 years	MIH 11	Yellow/ brown type 22	Saliva
Male, 9 years	MIH 17	Yellow/ brown type 22	Children pronamel
	MIH 9	Yellow/ brown type 22	Complete protection
Male, 9 years	MIH 4	Yellow/ brown type 22	Children pronamel
Female, 9 years	MIH 20	Yellow/ brown type 22	Saliva
Male, 9 years	MIH 19	Yellow/ brown type 22	Saliva
	MIH 8	Yellow/ brown type 22	Children pronamel
	MIH 18	Yellow/ brown type 22	Complete protection

Table 5.1 Details of samples selected in final model

5.4 Results

Saliva group

OCT images for the saliva group (control sample, C 9), are shown as these were representative of all the samples in the control group (figure 5.2). Minimal TSL was observed with less than 25µm after 100 cycles of brushing as indicated by the red arrows. The TSL was measured using the calculation method explained in section 4.5. The other MIH samples in the saliva group had a TSL of an average of 30µm and 63µm for MIH type 21 (white/cream) and type 22 (yellow/brown), respectively.

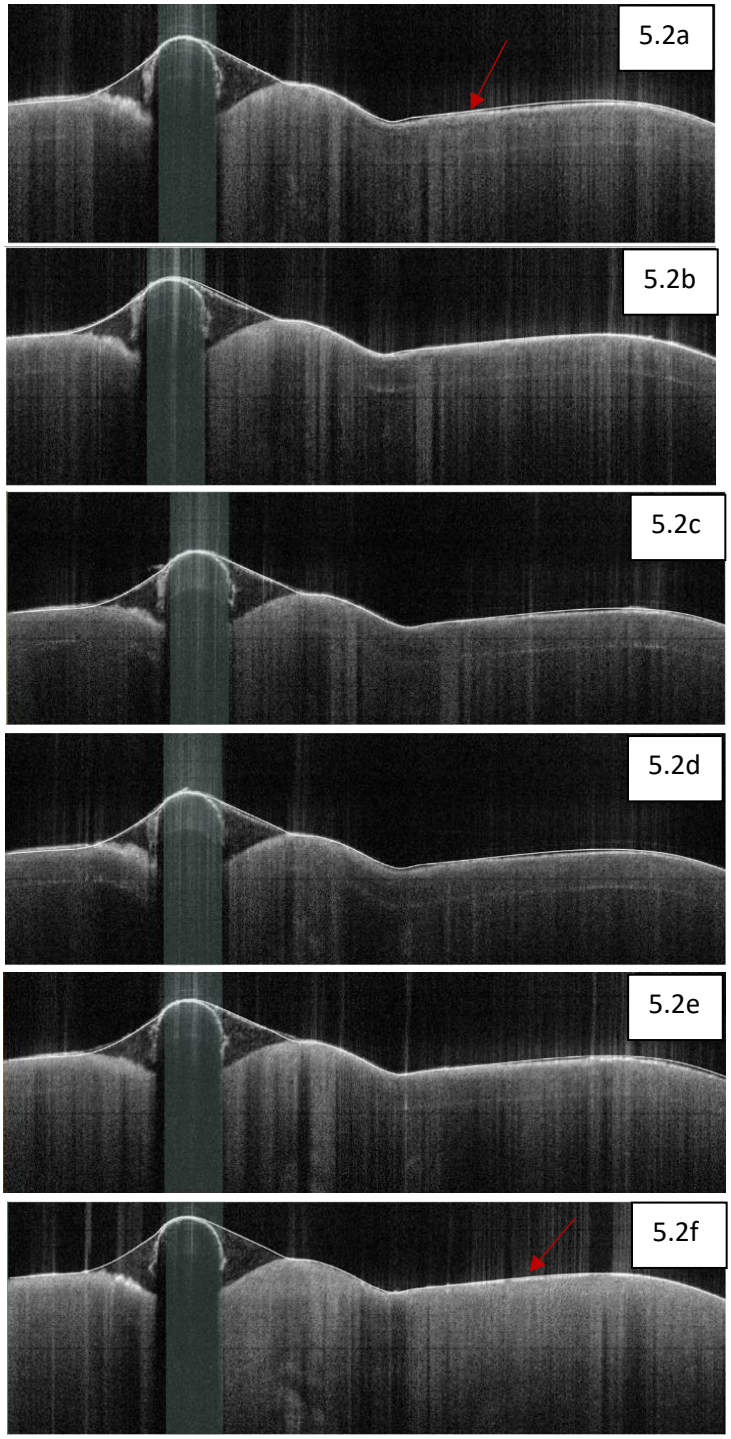

Figure 5.2 A control sample in saliva group,

5.2a (baseline image), 5.2b (20 cycles), 5.2c (40 cycles), 5.2d (60 cycles), 5.2e (80 cycles), 5.2f (100 cycles). Red arrows show the TSL between the baseline and 100 cycles images.

Sensodyne complete

Sensodyne complete, with the active ingredient Novamin®, (type 21 sample, MIH 5), representative of the other type 21 samples in this group, shown in figure 5.3 with a gradual TSL from baseline image to 100 cycles observed. Red arrows show how much TSL can be seen after the abrasion/erosion using complete protection toothpaste and 1% citric acid. The average TSL after 100 cycles in this group was 45µm compared to 93µm and 50µm in control and type 22 samples, respectively.

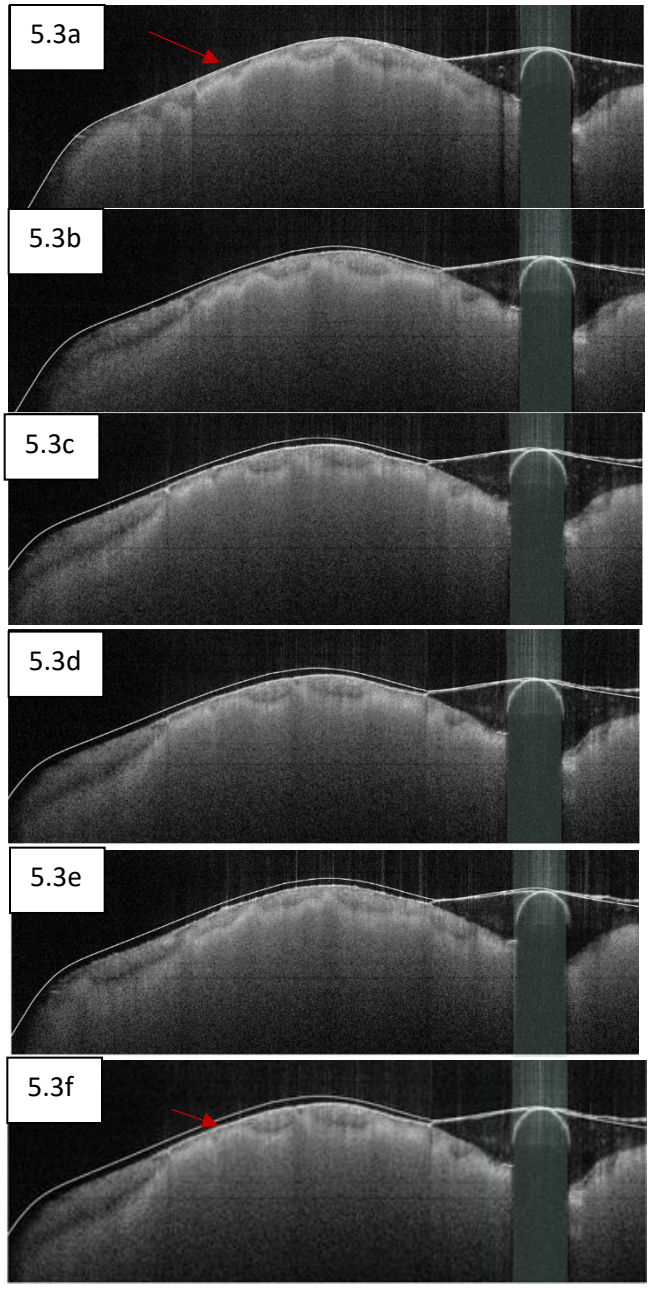

Figure 5.3 Type 21 sample in complete protection group,

5.3a (baseline image), 5.3b (20 cycles), 5.3c (40 cycles), 5.3d (60 cycles), 5.3e (80 cycles), 5.3f (100 cycles). Red arrows show the TSL between the baseline and 100 cycles images as can be seen by the gap using the white line drawn.

Children pronamel

In addition, the children pronamel group (type 22 sample, MIH 4), representing the other samples in the same group, showed a gradual TSL as presented in figure 5.4. Red arrows show the TSL and the difference between the baseline image and 100 cycles' image. The average TSL after 100 cycles in this group was 85µm compared to 99µm and 45µm in control and type 21 samples, respectively.

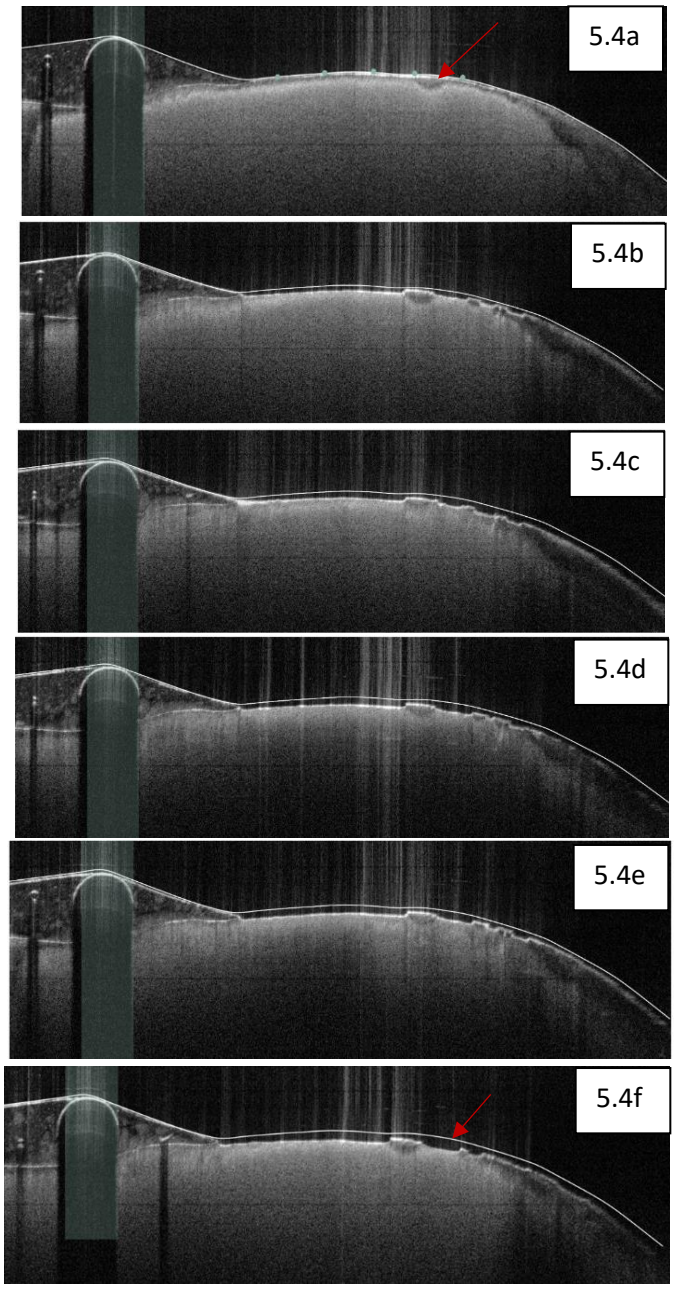

Figure 5.4 Type 22 sample in children pronamel group,

5.4a (baseline image), 5.4b (20 cycles), 5.4c (40 cycles), 5.4d (60 cycles), 5.4e (80 cycles), 5.4f (100 cycles). Red arrows show the TSL between the baseline and 100 cycles images as can be seen by the gap using the white line drawn.

It was noted from the OCT images presented in figures 5.2, 5.3, and 5.4 that the images were aligned in accordance with the reference needle. Also, the line drawn above the enamel surface showed the amount of TSL when compared with the baseline image.

Table 5.2 shows the average mean of TSL at 20, 40, 60, 80, and 100 cycles of brushing in each group, when calculated using the method described in section 4.3. In all samples, TSL increased following more cycles of brushing.

	Saliva samples	**Cycles**	**Mean TSL**	**Children pronamel samples**	**Cycles**	**Mean TSL**	**Complete protection samples**	**Cycles**	**Mean TSL**
Control group	(C 6, C 9, C 10)	20 40 60 80 100	7 µm 15 µm 17 µm 21 µm 25 µm	(C 3, C 7, C 11)	20 40 60 80 100	35 µm 44 µm 96 µm 67 µm 99 µm	(C 5, C 8, C 12)	20 40 60 80 100	52 µm 62 µm 87 µm 94 µm 93 µm
Type 21 (white/ cream)	(MIH 13, MIH 15, MIH 16)	20 40 60 80 100	10 µm 19 µm 24 µm 25 µm 30 µm	(MIH 3, MIH 10, MIH 12)	20 40 60 80 100	14 µm 19 µm 21 µm 26 µm 45 µm	(MIH 5, MIH 6, MIH 14)	20 40 60 80 100	23 µm 30 µm 35 µm 39 µm 45 µm
Type 22 (yellow/ brown)	(MIH 11, MIH 19, MIH 20)	20 40 60 80 100	36 µm 45 µm 54 µm 62 µm 63 µm	(MIH 4, MIH 8, MIH 17)	20 40 60 80 100	84 µm 62 µm 68 µm 71 µm 85 µm	(MIH 7, MIH 9, MIH 18)	20 40 60 80 100	17 µm 37 µm 44 µm 46 µm 50 µm

Table 5.2 Mean TSL at 20, 40, 60, 80, and 100 cycles of brushing.

For the final analysis, the amount of TSL in microns was tested in a regression model for each brushing group as described below.

5.4.1 Comparison in each brushing group

The regression model for control, type 21, and type 22 samples in saliva, complete protection, and children pronamel groups are represented in figures 5.5, 5.6, 5.7, 5.8, 5.9, and 5.10 respectively.

Saliva group, figure 5.5 shows positive correlation between TSL and increasing brushing cycle – as demonstrated by the positive slope of the regression. The highest positive correlation in control group was seen in sample C 10. It can be noticed that samples C 10 and C 6 have almost similar adjusted R-square values as seen in figure 5.6. These two samples are related to the same patient, which could indicate some correlation between the two numbers. Type 21 in saliva group had the highest positive correlation in sample MIH 16 compared to MIH 13 and MIH 13. In terms of the adjusted R-square value, the highest value was in sample MIH 16, indicating the best fit between the brushing cycles and TSL. In type 22 samples, the highest positive correlation was in sample MIH 19. However, sample MIH 11 showed a negative relation between the TSL and number of brushing cycles. This could be due to patient related factors as each sample responded differently as the amount of mineralization in each sample could be different which led to a higher TSL in some samples compared to the other.

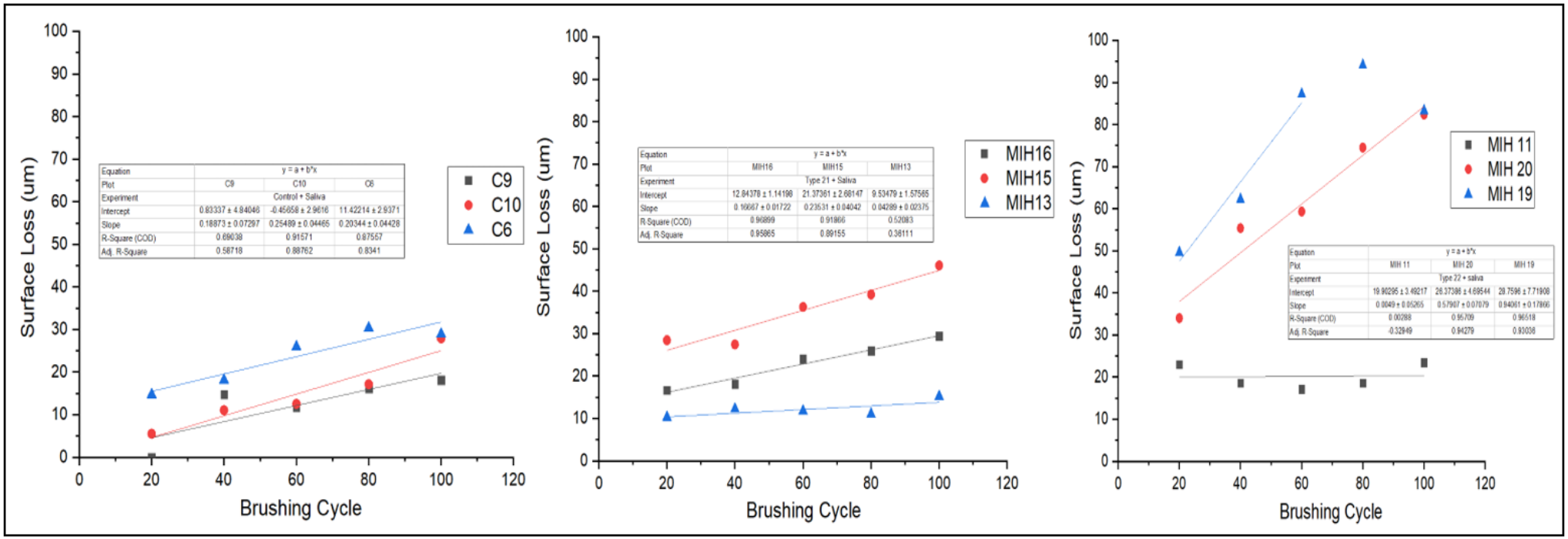

Figure 5.5 Control, type 21, and type 22 samples in saliva group

Equation	y = a + b*x		
Plot	C9	C10	C6
Experiment	Control + Saliva		
Intercept	0.83337 ± 4.84046	-0.45658 ± 2.9616	11.42214 ± 2.9371
Slope	0.18873 ± 0.07297	0.25489 ± 0.04465	0.20344 ± 0.04428
R-Square (COD)	0.69038	0.91571	0.87557
Adj. R-Square	0.58718	0.88762	0.8341

Equation	y = a + b*x		
Plot	MIH16	MIH15	MIH13
Experiment	Type 21 + Saliva		
Intercept	12.84378 ± 1.14198	21.37361 ± 2.68147	9.53479 ± 1.57565
Slope	0.16667 ± 0.01722	0.23531 ± 0.04042	0.04289 ± 0.02375
R-Square (COD)	0.96899	0.91866	0.52083
Adj. R-Square	0.95865	0.89155	0.36111

Equation	y = a + b*x		
Plot	MIH 11	MIH 20	MIH 19
Experiment	Type 22 + saliva		
Intercept	19.90295 ± 3.49217	26.37386 ± 4.69544	28.7596 ± 7.71908
Slope	0.0049 ± 0.05265	0.57907 ± 0.07079	0.94061 ± 0.17866
R-Square (COD)	0.00288	0.95709	0.96518
Adj. R-Square	-0.32949	0.94279	0.93036

Figure 5.6 Adjusted R-square numbers from the saliva group for the control, type 21, and type 22 samples.

Complete protection group, figure 5.7 shows the correlation in control, type 21, and type 22 samples that were in complete protection group. The control samples C 5 and C 8 did not show any correlation between the brushing cycles and TSL, as there was no TSL observed. However, a positive correlation between the brushing cycles and TSL was seen in sample C 12. In type 21, the highest TSL was observed in MIH 5 and the highest positive correlation was in MIH 6, as can be seen by the adjusted R-square value presented in figure 5.8. With type 22 samples, sample MIH 9 did not show a correlation between the brushing cycles and TSL. However, a positive correlation was observed with samples MIH 7 and MIH 18.

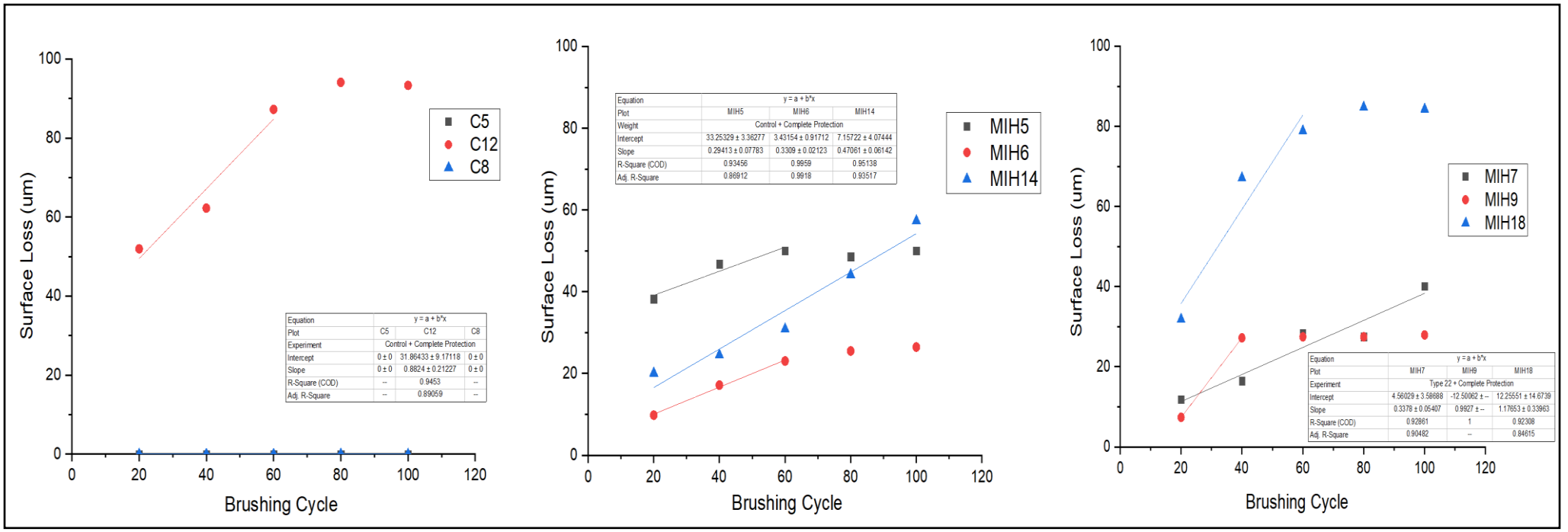

Figure 5.7 Control, type 21, and type 22 samples in complete protection group

Equation	y = a + b*x		
Plot	C5	C12	C8
Experiment	Control + Complete Protection		
Intercept	0 ± 0	31.86433 ± 9.17118	0 ± 0
Slope	0 ± 0	0.8824 ± 0.21227	0 ± 0
R-Square (COD)	--	0.9453	--
Adj. R-Square	--	0.89059	--

Equation	y = a + b*x		
Plot	MIH5	MIH6	MIH14
Weight	Type 21+ Complete Protection		
Intercept	33.25329 ± 3.36277	3.43154 ± 0.91712	7.15722 ± 4.07444
Slope	0.29413 ± 0.07783	0.3309 ± 0.02123	0.47061 ± 0.06142
R-Square (COD)	0.93456	0.9959	0.95138
Adj. R-Square	0.86912	0.9918	0.93517

Equation	y = a + b*x		
Plot	MIH7	MIH9	MIH18
Experiment	Type 22 + Complete Protection		
Intercept	4.56029 ± 3.58688	-12.50062 ± --	12.25551 ± 14.6739
Slope	0.3378 ± 0.05407	0.9927 ± --	1.17653 ± 0.33963
R-Square (COD)	0.92861	1	0.92308
Adj. R-Square	0.90482	--	0.84615

Figure 5.8 Adjusted R-square numbers from the complete protection group for the control, type 21, and type 22 samples.

Children pronamel group, all the samples in saliva group had a positive correlation between brushing cycles and TSL, with the highest rate observed in sample C 7 (figure 5.9). As for type 21 samples, a negative correlation was observed in sample MIH 12. This could be due to patient related factors, although a sample (MIH 6) from the same patient showed a positive correlation when brushed with complete protection toothpaste. In type 22 group, all the samples showed a positive correlation and the more brushing performed, the more TSL observed. The highest correlation was seen in sample MIH 4 as can be seen by the adjusted R-square value presented in figure 5.10.

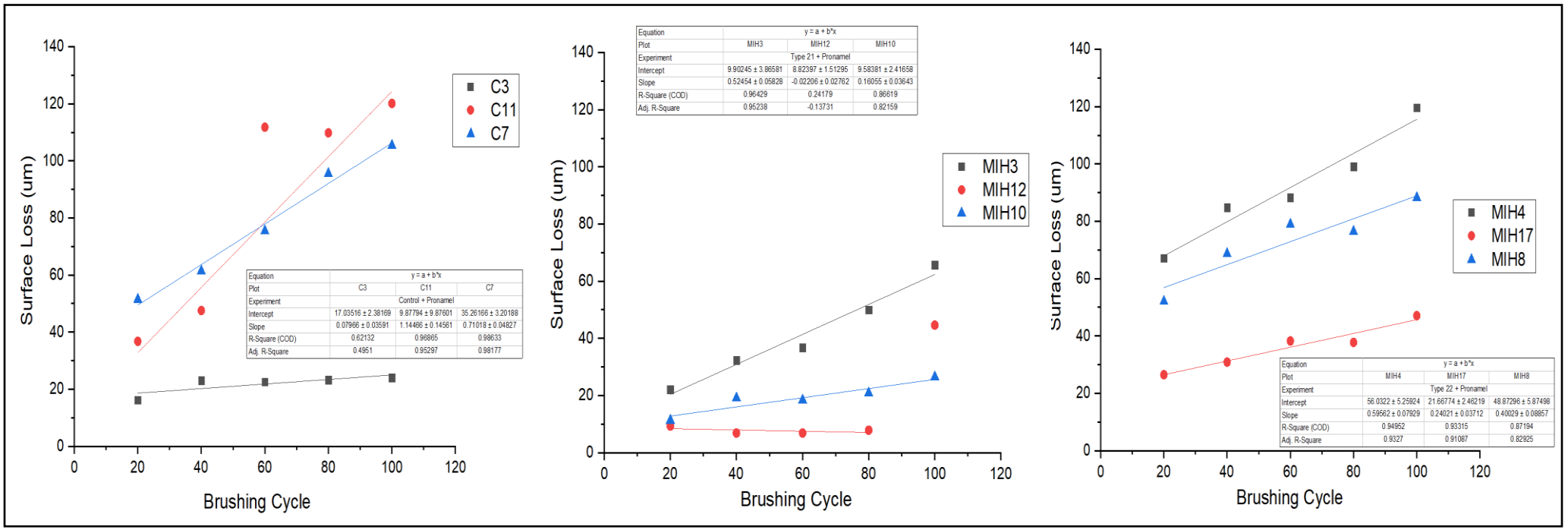

Figure 5.9 Control, type 21, and type 22 samples in children pronamel group.

Equation	y = a + b*x		
Plot	C3	C11	C7
Experiment	Control + Pronamel		
Intercept	17.03516 ± 2.38169	9.87794 ± 9.87601	35.26166 ± 3.20188
Slope	0.07966 ± 0.03591	1.14466 ± 0.14561	0.71018 ± 0.04827
R-Square (COD)	0.62132	0.96865	0.98633
Adj. R-Square	0.4951	0.95297	0.98177

Equation	y = a + b*x		
Plot	MIH3	MIH12	MIH10
Experiment	Type 21 + Pronamel		
Intercept	9.90245 ± 3.86581	8.82397 ± 1.51295	9.58381 ± 2.41658
Slope	0.52454 ± 0.05828	-0.02206 ± 0.02762	0.16055 ± 0.03643
R-Square (COD)	0.96429	0.24179	0.86619
Adj. R-Square	0.95238	-0.13731	0.82159

Equation	y = a + b*x		
Plot	MIH4	MIH17	MIH8
Experiment	Type 22 + Pronamel		
Intercept	56.0322 ± 5.25924	21.66774 ± 2.46219	48.87296 ± 5.87498
Slope	0.59562 ± 0.07929	0.24021 ± 0.03712	0.40029 ± 0.08857
R-Square (COD)	0.94952	0.93315	0.87194
Adj. R-Square	0.9327	0.91087	0.82925

Figure 5.10 Adjusted R-square numbers from the children pronamel group for the control, type 21, and type 22 samples.

5.4.2 Comparison between samples and groups

The average TSL from all the samples in each group was measured and plotted in a scatter plot. Control samples had higher TSL (99 µm) in children pronamel than complete protection and saliva after 100 cycles of brushing as shown in figure 5.11.

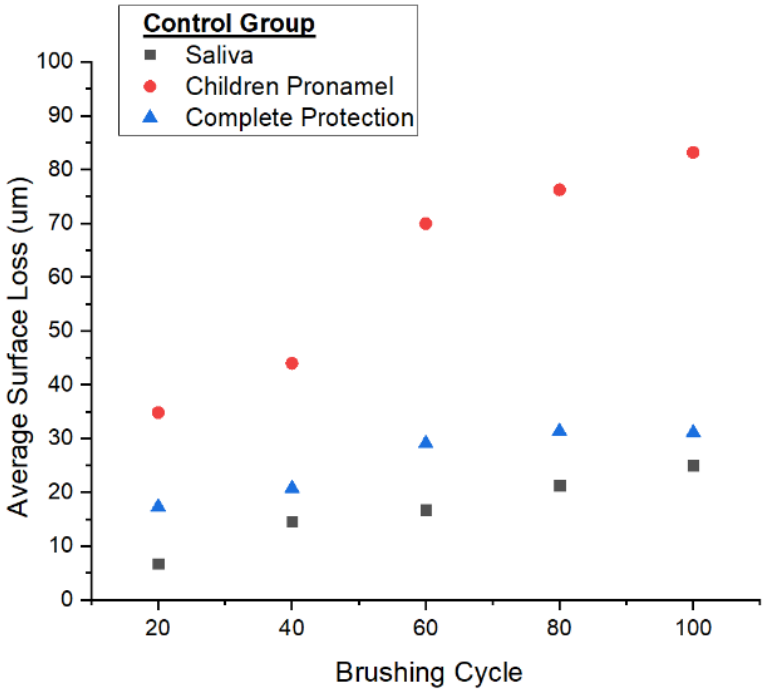

Figure 5.11 Comparison of brushing groups in control group.

In type 21 samples, children pronamel and complete protection toothpastes resulted in equal TSL (45 µm) and both were higher than saliva group after 100 cycles of brushing as shown in figure 5.12.

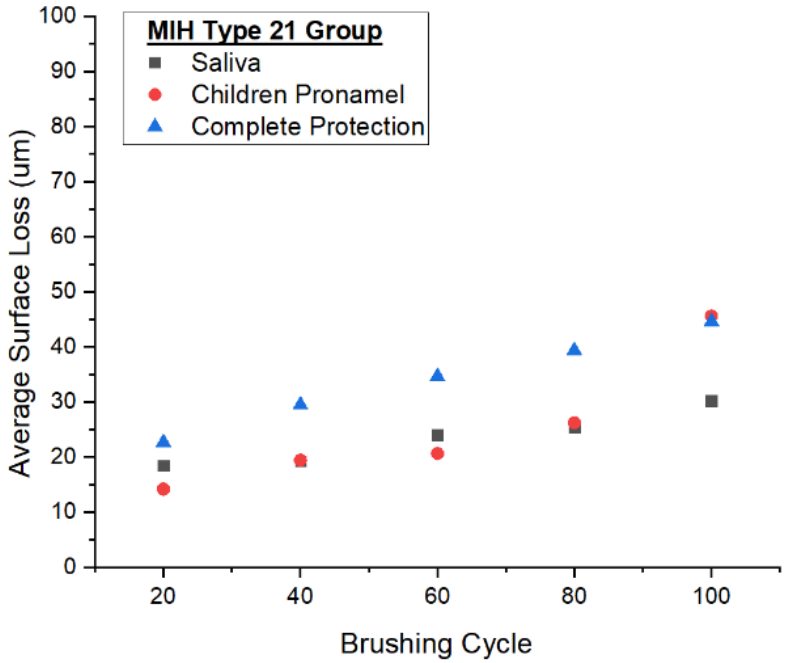

Figure 5.12 Comparison of brushing groups in type 21 group

Figure 5.13 illustrates that in type 22 samples, children pronamel resulted in a higher TSL (85 µm) than saliva and complete protection groups after 100 cycles of brushing.

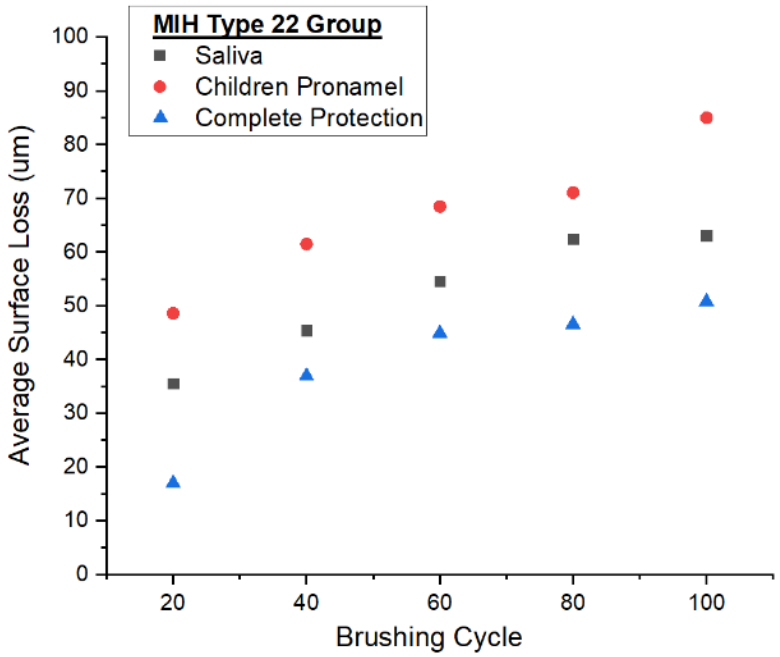

Figure 5.13 Comparison of brushing groups in type 22 group

From the 3 figures above, it can be observed that children pronamel resulted in the highest TSL in both control and type 22 groups. However, this toothpaste resulted in the lowest TSL in type 21 samples, except with at the 100 cycles of brushing, the result was similar to complete protection group.

Table 5.3 represents the confidence interval (CI) for the control, MIH type 21, and MIH type 22 groups. It can be noticed that the 95% CI in the control group lies between 23-45. The MIH type 21 groups had a 95% CI that lies between 23-32. However, type 22 group had the highest CI values as the mean loss lies between 44-61. These values indicate that the there was a difference in the mean TSL in each group.

	95% Confidence Interval			
	Mean TSL	Standard Deviation	Lower	Upper
Control Group	34.8110 µm	36.90146	23.7245	45.8974
MIH Type 21 Group	27.6266 µm	15.10587	23.0883	32.1650
MIH Type 22 Group	52.7891 µm	28.95138	44.0912	61.4871

Table 5.3 confidence intervals of each group

5.5 Discussion

In this section of the study the main objective was to perform abrasion/erosion using the brushing apparatus with electric toothbrushes and then calculate TSL from the OCT images using the protocol from pilot 3. This was performed to assess the difference of TSL between the control, MIH type 21 and type 22 samples when brushed using saliva, complete protection toothpaste, and children pronamel toothpaste. All the results were compared as explained above and more details explaining the results will be presented in the following paragraphs.

From the results it can be noted that the TSL between the samples and groups was different and did not follow a consistent pattern. This can be due to different factors such as the anatomy of the tooth sample, the degree of mineralization, and patient-related factors. For example, in the control and type 22 MIH groups, the children pronamel toothpaste resulted in more TSL than the samples brushed with saliva or complete protection toothpaste. In type 21 group, complete protection toothpaste resulted in more TSL than the saliva and children pronamel groups. These results don't indicate that children pronamel toothpaste causes more TSL as the sample size was small and such a conclusion cannot be reached. However, the Novamin® in complete protection toothpaste might have reduced the amount of TSL as this is the only difference between complete protection toothpaste and children pronamel.

Toothpastes were mixed in a slurry of artificial saliva of 3:1 ratio. Artificial saliva rather than water was used to try and mimic the clinical scenario and to enhance remineralisation of eroded enamel as saliva acts as a lubricant and conserves the dental enamel (Van Nieuw Amerongen et al., 2004). This is because it has been shown that water mixed with toothpaste results in more TSL than artificial saliva mixed with toothpaste, as the saliva is more lubricant and remineralises the enamel more than water (Attin et al., 1998). However, some studies used water mixed with toothpaste as a slurry (Binney et al., 1996, Joiner et al., 2008, Cassimiro-Silva et al., 2016).

An in vitro study concluded that brushing the samples with artificial saliva, after immersion in 0.65% citric acid or orange juice for 3 minutes, resulted in the least TSL compared to samples brushed with toothpaste slurry (Voronets and Lussi, 2010). This can explain why in current study control samples and type 21 (white/ cream) samples had the least TSL when brushed with saliva with an average of 25 µm and 30 µm at 100 cycles of brushing, respectively. However, the comparison is difficult as the immersion period in the acid was for 3 minutes compared to 30 minutes in the current study. Also, the number of brushing cycles were measured by strokes and the brushing load was less at 150 g compared to around 250 g in the present study.

Both toothpastes selected in this study contain 1450 ppm fluoride. In addition to fluoride, complete protection toothpaste has Novamin® as part of its components. Complete protection toothpaste had the lowest TSL (50 µm) in type 22 (yellow/brown) lesion after 100 cycles of brushing. This can be explained by the presence of Novamin® as it has been proven that bioglass forms a protective layer that

reduces erosion and abrasion effect (Burwell et al., 2009). Bioglass is formed of bioactive materials that react when exposed to saliva leading to deposition of calcium and phosphate (Andersson and Kangasniemi, 1991). In addition, it helps in forming a protective layer and reducing sensitivity that affects patients presented with MIH (Gillam et al., 2002, Burwell et al., 2009, Garg et al., 2012). Dentinal tubules are occluded by bioglass, which also results in reduced sensitivity (Curtis et al., 2010, Mitchell et al., 2011).

Children pronamel toothpaste resulted in the highest TSL (85 µm) in type 22 (yellow/brown) lesion after 100 cycles of brushing. However, with type 21 (white/cream) lesion, children pronamel toothpaste resulted in equal TSL (45 µm) with complete protection toothpaste after 100 cycles of brushing. This can be due to the type of the lesion, as the abrasion/erosion on white/cream lesions resulted in less TSL compared to yellow/brown lesions according to an in vitro study (Alqahtani, 2017). In their study, the TSL of type 21 lesions was between 42 to 96 µm, whereas with type 22 lesions, it ranged between 107 to 147 µm (Alqahtani, 2017).

Fluoride component in both children pronamel and complete protection toothpastes have also contributed to enamel protection and reduced TSL (Shannon and Trodahl, 1977, Wiegand and Attin, 2003). This is achieved as the NaF precipitates on the enamel surface as a CaF2-like material that results in a protective layer against abrasion and erosion challenges (Ganss et al., 2004, Magalhães et al., 2007, Rios et al., 2008). In vitro study found that fluoride in toothpastes with 1400 ppm F and 1460 ppm F protects enamel and promotes enamel re-hardening more than placebo toothpastes with 0 ppm fluoride; after exposure to 1% citric acid for 30 minutes (Fowler et al., 2006). However, the enamel wear was insignificant when a highly fluoridated toothpaste (5000 ppm F) was compared with a lower fluoridated toothpaste (1100 ppm F) in an in situ/ex vivo study (Rios et al., 2008). This could not be compared in this study as both toothpastes had equal concentrations of fluoride.

Chapter 6

Discussion

6 Discussion

6.1 Abrasion/erosion model

Most studies with erosion and/or abrasion models use human teeth or bovine teeth samples (Hooper et al., 2003, Attin et al., 2007, Wiegand et al., 2008, Wiegand et al., 2009, Moron et al., 2013). In this study, human samples were used as the enamel of MIH affected teeth was the target.

With regards to tooth wear model in this study, erosion was performed 30 minutes prior to abrasion cycles. The average duration of erosion cycles varied in the literature between 15s and 40 minutes (Wiegand and Attin, 2011). It is recommended that immersion time in erosion model should not exceed 2min/cycle for in vitro studies (Wiegand and Attin, 2011).

Many studies have demonstrated the harmful effect of soft drink consumption on children and adolescents (Al-Majed et al., 2002, Harding et al., 2003, Vartanian et al., 2007, Cheng et al., 2009, Chi and Scott, 2019). All juice drinks, bottle waters, fruit juices, and sport drinks may have erosive and cariogenic potential that cause caries and tooth wear (Tahmassebi and BaniHani, 2020). Also, studies showed a significant association between soft drinks consumption that contain high acidic content and tooth wear (Al-Majed et al., 2002, Tahmassebi et al., 2014, Pachori et al., 2018). The erosive potential of soft drinks comes from the acids such as malic acid, citric acid, phosphoric acid, and carbonic acid (Shenkin et al., 2003, Pineda et al., 2019).

Studies have used different demineralising substances to investigate erosion. One study used orange juice as an erosive substrate in an in-situ study to measure TSL and compare it with abrasive potential of different toothpastes (Hooper et al., 2003). Another study used carbonated beverage as a demineralising agent to study toothpastes with different fluoride concentrations in an in vitro study with bovine specimens (Moron et al., 2013). Other studies used citric acid as an erosive substrate due to its chelating property that results in binding to the minerals of enamel, for example calcium (Eisenburger et al., 2001, Attin et al., 2003, Hara et al., 2005). Concentrations of citric acid used to stimulate tooth wear in several studies varied between 0.1% to 5% (Hunter et al., 2000, Eisenburger et al., 2001, White et al., 2001, Attin et al., 2003, Hara et al., 2005, Voronets et al., 2008). However, most beverages contain a concentration of citric acid between 0.1% to 1% (West et al., 2001). A 1% citric acid was chosen in this study to perform as an erosive substrate due to its widespread use and to mimic high acidic beverages and soft drinks (Attin et al., 2003, Voronets et al., 2008, Voronets and Lussi, 2010). The differences between this study and the previous studies include acid application methods and TSL measurement methods.

The exposure time to acid varies in different studies. The minimum time was 1minute rinsing with citric acid to assess the remineralisation potential of artificial saliva and several minerals on bovine samples (Attin et al., 2003). Another study immersed bovine samples in 0.5% citric acid for 2 minutes to evaluate the mineral loss using OCT (Cassimiro-Silva et al., 2016). An in vitro study on MIH affected enamel

immersed the samples in 0.3% citric acid for 30 minutes as a demineralisation process (Alqahtani, 2017). In addition, 2 hours of immersion in 0.3% citric acid was implemented in an in vitro study to assess different times of remineralisation cycles in artificial saliva on the human enamel samples (Eisenburger et al., 2001). In the current study, 30 minutes immersion in citric acid was selected similar to a study that investigated the anti-erosive effect of different types of toothpastes on sound enamel surfaces (Fowler et al., 2006).

Abrasion can be delivered using electric or manual toothbrushes. Several studies used brushing machines with manual or electric toothbrushes, in which toothbrushes fixed in the toothbrush holder with maintenance of brushing force and direction (Sorensen and Nguyen, 2002, Attin et al., 2007, Wiegand et al., 2007b, Parry et al., 2008, Wiegand et al., 2013, Kumar et al., 2015). Brushing machine was used in pilot 1 with manual toothbrushes but the results were negligible because the samples were not secured and their removal from the machine affected the accuracy of the imaging. A decision was then made to shift to a custom-made apparatus with electric toothbrushes that was used in a previous study (Alqahtani, 2017). One study used powered toothbrushes to investigate the effect of brushing force on eroded dentine (Ganss et al., 2009a). Another study used an electric toothbrush, in which the brush heads were aligned parallel to the samples surface to investigate the effect of fluoride and pH concentrations in an abrasion/erosion model (Moron et al., 2013). In this study, a comparison between the brushing apparatus and the brushing machines mentioned in literature would not be possible as the purpose of using the apparatus was different in each study mentioned above and also the type of the machine.

A study comparing manual toothbrushes with electric toothbrushes found no significant difference in enamel abrasion between the two types (Wiegand et al., 2013). However, dentine abrasion was higher with manual toothbrushes than electric ones (Sorensen and Nguyen, 2002, Knezevic et al., 2010). Another study concluded that electric toothbrushes are less abrasive than the manual ones when both types were compared (Litonjua et al., 2005). In addition, studies showed that electric toothbrushes have more benefit than manual toothbrushes in decreasing gingival diseases and amount of plaque on the short and long terms (Yaacob et al., 2014, Van der Weijden and Slot, 2015). Also, brushing with soft or hard toothbrush bristles had insignificant differences in abrasion of eroded enamel (Voronets et al., 2008).

With regards to brushing force, insignificant difference in enamel abrasion was found when the brushing force was 4.5 N on sound enamel and 3.5 N on eroded enamel (Wiegand et al., 2007a). In addition, when the same brushing force was applied on a demineralised enamel, insignificant difference in enamel loss between manual and electric toothbrush noted (Wiegand et al., 2006a). The force of brushing varies in different studies between 0.2-4.5 N (Voronets et al., 2008, Ganss et al., 2009a). However, most reported brushing forces were between 2-3 N (Ganss et al., 2009b, Wiegand and Attin,

2011, Wiegand et al., 2013, Bizhang et al., 2017). In this study, 2.5 N selected for the brushing force as it is the most reported force clinically (Boyd et al., 1997, McCracken et al., 2001, Wiegand et al., 2007b).

One hundred cycles of brushing were performed, with each cycle equalling 2 minutes; equating to 50 days of brushing in accordance with a previous study (Alqahtani, 2017). A cycle of 2 minutes is the normal recommended brushing time twice per day (https://www.gov.uk/government/publications/delivering-better-oral-health-an-evidence-based-toolkit-for-prevention, 2017). One study performed brushing abrasion on extracted incisors for a period of 3 months; in which 2 cycles of 2 minutes were performed each day (Kumar et al., 2015). More brushing cycles have been performed in a study equalling a period of 8 years and 6 months to measure the effect of abrasion using 4 different types of toothbrushes (Bizhang et al., 2017).

6.2 OCT images

In this study, OCT was used to provide images of the teeth samples and help in calculating the enamel loss. OCT has been used widely in the medical field. Examples include images of the retina, monitoring retinal diseases, diagnosing cardiac and dermatological diseases, and examining hollow organs like gastrointestinal tract and bladder (Tearney et al., 1997, Jesser et al., 1999, Wang et al., 2001, Tsuboi et al., 2005, Low et al., 2006, Marschall et al., 2011).

In addition to using OCT in medical fields, in dentistry it has been used for multiple reasons and either as a quality measure or a quantity measure. One reason is to investigate the properties of enamel and dentine change in relation to demineralisation (Darling et al., 2006). Moreover, detecting caries using OCT proved to be superior to visual inspection and provides better contrast and resolution (Shimada et al., 2010, Chen et al., 2011). In regard to MIH lesions, two in vitro studies investigated the MIH lesions in terms of extent of lesions and concluded that it is a safe tool that helps to monitor patients if used clinically (Al-Azri et al., 2016, Alsabah, 2018).

Quantification of dental erosion and surface loss is limited clinically, especially in the longitudinal manner (Huysmans et al., 2011). This is because a reference would be needed each time the surface is examined, so that a comparison and quantification can be made. Example of studies using OCT to quantify the TSL include calculating the enamel loss using different types of toothpastes with different types of MIH (Alqahtani, 2017). Another in vivo study measured enamel demineralisation on patients taking anti erosive medications for GERD using OCT (Wilder Smith et al., 2009). The OCT has also been implemented in examining resin restorations and monitoring the quality of bonding between resin and dentine (Bakhsh et al., 2011). In addition, OCT was used to assess the quality and quantity of demineralised dentine affected by caries (de Azevedo et al., 2011).

The calculation of enamel loss using image J programme and measuring the enamel loss in microns from intensity profiles had been used in a previous study (Alqahtani, 2017). A similar process was

performed in this study; however, the calculation method is different. The main difference in calculation was that the study by Alqahtani measured each OCT image alone; in contrast to this study in which the baseline OCT image was compared with each image after 20, 40, 60, 80, and 100 cycles. This was done for the accuracy of the measurement as placing the baseline with each image from the cycles will ensure that the same frame of the sample was selected and compared properly. The measurement of depth of remaining enamel to DEJ can be also used to calculate the enamel loss (Wilder Smith et al., 2009). An in vitro study used OCT to quantify the micrometre gaps between resin and dentine from the OCT images and confirmed the results by comparing them with confocal laser scanning microscopy (Bakhsh et al., 2011). The above-mentioned studies used different methods of calculation compared to this study. Therefore, a direct comparison with the literature was difficult.

Another factor that has to be considered for the accuracy is the use of reference points. There are different types of reference points that can be used for the calculation of enamel loss and comparison between different images. In this study, a stainless-steel needle used as a reference point as it will not be affected by abrasion or erosion and it proved to be a more stable option compared to the literature. Subsurface characteristics have been used in a previous study as a reference (Alqahtani, 2017). Applying a varnish, as a reference that is resistant to erosion by acid, has also been utilized to cover half of enamel thereby protecting the subsurface and leaving unaffected enamel for comparison between OCT images (Fried et al., 2002, Cassimiro-Silva et al., 2016). Also, self-etch adhesive was used as a reference on the labial surface of enamel samples that were subjected to an erosive challenge (Chew et al., 2014).

In addition, indentations on the enamel surface have been performed to calculate the depth of indentations in abrasion studies using surface microhardness as a measurement method (Jaeggi and Lussi, 1999, Voronets and Lussi, 2010). Moreover, one study created indentations in dentine as a reference point to decrease variations of the b-scans when measuring enamel thickness (Algarni et al., 2016). In addition, two holes around the sides of white spot lesions have been created in one study using a laser as a guide with a distance of 2 mm away from the lesion borders (Espigares et al., 2015). However, in their study, demineralisation was not performed, and the lesion thickness was the only factor studied. In the current study, the indentations and holes cannot be created as a reference point as they will be affected by erosion from acid.

Using DEJ as a reference has also been suggested as a way of measuring TSL; in which any irregularities, indentations, or protrusions above the DEJ were noted from the baseline image and recorded as a landmark (Wilder Smith et al., 2009). However, the DEJ presents many challenges including not being a sharp boundary due to its scalloped shape and convexities and concavities directed towards dentine and enamel respectively (Chan et al., 2014). In addition, the resolution might be reduced as the light scattering is reduced after passing through enamel (Chan et al., 2014). Moreover,

if a subsurface demineralised layer is present beneath the enamel, the DEJ will not be accurately determined due to the sharp increase in light dispersing (Chan et al., 2013).

Other tools were also used to investigate TSL in abrasion/erosion studies. Optical profilometry was used in a study to quantify the surface abrasion in μm by comparing different types of toothbrushes (Bizhang et al., 2017). Other studies used scanning electron microscopy, microhardness, and atom force microscopy for calculation of surface erosion/abrasion (Jaeggi and Lussi, 1999, Voronets and Lussi, 2010, Attin and Wegehaupt, 2014, Kumar et al., 2015).

Chapter 7
Conclusion

7 Conclusion

As MIH prevalence is increasing worldwide, it was interesting to conduct this study to test the TSL in relation to MIH. In addition, the use of the OCT is increasing in the dental field. So, this study combined the use of OCT and the TSL to test the effect of different types of toothpastes on MIH affected teeth.

Different indices are available for diagnosing MIH lesions and classifying them. Also, different indices are available for measuring TSL clinically. However, this study assessed TSL on MIH affected teeth by quantifying TSL in microns using the OCT images.

The study showed that abrasion alone did not result in TSL. However, a combination of different factors including erosion/abrasion resulted in a TSL that can be measured on the OCT images.

This study showed that control samples had the least amount of TSL when brushed with saliva. Samples with white/cream lesions had equal TSL when brushed with children pronamel toothpaste and complete protection toothpaste. However, children pronamel toothpaste resulted in more TSL on MIH type 22 samples compared to complete protection toothpaste and saliva. This suggests Novamin in complete protection toothpaste may be beneficial in severely affected MIH teeth, but larger sample sizes are needed in future before a conclusion can be reached.

With regards to OCT, this study showed that clear images showing MIH lesions can be achieved and reproducibility can be maintained between the brushing cycles. It also showed the importance of reducing variations between images and how this affected the measurements of TSL.

Chapter 8
Limitations and future work

8 Limitations and future work

There are some limitations that need to be considered in a future study. For example, the types of toothpastes that were used in this study were only two. Both toothpastes contained the same amount of fluoride and the only difference was with the bioglass in complete protection. In the market and in literature, different types of toothpastes are available and were investigated. It would be interesting to compare different concentrations of fluoride such as 2800 ppm F and 5000 ppm F with 1450 ppm F, as these concentrations are usually recommended for high risk patients (https://www.gov.uk/government/publications/delivering-better-oral-health-an-evidence-based-toolkit-for-prevention, 2017). In addition, potassium nitrate can help reduce sensitivity (Nagata et al., 1994); and including a toothpaste that contain potassium nitrate and comparing it with a Novamin® toothpaste will help differentiate and identify the least abrasive material that reduces sensitivity.

The abrasivity of toothpastes should also be considered when brushing is performed and the TSL is measured. In the current study, the abrasivity of each toothpaste was not the scope of the project. However, including the abrasivity of each toothpaste will help in identifying the least abrasive toothpaste and this will reduce the TSL and sensitivity.

In addition, one type of toothbrush has been used in this study after the first pilot. Including different types of electric toothbrushes will help in discovering the effect of each toothbrush type. Moreover, the filament types of each toothbrush including soft, medium, and hard should be considered in future study as the abrasivity might be different in each type.

Another limitation in the current study is that all the abrasion cycles were completed in a single day for each sample. This was performed to maintain the position of the jack and the OCT probe in a stable position for each sample. Moreover, remineralisation periods using artificial saliva between the cycles were not considered and this does not represent the real-life scenario.

The sample size that was used in the final protocol was 27, with a total of 3 teeth in each subgroup only. Increasing the sample size in future would be more helpful for a better accuracy.

However, only one sample can be brushed using the brushing apparatus with electric toothbrushes compared with 8 samples using the manual brushing machine. The result is a total time of 5 hours per sample for brushing and scanning. This is because every 20 cycles of brushing take 40 minutes, so a total of 200 minutes for 100 cycles of brushing. Adding the erosion time of 30 minutes and scanning of 6 OCT images with 10 minutes per each scanned image equal around 5 hours. So, the long time for each sample and the fact that only one sample can be brushed in a day are limitations for the length and the sample size of the study.

The limitation of the need to use one toothbrush per 20 cycles with the risk of reduced power during the 20 cycles can be considered in future. This can be done by finding a way to keep the electric toothbrush charging while it is connected to a cable.

Although the OCT is a non-invasive device with a high resolution, its application in clinic for daily practice might be limited due to the high cost of the device (Espigares et al., 2015). Also, the system and the design require more adaptations in terms of the probe to be used intraorally (Espigares et al., 2015). In addition, the use of a reference needle can not be applied clinically and might be difficult to have a stable reference point to compare TSL in clinical situations. However, this study can be useful to test toothpastes and their abrasivity to discover the least abrasive toothpaste in relation to MIH affected teeth and recommend it to the patients.

Chapter 9
References

9 References

ABSI, E. G., ADDY, M. & ADAMS, D. 1992. Dentine hypersensitivity--the effect of toothbrushing and dietary compounds on dentine in vitro: an SEM study. *Journal of Oral Rehabilitation,* 19**,** 101-110.

ADDY, M. & HUNTER, M. L. 2003. Can tooth brushing damage your health? Effects on oral and dental tissues. *International Dental Journal,* 53 Suppl 3**,** 177-186.

AL-AZRI, K., MELITA, L. N., STRANGE, A. P., FESTY, F., AL-JAWAD, M., COOK, R., PAREKH, S. & BOZEC, L. 2016. Optical coherence tomography use in the diagnosis of enamel defects. *Journal of biomedical optics,* 21**,** 036004.

ALALUUSUA, ALALUUSUA, S., LUKINMAA, P.-L., KOSKIMIES, M., PIRINEN, S., HÖLTTÄ, P., KALLIO, M., HOLTTINEN, T. & SALMENPERÄ, L. 1996. Developmental dental defects associated with long breast feeding. *European Journal of Oral Sciences,* 104**,** 493-497.

ALALUUSUA, S. 2010. Aetiology of molar-incisor hypomineralisation: a systematic review. *European Archives of Paediatric Dentistry,* 11**,** 53-58.

ALGARNI, A., KANG, H., FRIED, D., ECKERT, G. J. & HARA, A. T. 2016. Enamel thickness determination by optical coherence tomography: in vitro validation. *Caries research,* 50**,** 400-406.

ALGHILAN, M. A., LIPPERT, F., PLATT, J. A., ECKERT, G. J., GONZÁLEZ-CABEZAS, C., FRIED, D. & HARA, A. T. 2019. In vitro longitudinal evaluation of enamel wear by cross-polarization optical coherence tomography. *Dental Materials,* 35**,** 1464-1470.

ALLAZZAM, S. M., ALAKI, S. M. & EL MELIGY, O. A. S. 2014. Molar incisor hypomineralization, prevalence, and etiology. *International journal of dentistry,* 2014.

ALQAHTANI, M. 2017. *The impact of tooth brushing on enamel affected by molar incisor hypomineralisation (MIH).*

ALSABAH, D. K. 2018. The investigation of optical coherence tomography as a clinical tool to determine the extent of molar incisor hypomineralisation (MIH) lesions. UCL (University College London).

ANDERSSON, Ö. & KANGASNIEMI, I. 1991. Calcium phosphate formation at the surface of bioactive glass in vitro. *Journal of biomedical materials research,* 25**,** 1019-1030.

ARROW, P. 2009. Risk factors in the occurrence of enamel defects of the first permanent molars among schoolchildren in Western Australia. *Community dentistry and oral epidemiology,* 37**,** 405-415.

ATTIN, T., WEGEHAUPT, F., GRIES, D. & WIEGAND, A. 2007. The potential of deciduous and permanent bovine enamel as substitute for deciduous and permanent human enamel: Erosion–abrasion experiments. *Journal of dentistry,* 35**,** 773-777.

AZARPAZHOOH, A. & LIMEBACK, H. 2008. Clinical Efficacy of Casein Derivatives. *Journal of the American Dental Association,* 139**,** 915-924.

BALMER, R., TOUMBA, J., GODSON, J. & DUGGAL, M. 2012. The prevalence of molar incisor hypomineralisation in Northern England and its relationship to socioeconomic status and water fluoridation. *International journal of paediatric dentistry,* 22**,** 250-257.

BARDSLEY, P., TAYLOR, S. & MILOSEVIC, A. 2004. Epidemiological studies of tooth wear and dental erosion in 14-year-old children in North West England. Part 1: The relationship with water fluoridation and social deprivation. *British dental journal,* 197**,** 413-416.

BARTLETT, D., GANSS, C. & LUSSI, A. 2008. Basic Erosive Wear Examination (BEWE): a new scoring system for scientific and clinical needs. *Clinical oral investigations,* 12**,** 65-68.

BARTLETT, D., PHILLIPS, K. & SMITH, B. 1999. A difference in perspective--the North American and European interpretations of tooth wear. *International journal of prosthodontics,* 12.

BARTLETT, D. & SMITH, B. G. 2000. Definition, classification and clinical assessment of attrition, erosion and abrasion of enamel and dentine. *Tooth Wear and Sensitivity. London, Martin Dunitz***,** 87-92.

BEENTJES, V., WEERHEIJM, K. & GROEN, H. 2002. Factors involved in the aetiology of molar-incisor hypomineralisation (MIH). *European Journal of Paediatric Dentistry,* 3**,** 9-13.

BENIASH, E., METZLER, R. A., LAM, R. S. & GILBERT, P. 2009. Transient amorphous calcium phosphate in forming enamel. *Journal of structural biology,* 166**,** 133-143.

BIESBROCK, A. R., GERLACH, R. W., BOLLMER, B. W., FALLER, R. V., JACOBS, S. A. & BARTIZEK, R. D. 2001. Relative anti-caries efficacy of 1100, 1700, 2200, and 2800 ppm fluoride ion in a sodium fluoride dentifrice over 1 year. *Community dentistry and oral epidemiology,* 29**,** 382-389.

BISHOP, K., KELLEHER, M., BRIGGS, P. & JOSHI, R. 1997. Wear now? An update on the etiology of tooth wear. *Quintessence International,* 28.

BLONG, M., VOLDING, B., THRASH, W. & JONES, D. 1985. Effects of a gel containing 0.4 percent stannous fluoride on dentinal hypersensitivity. *Dental hygiene,* 59**,** 489.

BOUMA, B. 2001. *Handbook of optical coherence tomography*, CRC Press.

BOZAL, C. B., KAPLAN, A., ORTOLANI, A., CORTESE, S. G. & BIONDI, A. M. 2015. Ultrastructure of the surface of dental enamel with molar incisor hypomineralization (MIH) with and without acid etching. *Acta Odontológica Latinoamericana,* 28**,** 192-198.

BURWELL, A., LITKOWSKI, L. & GREENSPAN, D. 2009. Calcium sodium phosphosilicate (NovaMin®): remineralization potential. *Advances in Dental Research,* 21**,** 35-39.

CASSIMIRO-SILVA, P. F., MAIA, A. M. A., DE MELO MONTEIRO, G. Q. & GOMES, A. S. L. Mitigation of enamel erosion using commercial toothpastes evaluated with optical coherence tomography. Sixth International Conference on Lasers in Medicine, 2016. International Society for Optics and Photonics, 96700Y.

CHAN, Y., NGAN, A. & KING, N. 2010. Degraded prism sheaths in the transition region of hypomineralized teeth. *Journal of dentistry,* 38**,** 237-244.

CHAWLA, N., MESSER, L. B. & SILVA, M. 2008. Clinical Studies on Molar-Incisor-Hypomineralisation Part 2: Development of a Severity Index. *European Archives of Paediatric Dentistry,* 9**,** 191-199.

CHEN, Y. L., YANG, Y., MA, J., YAN, J., SHOU, Y., WANG, T., RAMESH, A., ZHAO, J. & ZHU, Q. 2011. 3D imaging of dental hard tissues with Fourier domain optical coherence tomography.

CHEW, H. P., ZAKIAN, C. M., PRETTY, I. A. & ELLWOOD, R. P. 2014. Measuring Initial Enamel Erosion with Quantitative Light-Induced Fluorescence and Optical Coherence Tomography: An in vitro Validation Study. *Caries Research,* 48**,** 254-262.

CLARKSON, D. M. G. 2014. An update on optical coherence tomography in dentistry. *Dental update,* 41**,** 174.

CLARKSON, J. 1992. FDI commission on oral health, research & epidemiology. A review of the developmental defects of enamel index (DDE Index). *Int Dent J,* 42**,** 411-426.

CLEMENTINO-LUEDEMANN, T. N. R. & KUNZELMANN, K.-H. 2006. Mineral concentration of natural human teeth by a commercial micro-CT. *Dental materials journal,* 25**,** 113-119.

CROMBIE, F. A., MANTON, D. J., PALAMARA, J. E., ZALIZNIAK, I., COCHRANE, N. J. & REYNOLDS, E. C. 2013. Characterisation of developmentally hypomineralised human enamel. *Journal of dentistry,* 41**,** 611-618.

CURTIS, A., WEST, N. & SU, B. 2010. Synthesis of nanobioglass and formation of apatite rods to occlude exposed dentine tubules and eliminate hypersensitivity. *Acta biomaterialia,* 6**,** 3740-3746.

DARLING, C. L., HUYNH, G. & FRIED, D. 2006. Light scattering properties of natural and artificially demineralized dental enamel at 1310 nm. *Journal of biomedical optics,* 11**,** 034023.

DAVE, M. & TAYLOR, G. 2018. Global prevalence of molar incisor hypomineralisation. *Evidence-based dentistry,* 19**,** 78-79.

DAVIES, R., SCULLY, C. & PRESTON, A. J. 2010. Dentifrices-an update. *Med Oral Patol Oral Cir Bucal,* 15**,** e976-82.

DAVIES, R. M. 2004. What's in toothpaste and why? *Dental update,* 31**,** 67-71.

DIETRICH, G., SPERLING, S. & HETZER, G. 2003. Molar incisor hypomineralisation in a group of children and adolescents living in Dresden (Germany). *European Journal of Paediatric Dentistry,* 4**,** 133-137.

DURMUS, B., ABBASOGLU, Z. & KARGUL, B. 2013. Possible medical aetiological factors and characteristics of molar incisor hypomineralisation in a group of turkish children. *Acta stomatologica Croatica,* 47**,** 297-305.

DYER, D., ADDY, M. & NEWCOMBE, R. G. 2000. Studies in vitro of abrasion by different manual toothbrush heads and a standard toothpaste. *Journal of Clinical Periodontology,* 27**,** 99-103.

EARL, J., LEARY, R., MULLER, K., LANGFORD, R. & GREENSPAN, D. 2011. Physical and chemical characterization of dentin surface following treatment with NovaMin technology. *The Journal of clinical dentistry,* 22**,** 62-67.

ELFRINK, M. E. C., GHANIM, A., MANTON, D. J. & WEERHEIJM, K. L. 2015. Standardised studies on Molar Incisor Hypomineralisation (MIH) and Hypomineralised Second Primary Molars (HSPM): a need. *European Archives of Paediatric Dentistry,* 16**,** 247-255.

ELFRINK, M. E. C., SCHULLER, A. A., WEERHEIJM, K. L. & VEERKAMP, J. S. J. 2008. Hypomineralized Second Primary Molars: Prevalence Data in Dutch 5-Year-Olds. *Caries Research,* 42**,** 282-285.

ELHENNAWY, K., MANTON, D., CROMBIE, F., ZASLANSKY, P., RADLANSKI, R., JOST BRINKMANN, P.-G. & SCHWENDICKE, F. 2017. Structural, mechanical and chemical evaluation of molar-incisor hypomineralization-affected enamel: A systematic review. *Archives of oral biology,* 83**,** 272-281.

ESPIGARES, J., SADR, A., HAMBA, H., SHIMADA, Y., OTSUKI, M., TAGAMI, J. & SUMI, Y. 2015. Assessment of natural enamel lesions with optical coherence tomography in comparison with microfocus x-ray computed tomography. *Journal of Medical Imaging,* 2**,** 014001.

FAGRELL, T. G., DIETZ, W., JÄLEVIK, B. & NORÉN, J. G. 2010. Chemical, mechanical and morphological properties of hypomineralized enamel of permanent first molars. *Acta Odontologica Scandinavica,* 68**,** 215-222.

FAGRELL, T. G., LUDVIGSSON, J., ULLBRO, C., LUNDIN, S.-A. & KOCH, G. 2011. Aetiology of severe demarcated enamel opacities-an evaluation based on prospective medical and social data from 17,000 children. *Swed Dent J,* 35**,** 57-67.

FALLER, R. V., EVERSOLE, S. L. & TZEGHAI, G. E. 2011. Enamel protection: a comparison of marketed dentifrice performance against dental erosion. *American Journal of Dentistry,* 24**,** 205.

FAN, Y., NELSON, J. R., ALVAREZ, J. R., HAGAN, J., BERRIER, A. & XU, X. 2011. Amelogenin-assisted ex vivo remineralization of human enamel: Effects of supersaturation degree and fluoride concentration. *Acta biomaterialia,* 7**,** 2293-2302.

FARAH, R. A., MONK, B. C., SWAIN, M. V. & DRUMMOND, B. K. 2010. Protein content of molar–incisor hypomineralisation enamel. *Journal of dentistry,* 38**,** 591-596.

FEARNE, J., ANDERSON, P. & DAVIS, G. 2004. 3D X-ray microscopic study of the extent of variations in enamel density in first permanent molars with idiopathic enamel hypomineralisation. *British dental journal,* 196**,** 634.

FERCHER, A. F., HITZENBERGER, C. K., KAMP, G. & EL-ZAIAT, S. Y. 1995. Measurement of intraocular distances by backscattering spectral interferometry. *Optics communications,* 117**,** 43-48.

FINCHAM, A., MORADIAN-OLDAK, J., DIEKWISCH, T., LYARUU, D., WRIGHT, J., BRINGAS JR, P. & SLAVKIN, H. 1995. Evidence for amelogenin" nanospheres" as functional components of secretory-stage enamel matrix. *Journal of structural biology,* 115**,** 50-59.

FINCHAM, A., MORADIAN-OLDAK, J. & SIMMER, J. 1999. The structural biology of the developing dental enamel matrix. *Journal of structural biology,* 126**,** 270-299.

FINCHAM, A. G. & SIMMER, J. P. Amelogenin proteins of developing dental enamel. Ciba Foundation Symposium 205-Dental Enamel: Dental Enamel: Ciba Foundation Symposium 205, 2007. Wiley Online Library, 118-134.

FTEITA, D., ALI, A. & ALALUUSUA, S. 2006. Molar-incisor hypomineralization (MIH) in a group of school-aged children in Benghazi, Libya. *European Archives of Paediatric Dentistry,* 1**,** 92-95.

FUJIMOTO, J. & DREXLER, W. 2008. Introduction to optical coherence tomography. *Optical coherence tomography.* Springer.
GANSS, C., KLIMEK, J., BRUNE, V. & SCHÜRMANN, A. 2004. Effects of two fluoridation measures on erosion progression in human enamel and dentine in situ. *Caries Research,* 38**,** 561-566.
GANSS, C., LUSSI, A., GRUNAU, O., KLIMEK, J. & SCHLUETER, N. 2011. Conventional and Anti-Erosion Fluoride Toothpastes: Effect on Enamel Erosion and Erosion-Abrasion. *Caries Research,* 45**,** 581-589.
GARG, N., JAIN, A. K., SAHA, S. & SINGH, J. 2012. Essentiality of early diagnosis of molar incisor hypomineralization in children and review of its clinical presentation, etiology and management. *International journal of clinical pediatric dentistry,* 5**,** 190.
GHANIM, A., ELFRINK, M., WEERHEIJM, K., MARIÑO, R. & MANTON, D. 2015. A practical method for use in epidemiological studies on enamel hypomineralisation. *European Archives of Paediatric Dentistry,* 16**,** 235-246.
GHANIM, A., MANTON, D., BAILEY, D., MARINO, R. & MORGAN, M. 2013a. Risk factors in the occurrence of molar–incisor hypomineralization amongst a group of Iraqi children. *International journal of paediatric dentistry,* 23**,** 197-206.
GHANIM, A., MARIÑO, R., MORGAN, M., BAILEY, D. & MANTON, D. 2013b. Anin vivoinvestigation of salivary properties, enamel hypomineralisation, and carious lesion severity in a group of Iraqi schoolchildren. *International Journal of Paediatric Dentistry,* 23**,** 2-12.
GHANIM, A., MORGAN, M., MARINO, R., BAILEY, D. & MANTON, D. 2011. Molar-incisor hypomineralisation: prevalence and defect characteristics in Iraqi children. *International journal of paediatric dentistry,* 21**,** 413-421.
GILLAM, D., TANG, J., MORDAN, N. & NEWMAN, H. 2002. The effects of a novel Bioglass® dentifrice on dentine sensitivity: a scanning electron microscopy investigation. *Journal of Oral Rehabilitation,* 29**,** 305-313.
GRAHNEN, H. & SELANDER, P. 1954. The effect of rickets and spasmophilia on the permanent dentition. I. The effect on the teeth. *Odontologisk revy,* 5**,** 7.
GRIPPO, J. O. 1991. Abfractions: a new classification of hard tissue lesions of teeth. *Journal of Esthetic and Restorative Dentistry,* 3**,** 14-19.
GROBLER, S., SENEKAL, P. & KOTZE, T. 1989. The degree of enamel erosion by five different kinds of fruit. *Clinical preventive dentistry,* 11**,** 23-28.
HAITER-NETO, F., WENZEL, A. & GOTFREDSEN, E. 2008. Diagnostic accuracy of cone beam computed tomography scans compared with intraoral image modalities for detection of caries lesions. *Dentomaxillofacial Radiology,* 37**,** 18-22.
HALL, A., BUCHANAN, C., MILLETT, D., CREANOR, S., STRANG, R. & FOYE, R. 1999. The effect of saliva on enamel and dentine erosion. *Journal of dentistry,* 27**,** 333-339.
HTTPS://WWW.GOV.UK/GOVERNMENT/PUBLICATIONS/DELIVERING-BETTER-ORAL-HEALTH-AN-EVIDENCE-BASED-TOOLKIT-FOR-PREVENTION. 2017. *Delivering better oral health: An evidence-based toolkit for prevention* [Online]. [Accessed 15 June 2020].
HU, D., ZHANG, Y. P., CHAKNIS, P., PETRONE, M. E., VOLPE, A. & DEVIZIO, W. 2004. Comparative investigation of the desensitizing efficacy of a new dentifrice containing 5.5% potassium citrate: an eight-week clinical study. *The Journal of clinical dentistry,* 15**,** 6-10.
HU, J. C. C., CHUN, Y. H. P., AL HAZZAZZI, T. & SIMMER, J. P. 2007. Enamel Formation and Amelogenesis Imperfecta. *Cells Tissues Organs,* 186**,** 78-85.
HUANG, D., SWANSON, E., LIN, C., SCHUMAN, J., STINSON, W., CHANG, W., HEE, M., FLOTTE, T., GREGORY, K., PULIAFITO, C. & ET, A. 1991. Optical coherence tomography. *Science,* 254**,** 1178-1181.
IIJIMA, M. & MORADIAN-OLDAK, J. 2004. Control of octacalcium phosphate and apatite crystal growth by amelogenin matrices. *Journal of Materials Chemistry,* 14**,** 2189-2199.
IMFELD, T. 1996. Dental erosion. Definition, classification and links. *European journal of oral sciences,* 104**,** 151-155.

JÄLEVIK, B. 2010. Prevalence and diagnosis of molar-incisor-hypomineralisation (MIH): a systematic review. *European archives of paediatric dentistry,* 11**,** 59-64.
JÄLEVIK, B., DIETZ, W. & NOREN, J. G. 2005. Scanning electron micrograph analysis of hypomineralized enamel in permanent first molars. *International Journal of Paediatric Dentistry,* 15**,** 233-240.
JÄLEVIK, B. & KLINGBERG, G. 2002. Dental treatment, dental fear and behaviour management problems in children with severe enamel hypomineralization of their permanent first molars. *International Journal of Paediatric Dentistry,* 12**,** 24-32.
JÄLEVIK, B., NOREN, J., KLINGBERG, G. & BARREGARD, L. 2001. Etiologic factors influencing the prevalence of demarcated opacities in permanent first molars in a group of Swedish children. *European Journal of Oral Sciences,* 109**,** 230-234.
JAN, J., SOVCIKOVA, E., KOČAN, A., WSOLOVA, L. & TRNOVEC, T. 2007. Developmental dental defects in children exposed to PCBs in eastern Slovakia. *Chemosphere,* 67**,** S350-S354.
JAN, J. & VRBIČ, V. 2000. Polychlorinated Biphenyls Cause Developmental Enamel Defects in Children. *Caries Research,* 34**,** 469-473.
JESSER, C., BOPPART, S., PITRIS, C., STAMPER, D., NIELSEN, G. P., BREZINSKI, M. & FUJIMOTO, J. 1999. High resolution imaging of transitional cell carcinoma with optical coherence tomography: feasibility for the evaluation of bladder pathology. *The British journal of radiology,* 72**,** 1170-1176.
JOHANSSON, A.-K., JOHANSSON, A., BIRKHED, D., OMAR, R., BAGHDADI, S. & CARLSSON, G. E. 1996. Dental erosion, soft-drink intake, and oral health in young Saudi men, and the development of a system for assessing erosive anterior tooth wear. *Acta Odontologica Scandinavica,* 54**,** 369-378.
JONES, J. R. 2013. Review of bioactive glass: from Hench to hybrids. *Acta biomaterialia,* 9**,** 4457-4486.
KAIDONIS, J. A. 2008. Tooth wear: the view of the anthropologist. *Clinical oral investigations,* 12**,** 21-26.
KAISER, P. K., BLODI, B. A., SHAPIRO, H., ACHARYA, N. R. & GROUP, M. S. 2007. Angiographic and optical coherence tomographic results of the MARINA study of ranibizumab in neovascular age-related macular degeneration. *Ophthalmology,* 114**,** 1868-1875. e4.
KARAN, K., YAO, X., XU, C. & WANG, Y. 2009. Chemical profile of the dentin substrate in non-carious cervical lesions. *Dental materials,* 25**,** 1205-1212.
KELLEHER, M. & BISHOP, K. 1999. Tooth surface loss: an overview. *British Dental Journal,* 186**,** 61.
KEMOLI, A. 2008. Prevalence of molar incisor hypomineralisation in six to eight year-olds in two rural divisions in Kenya. *East African medical journal,* 85**,** 514-520.
KIM, J.-M., KANG, S.-R. & YI, W.-J. 2017. Automatic detection of tooth cracks in optical coherence tomography images. *Journal of periodontal & implant science,* 47**,** 41-50.
KREULEN, C. M., VAN 'T SPIJKER, A., RODRIGUEZ, J. M., BRONKHORST, E. M., CREUGERS, N. H. J. & BARTLETT, D. W. 2010. Systematic Review of the Prevalence of Tooth Wear in Children and Adolescents. *Caries Research,* 44**,** 151-159.
KÜHNISCH, J., MACH, D., THIERING, E., BROCKOW, I., HOFFMANN, U., NEUMANN, C., HEINRICH-WELTZIEN, R., BAUER, C. P., BERDEL, D. & KOLETZKO, S. 2014. Respiratory diseases are associated with molar-incisor hypomineralizations. *Swiss dental journal,* 124**,** 286-293.
KUKLEVA, M. 2008. Molar incisor hypomineralisation in 7-to-14-year old children in Plovdiv, Bulgaria--an epidemiologic study. *Folia Medica,* 50**,** 71-5.
KUSCU, O., ÇAGLAR, E., ASLAN, S., DURMUSOGLU, E., KARADEMIR, A. & SANDALLI, N. 2009. The prevalence of molar incisor hypomineralization (MIH) in a group of children in a highly polluted urban region and a windfarm-green energy island. *International Journal of Paediatric Dentistry,* 19**,** 176-185.
KUTSCH, V. K. 2013. Reconsidering remineralization strategies to include nanoparticle hydroxyapatite. *Compendium of continuing education in dentistry,* 34**,** 170-6.

LAISI, S., KIVIRANTA, H., LUKINMAA, P., VARTIAINEN, T. & ALALUUSUA, S. 2008. Molar-incisor-hypomineralisation and dioxins: new findings. *European Archives of Paediatric Dentistry,* 9**,** 224-227.

LEPPANIEMI, A., LUKINMAA, P.-L. & ALALUUSUA, S. 2001. Nonfluoride hypomineralizations in the permanent first molars and their impact on the treatment need. *Caries research,* 35**,** 36-40.

LEVRINI, L., DI BENEDETTO, G. & RASPANTI, M. 2014. Dental Wear: A Scanning Electron Microscope Study. *BioMed Research International,* 2014**,** 1-7.

LI, X., WANG, J., JOINER, A. & CHANG, J. 2014. The remineralisation of enamel: a review of the literature. *Journal of dentistry,* 42**,** S12-S20.

LITONJUA, L., ANDREANA, S., BUSH, P. & COHEN, R. 2003. Tooth wear: attrition, erosion, and abrasion. *Quintessence international,* 34**,** 435-446.

LIU, B. & BREZINSKI, M. E. 2007. Theoretical and practical considerations on detection performance of time domain, Fourier domain, and swept source optical coherence tomography. *Journal of biomedical optics,* 12**,** 044007.

LOPEZ FRIAS, F. J., CASTELLANOS COSANO, L., MARTIN GONZALEZ, J., LLAMAS CARRERAS, J. M. & SEGURA EGEA, J. J. 2012. Clinical measurement of tooth wear: Tooth Wear Indices. *Journal of Clinical and Experimental Dentistry,* 4**,** e48-e53.

LOW, A. F., TEARNEY, G. J., BOUMA, B. E. & JANG, I.-K. 2006. Technology insight: optical coherence tomography—current status and future development. *Nature Reviews Cardiology,* 3**,** 154.

LUSSI, A., JAEGGI, T. & SCHÄRER, S. 1993. The influence of different factors on in vitro enamel erosion. *Caries research,* 27**,** 387-393.

LYGIDAKIS, N., DIMOU, G. & MARINOU, D. 2008. Molar-Incisor-Hypomineralisation (MIH). A retrospective clinical study in Greek children. II. Possible medical aetiological factors. *European Archives of Paediatric Dentistry,* 9**,** 207-217.

LYGIDAKIS, N., WONG, F., JÄLEVIK, B., VIERROU, A., ALALUUSUA, S. & ESPELID, I. 2010. Best Clinical Practice Guidance for clinicians dealing with children presenting with Molar-Incisor-Hypomineralisation (MIH). *European Archives of Paediatric Dentistry,* 11**,** 75-81.

LYGIDAKIS, N. A., DIMOU, G. & STAMATAKI, E. 2009. Retention of fissure sealants using two different methods of application in teeth with hypomineralised molars (MIH): A 4 year clinical study. *European Archives of Paediatric Dentistry,* 10**,** 223-226.

MACHOY, M., SEELIGER, J., SZYSZKA-SOMMERFELD, L., KOPROWSKI, R., GEDRANGE, T. & WOŹNIAK, K. 2017. The use of optical coherence tomography in dental diagnostics: a state-of-the-art review. *Journal of healthcare engineering,* 2017.

MAGALHAES, A., WIEGAND, A. & BUZALAF, M. A. R. 2014. Use of dentifrices to prevent erosive tooth wear: harmful or helpful? *Brazilian Oral Research,* 28 Spec No**,** 1-6.

MAHONEY, E., ISMAIL, F. S. M., KILPATRICK, N. & SWAIN, M. 2004. Mechanical properties across hypomineralized/hypoplastic enamel of first permanent molar teeth. *European journal of oral sciences,* 112**,** 497-502.

MAJKUT, P., SADR, A., SHIMADA, Y., SUMI, Y. & TAGAMI, J. 2015. Validation of optical coherence tomography against micro–computed tomography for evaluation of remaining coronal dentin thickness. *Journal of endodontics,* 41**,** 1349-1352.

MARCAUTEANU, C., BRADU, A., SINESCU, C., TOPALA, F. I., NEGRUTIU, N. L. & PODOLEANU, A. G. 2013. Quantitative evaluation of dental abfraction and attrition using a swept-source optical coherence tomography system. *Journal of Biomedical Optics,* 19**,** 021108.

MARGOLIS, H., BENIASH, E. & FOWLER, C. 2006. Role of macromolecular assembly of enamel matrix proteins in enamel formation. *Journal of dental research,* 85**,** 775-793.

MARINHO, V., HIGGINS, J., SHEIHAM, A. & LOGAN, S. 2003. Fluoride toothpastes for preventing dental caries in children and adolescents. *Cochrane Database Syst Rev,* 1.

MARSCHALL, S., SANDER, B., MOGENSEN, M., JØRGENSEN, T. & ANDERSEN, P. 2011. Optical coherence tomography—current technology and applications in clinical and biomedical research. *Analytical and Bioanalytical Chemistry,* 400**,** 2699-2720.

MAST, P., RODRIGUEZTAPIA, M. T., DAENIKER, L. & KREJCI, I. 2013. Understanding MIH: definition, epidemiology, differential diagnosis and new treatment guidelines. *Eur J Paediatr Dent,* 14**,** 204-8.

MCKNIGHT-HANES, C. & WHITFORD, G. M. 1992. Fluoride release from three glass ionomer materials and the effects of varnishing with or without finishing. *Caries research,* 26**,** 345-350.

MEURMAN, J. & TEN GATE, J. 1996. Pathogenesis and modifying factors of dental erosion. *European Journal of Oral Sciences,* 104**,** 199-206.

MILOSEVIC, A., BRODIE, D. A. & SLADE, P. D. 1997. Dental erosion, oral hygiene, and nutrition in eating disorders. *International Journal of Eating Disorders,* 21**,** 195-199.

MITCHELL, J. C., MUSANJE, L. & FERRACANE, J. L. 2011. Biomimetic dentin desensitizer based on nano-structured bioactive glass. *Dental Materials,* 27**,** 386-393.

MOGENSEN, M., NÜRNBERG, B., FORMAN, J., THOMSEN, J. B., THRANE, L. & JEMEC, G. 2009. In vivo thickness measurement of basal cell carcinoma and actinic keratosis with optical coherence tomography and 20-MHz ultrasound. *British Journal of Dermatology,* 160**,** 1026-1033.

MOHD NOOR, M. 2014. Phenotypic properties of enamel in molarincisor hypomineralisation (mih) and amelogenesis imperfecta (ai) teeth. ProQuest Dissertations Publishing.

MOHLER, K. J., DRAXINGER, W., KLEIN, T., KOLB, J. P., WIESER, W., HARITOGLOU, C., KAMPIK, A., FUJIMOTO, J. G., NEUBAUER, A. S. & HUBER, R. 2015. Combined 60 wide-field choroidal thickness maps and high-definition en face vasculature visualization using swept-source megahertz OCT at 1050 nm. *Investigative ophthalmology & visual science,* 56**,** 6284-6293.

MORADIAN-OLDAK, J. 2001. Amelogenins: assembly, processing and control of crystal morphology. *Matrix Biology,* 20**,** 293-305.

NAGATA, T., ISHIDA, H., SHINOHARA, H., NISHIKAWA, S., KASAHARA, S., WAKANO, Y., DAIGEN, S. & TROULLOS, E. S. 1994. Clinical evaluation of a potassium nitrate dentifrice for the treatment of dentinal hypersensitivity. *Journal of clinical periodontology,* 21**,** 217-221.

NAKAGAWA, H., SADR, A., SHIMADA, Y., TAGAMI, J. & SUMI, Y. 2013. Validation of swept source optical coherence tomography (SS-OCT) for the diagnosis of smooth surface caries in vitro. *Journal of dentistry,* 41**,** 80-89.

NANCI, A. 2014. *Ten Cate's Oral Histology : Development, Structure, and Function (8th Edition)*.

NATSUME, Y., NAKASHIMA, S., SHIMADA, Y., SADR, A., TAGAMI, J. & SUMI, Y. 2011. Estimation of lesion progress in artificial root caries by swept source optical coherence tomography in comparison to transverse microradiography. *Journal of biomedical optics,* 16**,** 071408.

OLIVER, K., MESSER, L., MANTON, D., KAN, K., NG, F., OLSEN, C., SHEAHAN, J., SILVA, M. & CHAWLA, N. 2014. Distribution and severity of molar hypomineralisation: trial of a new severity index. *International Journal of Paediatric Dentistry,* 24**,** 131-151.

PANAGAKOS, F. S., VOLPE, A. R., PETRONE, M. E., DEVIZIO, W., DAVIES, R. M. & PROSKIN, H. M. 2005. Advanced oral antibacterial/anti-inflammatory technology: A comprehensive review of the clinical benefits of a triclosan/copolymer/fluoride dentifrice. *The Journal of clinical dentistry,* 16**,** S1-19.

PITIPHAT, W., LUANGCHAICHAWENG, S., PUNGCHANCHAIKUL, P., ANGWARAVONG, O. & CHANSAMAK, N. 2014. Factors associated with molar incisor hypomineralization in Thai children. *European journal of oral sciences,* 122**,** 265-270.

POTSAID, B., BAUMANN, B., HUANG, D., BARRY, S., CABLE, A. E., SCHUMAN, J. S., DUKER, J. S. & FUJIMOTO, J. G. 2010. Ultrahigh speed 1050nm swept source/Fourier domain OCT retinal and anterior segment imaging at 100,000 to 400,000 axial scans per second. *Optics express,* 18**,** 20029-20048.

PRADEEP, A. & SHARMA, A. 2010. Comparison of clinical efficacy of a dentifrice containing calcium sodium phosphosilicate to a dentifrice containing potassium nitrate and to a placebo on dentinal hypersensitivity: a randomized clinical trial. *Journal of Periodontology,* 81**,** 1167-1173.

RANJITKAR, S., RODRIGUEZ, J., KAIDONIS, J., RICHARDS, L., TOWNSEND, G. & BARTLETT, D. 2009. The effect of casein phosphopeptide–amorphous calcium phosphate on erosive enamel and dentine wear by toothbrush abrasion. *Journal of dentistry,* 37**,** 250-254.

REES, J., LOYN, T. & CHADWICK, B. 2007. Pronamel and tooth mousse: an initial assessment of erosion prevention in vitro. *Journal of Dentistry,* 35**,** 355-357.

REICHENMILLER, K. & KLEIN, C. 2007. Formation of teeth. *Handbook of Biomineralization: Biological Aspects and Structure Formation***,** 159-176.

ROBERTS, J., DRAGE, N., DAVIES, J. & THOMAS, D. W. 2009. Effective dose from cone beam CT examinations in dentistry. *The British journal of radiology,* 82**,** 35-40.

RUAN, Q. & MORADIAN-OLDAK, J. 2015. Amelogenin and enamel biomimetics. *Journal of Materials Chemistry B,* 3**,** 3112-3129.

SALEHI, H. S., MAHDIAN, M., MURSHID, M. M., JUDEX, S. & TADINADA, A. Deep learning-based quantitative analysis of dental caries using optical coherence tomography: an ex vivo study. Lasers in Dentistry XXV, 2019. International Society for Optics and Photonics, 108570H.

SALVATO, A. R., CLARK, G., GINGOLD, J. & CURRO, F. 1992. Clinical effectiveness of a dentifrice containing potassium chloride as a desensitizing agent. *American journal of dentistry,* 5**,** 303-306.

SCHIFF, T., DOS, M. S., LAFFI, S., YOSHIOKA, M., BAINES, E., BRASIL, K., MCCOOL, J. & DE, W. V. 1998. Efficacy of a dentifrice containing 5% potassium nitrate and 1500 PPM sodium monofluorophosphate in a precipitated calcium carbonate base on dentinal hypersensitivity. *The Journal of clinical dentistry,* 9**,** 22-25.

SCHIFF, T., SALETTA, L., BAKER, R., WINSTON, J. & HE, T. 2005. Desensitizing effect of a stabilized stannous fluoride/Sodium hexametaphosphate dentifrice. *Compendium of continuing education in dentistry (Jamesburg, NJ: 1995),* 26**,** 35-40.

SCHUURS, A. 2012. *Pathology of the hard dental tissues*, John Wiley & Sons.

SCHWENDICKE, F., ELHENNAWY, K., REDA, S., BEKES, K., MANTON, D. J. & KROIS, J. 2018. Global burden of molar incisor hypomineralization. *Journal of dentistry,* 68**,** 10-18.

SEGARRA, M., SHIMADA, Y., SADR, A., SUMI, Y. & TAGAMI, J. 2017. Three-dimensional analysis of enamel crack behavior using optical coherence tomography. *Journal of dental research,* 96**,** 308-314.

SHANNON, I. L. & TRODAHL, J. N. 1977. Effect of waterborne fluoride on fluoride concentration and solubility of dental enamel. *Australian dental journal,* 22**,** 428-431.

SHARMA, N., ROY, S., KAKAR, A., GREENSPAN, D. C. & SCOTT, R. 2010. A clinical study comparing oral formulations containing 7.5% calcium sodium phosphosilicate (NovaMin), 5% potassium nitrate, and 0.4% stannous fluoride for the management of dentin hypersensitivity. *The Journal of clinical dentistry,* 21**,** 88-92.

SHELLIS, R. P. & ADDY, M. 2014. The Interactions between Attrition, Abrasion and Erosion in Tooth Wear

Erosive Tooth Wear. *Erosive Tooth Wear,* 25**,** 32-45.

SHEN, P., CAI, F., NOWICKI, A., VINCENT, J. & REYNOLDS, E. C. 2001. Remineralization of Enamel Subsurface Lesions by Sugar-free Chewing Gum Containing Casein Phosphopeptide-Amorphous Calcium Phosphate. *Journal of Dental Research,* 80**,** 2066-2070.

SHI, X.-Q., WELANDER, U. & ANGMAR-MÅNSSON, B. 2000. Occlusal caries detection with KaVo DIAGNOdent and radiography: an in vitro comparison. *Caries research,* 34**,** 151-158.

SHIMADA, Y., SADR, A., BURROW, M. F., TAGAMI, J., OZAWA, N. & SUMI, Y. 2010. Validation of swept-source optical coherence tomography (SS-OCT) for the diagnosis of occlusal caries. *Journal of dentistry,* 38**,** 655-665.

SILVA, M. J., SCURRAH, K. J., CRAIG, J. M., MANTON, D. J. & KILPATRICK, N. 2016. Etiology of molar incisor hypomineralization–A systematic review. *Community dentistry and oral epidemiology,* 44**,** 342-353.

SIMMER, J. & FINCHAM, A. 1995. Molecular mechanisms of dental enamel formation. *Critical Reviews in Oral Biology & Medicine,* 6**,** 84-108.
SIMRATVIR, M. 2011. Extensive Hypoplasia of Permanent Dentition Due to Childhood Illness and Antibiotic Use-A Case Report. *Dentistry,* 1**,** 2161-1122.100010.
SMITH, B. 1984. An index for measuring the wear of teeth. *Br Dent J,* 156**,** 435-438.
SOARES, G., MAGALHÃES, P., FONSECA, A. B. M., TOSTES, M., DA SILVA, E. & COUTINHO, T. C. L. 2017. Preventive Effect of CPP-ACPF Paste and Fluoride Toothpastes Against Erosion and Erosion Plus Abrasion In Vitro - A 3D Profilometric Analysis. *Oral health & preventive dentistry,* 15**,** 269-277.
SOLIMAN, W., SANDER, B., SOLIMAN, K. A. E. N., YEHYA, S., RAHAMN, M. S. A. & LARSEN, M. 2008. The predictive value of optical coherence tomography after grid laser photocoagulation for diffuse diabetic macular oedema. *Acta ophthalmologica,* 86**,** 284-291.
SOUZA, J., COSTA-SILVA, C., JEREMIAS, F., SANTOS-PINTO, L., ZUANON, A. C. C. & CORDEIRO, R. D. C. L. 2012. Molar incisor hypomineralisation: possible aetiological factors in children from urban and rural areas. *European Archives of Paediatric Dentistry,* 13**,** 164-170.
SOVIERO, V., HAUBEK, D., TRINDADE, C., DA MATTA, T. & POULSEN, S. 2009. Prevalence and distribution of demarcated opacities and their sequelae in permanent 1st molars and incisors in 7 to 13-year-old Brazilian children. *Acta odontologica scandinavica,* 67**,** 170-175.
STEFFEN, R., KRÄMER, N. & BEKES, K. 2017. The Würzburg MIH concept: the MIH treatment need index (MIH TNI). *European Archives of Paediatric Dentistry,* 18**,** 355-361.
SUGA, S. 1989. Enamel Hypomineralization Viewed From the Pattern of Progressive Mineralization of Human and Monkey Developing Enamel. *Advances in Dental Research,* 3**,** 188-198.
SWAIN, M. V. & XUE, J. 2009. State of the art of micro-CT applications in dental research. *International journal of oral science,* 1**,** 177-188.
TAN, O., LI, G., LU, A. T.-H., VARMA, R., HUANG, D. & GROUP, A. I. F. G. S. 2008. Mapping of macular substructures with optical coherence tomography for glaucoma diagnosis. *Ophthalmology,* 115**,** 949-956.
TAPIAS-LEDESMA, M. A., JIMÉNEZ, R., LAMAS, F., GONZÁLEZ, A., CARRASCO, P. & DE MIGUEL, A. G. 2003. Factors associated with first molar dental enamel defects: a multivariate epidemiological approach. *Journal of dentistry for children,* 70**,** 215-220.
TARBET, W. J., SILVERMAN, G., STOLMAN, J. M. & FRATARCANGELO, P. A. 1980. Clinical evaluation of a new treatment for dentinal hypersensitivity. *Journal of periodontology,* 51**,** 535-540.
TEARNEY, G. J., BREZINSKI, M. E., BOUMA, B. E., BOPPART, S. A., PITRIS, C., SOUTHERN, J. F. & FUJIMOTO, J. G. 1997. In vivo endoscopic optical biopsy with optical coherence tomography. *Science,* 276**,** 2037-2039.
TEZEL, H., ERGÜCÜ, Z. & ÖNAL, B. 2002. Effects of topical fluoride agents on artificial enamel lesion formation in vitro. *Quintessence international,* 33.
THRASH, W., DODDS, M. & JONES, D. 1994. The effect of stannous fluoride on dentinal hypersensitivity.
TSAI, M.-T., WANG, Y.-L., YEH, T.-W., LEE, H.-C., CHEN, W.-J., KE, J.-L. & LEE, Y.-J. 2019. early detection of enamel demineralization by optical coherence tomography. *Scientific reports,* 9**,** 1-9.
TSUBOI, M., HAYASHI, A., IKEDA, N., HONDA, H., KATO, Y., ICHINOSE, S. & KATO, H. 2005. Optical coherence tomography in the diagnosis of bronchial lesions. *Lung cancer,* 49**,** 387-394.
TWETMAN, S., AXELSSON, S., DAHLGREN, H., HOLM, A. K., KÄLLESTÅL, C., LAGERLÖF, F., LINGSTROÈM, P., MEJÀRE, I., NORDENRAM, G. & NORLUND, A. 2003. Caries-preventive effect of fluoride toothpaste: a systematic review. *Acta Odontologica Scandinavica,* 61**,** 347-355.
VAARKAMP, J., TEN BOSCH, J. & VERDONSCHOT, E. 1995. Propagation of light through human dental enamel and dentine. *Caries Research,* 29**,** 8-13.

VAN DER VEEN, M. & DE JONG, E. D. J. 2000. Application of quantitative light-induced fluorescence for assessing early caries lesions. *Assessment of Oral Health.* Karger Publishers.

VOLPE, A., PETRONE, M., DE VIZIO, W., DAVIES, R. & PROSKIN, H. 1996. A review of plaque, gingivitis, calculus and caries clinical efficacy studies with a fluoride dentifrice containing triclosan and PVM/MA copolymer. *The Journal of clinical dentistry,* 7**,** S1.

WANG, R. K., ELDER, J. B. & SMITH, V. High-resolution imaging of colonic mucosa using optical coherence tomography. Coherence Domain Optical Methods in Biomedical Science and Clinical Applications V, 2001. International Society for Optics and Photonics, 242-247.

WEERHEIJM, K. L., DUGGAL, M., MEJÀRE, I., PAPAGIANNOULIS, L., KOCH, G., MARTENS, L. & HALLONSTEN, A. 2003. Judgement criteria for Molar Incisor Hypomincralisation (MIH) in epidemiologic studies: a summary of the European meeting on MIH held in Athens, 2003. *European Journal of Paediatric Dentistry,* 4**,** 110-114.

WEGEHAUPT, F., GRIES, D., WIEGAND, A. & ATTIN, T. 2008. Is bovine dentine an appropriate substitute for human dentine in erosion/abrasion tests? *Journal of Oral Rehabilitation,* 35**,** 390-394.

WHATLING, R. & FEARNE, J. M. 2008. Molar incisor hypomineralization: a study of aetiological factors in a group of UK children. *International journal of paediatric dentistry,* 18**,** 155-162.

WIEGAND, A. & ATTIN, T. 2003. Influence of fluoride on the prevention of erosive lesions--a review. *Oral Health & Preventive Dentistry,* 1.

WIEGAND, A., EGERT, S. & ATTIN, T. 2008. Toothbrushing before or after an acidic challenge to minimize tooth wear? An in situ/ex vivo study. *American journal of dentistry,* 21**,** 13-16.

WIEGAND, A., KUHN, M., SENER, B., ROOS, M. & ATTIN, T. 2009. Abrasion of eroded dentin caused by toothpaste slurries of different abrasivity and toothbrushes of different filament diameter. *Journal of dentistry,* 37**,** 480-484.

WIEGAND, A., LEMMRICH, F. & ATTIN, T. 2006. Influence of rotating–oscillating, sonic and ultrasonic action of power toothbrushes on abrasion of sound and eroded dentine. *Journal of periodontal research,* 41**,** 221-227.

WILDER SMITH, C., WILDER SMITH, P., KAWAKAMI WONG, H., VORONETS, J., OSANN, K. & LUSSI, A. 2009. Quantification of Dental Erosions in Patients With GERD Using Optical Coherence Tomography Before and After Double-Blind, Randomized Treatment With Esomeprazole or Placebo. *The American journal of gastroenterology,* 104**,** 2788-2795.

WILLIAM, V., MESSER, L. B. & BURROW, M. F. 2006. Molar incisor hypomineralization: review and recommendations for clinical management. *Pediatric dentistry,* 28**,** 224-232.

WILLMOTT, N. S., BRYAN, R. A. E. & DUGGAL, M. S. 2008. Molar-Incisor-Hypomineralisation: A literature review. *European Archives of Paediatric Dentistry,* 9**,** 172-179.

XIE, Z., KILPATRICK, N., SWAIN, M., MUNROE, P. & HOFFMAN, M. 2008. Transmission electron microscope characterisation of molar-incisor-hypomineralisation. *Journal of materials science. Materials in medicine,* 19**,** 3187-3192.

YANG, X., WANG, L., QIN, Y., SUN, Z., HENNEMAN, Z. J., MORADIAN-OLDAK, J. & NANCOLLAS, G. H. 2010. How amelogenin orchestrates the organization of hierarchical elongated microstructures of apatite. *The Journal of Physical Chemistry B,* 114**,** 2293-2300.

ZERO, D. T. 1996. Etiology of dental erosion–extrinsic factors. *European journal of oral sciences,* 104**,** 162-177.

ZHANG, Z.-L., QU, X.-M., LI, G., ZHANG, Z.-Y. & MA, X.-C. 2011. The detection accuracies for proximal caries by cone-beam computerized tomography, film, and phosphor plates. *Oral Surgery, Oral Medicine, Oral Pathology, Oral Radiology, and Endodontology,* 111**,** 103-108.

Chapter 10

Appendices

10 Appendices

10.1 Appendix 1

Patient information leaflet

Research team:
Dr Susan Parekh,
Dr Agnes Bloch Zupan,
Dr Peter Brett,
Dr Laurent Bozec
Mashael Abdullatif
Nurjehan Ibrahim
Nabilah Harith
Amanda O`Donnell

Contact details:
Dr Susan Parekh
Tel: 020 3456 1067
Fax: 020 3456 2329
Unit of Paediatric Dentistry
The Eastman Dental Hospital and Institute
256 Gray's Inn Road
London WC1X 8LD
s.parekh@eastman.ucl.ac.uk

Website: www.uclh.nhs.uk

UCL Hospitals cannot accept responsibility for information provided by external organisations.

UCL HOSPITALS

If you need a large print, audio or translated copy of this document, please contact us on 0207 915 1022. We will try our best to meet your needs.

If you wish to discuss this study with a member of the research team or an independent expert who is not part of the research team, please ask Dr Susan Parekh

Thank you for taking the time to read this leaflet.

University College London Hospitals NHS
NHS Foundation Trust

A study of the genetics and the physical properties of dental anomalies

Publication date: 08/08/11

Date last reviewed

Version number **3**

Patient's Information Leaflet

A Study of the genetics and the physical properties of dental anomalies

Invitation

You are being invited to take part in a research study. Before you make a decision, it is important that you know why the research is being done and what it would involve from you. Please take time to read the following information carefully and discuss it with others if you wish. Ask us if anything is not clear at any time before or after participating. If you need more information we are willing to spend more time to satisfy you before taking any decision.

What is the purpose of the study?

To obtain and gather more information about dental anomalies, such as Enamel defects (Amelogenesis Imperfecta AI), and dentine defects (Dentinogenesis Imperfecta DI). We want to use this information to improve our knowledge of genetics and the properties of the teeth, to provide better support and long term care.

Why has I have been chosen?

We are asking all patients who have been diagnosed with dental anomalies and members of their families with the same or other dental conditions to participate in the study

Do I have to take part?

No. It is up to you to decide. If you do decide to participate we will ask you to sign a consent form. If you change your mind, you are free to withdraw at any time, without giving a reason. The standard of care you will receive will not be affected in any way.

What will happen to me if I take part?

We will ask you some questions about your teeth and your medical history, and examine your teeth, take photographs, and a saliva sample. The saliva sample will be used to link your DNA with the physical properties of your teeth. If you require any teeth to be extracted as part of your treatment, these will be collected for laboratory testing of the teeth. You will not need to do anything else. If any member of your family has similar teeth, we will invite them to take part as well, as this will help to detect the common dental genes in families. If you do not want other members of your family to participate, you can refuse and your treatment will not be affected in any way.

What are the possible disadvantages or risks of taking part?

There are no risks anticipated. None of your answers will affect your treatment in any way.

What are the possible benefits?

The information from this study will hopefully be used to help us expand our knowledge about the genetics of dental anomalies, and relate this to the appearance of the teeth, identify affected families and provide better support and treatment.

What will happen with the results?

Any samples that we collect will be stored using a study ID number, so that they cannot be directly linked to you. We hope to publish the results of the study on completion. All confidential information will be coded and you will not be identifiable in any way.

Will my taking part in the study remain confidential?

Yes. All information that is collected about you during the research will remain strictly confidential and will be seen only by the investigators named on this sheet. The safety and security of the data will be the responsibility of the principal investigator (Miss Susan Parekh). This information will be recorded in such a way that it is completely anonymous and you cannot be individually identified in anyway.

The information will also be stored in a database developed by Strasbourg University (phenodent database), who we work closely with. All information will be anonymised before putting on the phenodent database.

Who has reviewed the study?

All research in the NHS is looked at by independent group, called a Research Ethics Committee to protect your safety, rights, wellbeing and dignity. This study has been reviewed and given favourable opinion by the Joint Research Ethics Committee. If you would like to see a summary of the findings from the study when it is completed, please tell Miss Parekh or any of the other dentists you see.

10.2 Appendix 2

Consent form given to parents to collect teeth samples

University College London Hospitals NHS
NHS Foundation Trust

The Eastman Dental Hospital
256 Gray's Inn road
London
WC1X 8LD

Telephone: 020 3456 - 7899
Direct Line: 020-3456 - 1067
Fax: 020-3456-2329
Web-site: www.uclh.nhs.uk

Version 1
Study Number:
Patient Identification Number for this trial: .....

PARENT CONSENT FORM

Title of Project:

A Study of the genetics and the physical properties of dental anomalies.

Name of Researchers: Dr Susan Parekh, Dr Laurent Bozec, Dr Agnes Bloch-Zupan, Ms Kathy Harley, Khalifa Al-Azri, Salwa Ibrahim, May Alqatani, Shaima Sarkhouh and Alba tool Shinawi

Please initial box

1. I confirm that I have read and understood the information sheet dated 07/07/11 (version 2) for the study. I have been allowed some time to think about this, ask questions, and have had these answered in a way that I understand. ☐

2. I understand that my child's is voluntary and that I am free to withdraw at any time, without giving any reason, without their medical care or legal rights being affected. ☐

3. I understand that sections of any medical notes may be looked at by the researchers and responsible individuals from regulatory authorities where it is relevant to my child taking part in research. I give permission for these individuals to have access to my child's records. ☐

4. I give permission to the investigators to pass clinical data collected from my child's examination to my General Practitioner or General Dental Practitioner ☐

5. I understand that the samples taken from my child may be stored and used for the purpose of further research at a later date. I understand that these results will also remain anonymous. ☐

6. I understand that (this project or future research) will include genetic research aimed at understanding the genetic influences on dental defects in children. ☐

7. I agree for my child to take part in the above study. ☐

Name of Patient	Date		Signature of parent
Name of Person taking consent	Date		Signature

When completed, 1 for patient; 1 for researcher site file; 1 (original) to be kept in medical notes

UCL HOSPITALS

UCL Hospitals is an NHS Foundation Trust comprising: The Eastman Dental Hospital, The Heart Hospital, Hospital for Tropical Diseases, National Hospital for Neurology and Neurosurgery, The Royal London Homoeopathic Hospital and University College Hospital (incorporating the former Middlesex and Elizabeth Garrett Anderson Hospitals).

S Parekh Version 1

10.3 Appendix 3

A list of the three groups with the teeth samples in each group

Saliva		**Sensodyne complete protection**		**Sensodyne pronamel**	
Tooth number	Classification	Tooth number	Classification	Tooth number	Classification
MIH 1	21, II	MIH 24	21, I	C 1	Sound
C 0	Sound	C 13	Sound	MIH 29	21, I
MIH2	22, I	MIH 25	22, I	MIH 31	22, III
C 2	Sound	C 4	Sound	C 14	Sound
MIH 21	21, I	MIH 28	21, II	MIH 3	21, I
MIH 11	22, I	MIH 22	22, I	MIH 34	22, I
MIH 16	21, I	MIH 23	22, II	C 15	Sound
C 9	Sound	C 5	Sound	C 3	Sound
C 10	Sound	MIH 5	21, I	MIH 35	21, I
MIH 15	21, I	MIH 7	22, I	MIH 4	22, I
MIH 20	22, II	C 12	Sound	C 11	Sound
C 6	Sound	MIH 6	21, I	MIH 12	21, I
MIH 13	21, I	MIH 9	22, II	MIH 17	22, II
MIH 19	22, I	C 8	Sound	C 7	Sound
		MIH 14	21, I	MIH 10	21, I
		MIH 18	22, I	MIH 8	22, II
		C 19	Sound	C 3	Sound
		MIH 5	21, I	MIH 35	21, I
		MIH 30	22, I	MIH37	22,I